

https://dspace.org/

A seismic investigation of the Kaapvaal craton

Durrheim, Raymond John

2015-03-10
http://hdl.handle.net/10539/17215

Downloaded from a DSpace repository. https://dspace.org/

A SEISMIC INVESTIGATION OF THE KAAPVAAL CRATON

Raymond John Durrheim

A thesis submitted to the Faculty of Science,
University of the Witwatersrand, Johannesburg,
in fulfilment of the requirements for the
degree of Doctor of Philosophy.

Johannesburg 1989

ABSTRACT

The structure of the Kaapvaal Craton of southern Africa has been investigated by means of deep seismic sounding using mine tremors as the energy source, and by deep seismic reflection profiling. Seismometers were deployed at 10 km intervals on two profiles stretching between the major mine tremor source regions. Each profile is about 250 km in length. Record sections have been compiled for both P- and S-waves, and the travel-times and amplitudes interpreted using ray-tracing techniques. Synthetic seismograms have also been computed using the reflectivity method. A 16 s two-way-time seismic reflection profile, 112 km in length and traversing the northwestern portion of the Witwatersrand Basin, was surveyed during 1988 under the auspices of the National Geophysics Programme and the Geological Survey of South Africa. The reflection profile, which intersects both the refraction profiles, has been interpreted. The seismic models have been integrated with other geophysical and geological data.

This study has shown that the use of mine tremors for deep seismic sounding has particular advantages. Tremors are rich in shear energy, enabling joint interpretation of P- and S-waves and the estimation of Poisson's ratio. Tremors also have a wide bandwidth, with significant energy at frequencies as low as 3 Hz. Consequently reflections are produced from velocity gradient zones which are invisible to conventional reflection profiling using vibrators as the energy source. The seismic model for the Kaapvaal Craton has the following features: supracrustal strata 0-10 km thick; upper crystalline basement with P-velocities of 6.0-6.2 km/s; the boundary between upper and lower crust at a depth of ca. 14 km is either a discontinuity giving rise to reflections, or a gradient zone giving rise to a caustic; the lower crust has a uniform seismic velocity in the range 6.4-6.7 km/s; the crust mantle transition takes place over 1-3 km; and Moho at a depth of ca. 35 km. The lower crust was also found to be strongly attenuating, and to have a Poisson's ratio of ca. 0.28. It is also known to be electrically conductive. These observations are in accord with the presence of hydrated mantle rock at the base of the crust.

DECLARATION

I declare that this thesis is entirely my own work, except where explicitly stated in the Preface. It is being submitted for the degree of Doctor of Philosophy in the University of the Witwatersrand, Johannesburg. It has not been submitted before for any other degree or examination in any other University.

Raymond John Durrheim R J Durrheim

10 day of July, 1989.

DEDICATION

To Margie

PREFACE

During the 1950's seismologists at the University of the Witwatersrand pioneered the use of mine tremors as the energy source for deep seismic sounding of the Kaapvaal Craton. In the intervening three decades there have been advances in recording instrumentation and interpretation methods, which have been used in this study to obtain a substantially more detailed model of the Craton. By happy coincidence, the National Geophysics Programme and Geological Survey of South Africa financed the trans-Witwatersrand Basin deep seismic reflection profile during 1988. This allowed a joint interpretation of the reflection and refraction data sets, and provided valuable constraints on the interpretation.

Dr Rod Green supervised this project. I deeply appreciate his encouragement and advice, and his willingness to discuss problems and provide practical assistance.

The project involved more than thirty months of field recording, requiring weekly visits to service the seismographs. I would like to thank the following technicians who worked with me at various times during this period, preparing and repairing seismographs, digging holes, opening gates, charging batteries. They are Peter Chipkin, Migael Goldberg, Alan Robertson and John Sorour.

Mpho Nkwana was responsible for much of the replaying and digitizing the field tapes. I am grateful for his reliable work.

The trans-Witwatersrand Basin seismic reflection profile was acquired and processed by Rockplan (Pty) Ltd. I was a member of a group of four persons appointed by the Steering Committee of the National Geophysics Programme to supervise this. The other members of the group were Messrs A du Plessis and J H T Beukes of the Geological Survey of South Africa, and Dr J Potocki-Szwejkowski, at that time a member at staff of Witwatersrand University.

Mark Muller was responsible for running the reflectivity method synthetic seismogram computer programme. Gordon Cooper provided general computing support, both on the PC and on the Microvax. Dr Artur Cichowicz provided many insights into the philosophy of seismology. Annette Maher assisted with the interpretation of the reflection seismic section across the collar of the Vredefort Dome. Studies of the gravity and magnetic fields of the Kaapvaal Craton, in which I have collaborated, have contributed to this thesis. The leader of this research is Prof Brankc Corner.

Financial support for this project was provided by the National Geophysics Programme, and the Chamber of Mines.

The major findings of this study have not yet been submitted for publication. However I have authored or co-authored several publications related to this study which have appeared, or been accepted for publication, in refereed international journals.

Corner, B., R J. Durrheim and L. O. Nicolaysen, Relationships between the Vredefort structure and the Witwatersrand Basin, within the tectonic framework of the Kaapvaal Craton, as interpreted from regional gravity and aeromagnetic data, Tectonophysics, in press.

Durrheim, R. J., Recent reflection seismic developments in the Witwatersrand Basin, in Reflection Seismology: a global perspective, M. Barazangi and L. Brown (eds.), Geodynamics Series, 13, 77-83, American Geophysical Union, Washington, 1986.

Durrheim, R. J., Seismic reflection and refraction studies of the deep structure of the Agulhas Bank, Geophys. J. R. astr. Soc., 89, 395-398, 1987.

Green, R. W. E. and R. J. Durrheim, A seismic refraction investigation of the Namaqualand Metamorphic Complex, South Africa, J. Geophys. Res., in press.

Hart, R. J., M. A. G. Andreoli, C. B. Smith, M. L. Otter and R. J. Durrheim, Ultramafic rocks in the centre of the Vredefort structure: possible exposure of the upper mantle ? Chemical Geology, in press.

CONTENTS

page

ABSTRACT i

DECLARATION ii

DEDICATION iii

PREFACE iv

LIST OF FIGURES ix

LIST OF TABLES xiii

1. INTRODUCTION 1

1.1 Seismology and the earth's interior 1
1.2 Aim and scope of this study 1

2. KAAPVAAL CRATON 4

2.1 Geology 4
2.1.1 Tectonic evolution 4
2.1.2 Vredefort structure 6
2.1.3 Kimberlites and xeroliths 9
2.2 Seismic investigations 12
2.2.1 Mine tremor studies 12
2.2.2 Refraction surveys using explosive sources 14
2.2.3 Long period surface wave studies 14
2.2.4 Reflection seismics 15

2.3 Other Geophysical Investigations 17
2.3.1 Gravity and magnetics 17
2.3.2 Deep electrical soundings 19
2.3.3 Heat flow 20

3. MINE TREMORS - THE SEISMIC ENERGY SOURCE 21

3.1 Mining induced seismicity 21
3.2 Location, origin time and local magnitude 22
3.3 Source parameters 23
3.4 Source mechanism and radiation pattern 27
3.5 Magnitude distribution 28

4. DATA ACQUISITION, PROCESSING AND DISPLAY 31

4.1 Seismograph locations 31
4.2 Seismometers 31
4.3 Recording instrumentation 33
4.4 Digitization 36
4.5 Calibration and system response 38
4.6 Noise removal 38
4.7 Compilation and display of record sections 40

5. INTERPRETATION OF DEEP SEISMIC SOUNDING PROFILES . 44

5.1 Analysis techniques 44
5.2 Description of record sections 53
5.2.1 Klerksdorp - East Rand - Witbank profile . 53
5.2.2 East Rand - O F S profile 68
5.3 Qualitative interpretation of record sections ... 78

5.4 Raytrace modelling 85
5.4.1 Klerksdorp - East Rand - Witbank profile . 85
5.4.2 East Rand - O F S profile 96
5.5 Reflectivity method modelling 102

6. TRANS-WITWATERSRAND BASIN DEEP SEISMIC REFLECTION PROFILE 106

6.1 Objectives 106
6.2 Acquisition parameters 108
6.3 Data processing sequence 111
6.4 Interpretation 114
6.4.1 Supracrustal strata 115
6.4.2 Crystalline Basement 121

7. STRUCTURE OF THE KAAPVAAL CRATON 129

7.1 Synthesis of the seismic refraction, reflection and surface wave models 129
7.2 Geological and geophysical synthesis 133
7.3 Comparison with other Archaean cratons 138
7.4 Comparison with adjacent geological provinces .. 145
7.5 Implications for crustal evolution 148

8. CONCLUSIONS 151

9. REFERENCES 156

APPENDIX A Seismograph locations 170

LIST OF FIGURES

Figure 2.1. Generalized distribution of the major tectonic provinces in southern Africa (after Hartnady et al., 1985 and Jones, 1988) 5

Figure 2.2. Geological map of the Witwatersrand Basin with the Palaeozoic cover removed (after Borchers, 1964 and Jones, 1988) 8

Figure 2.3. Seismic velocity models of the Kaapvaal Craton 13

Figure 2.4. Shear wave velocity model for the Kariba-Pretoria path derived by Bloch et al. (1969) 15

Figure 2.5. Bouguer gravity map of the Witwatersrand Basin and environs (Durrheim et al., 1986) 18

Figure 3.1. Normalized vertical component velocity density spectra of Klerksdorp goldfield tremors recorded at a station in the Vredefort Dome (about 65 km southeast of the source region) 25

Figure 3.2. Magnitude-frequency distribution for mine tremors in the Witwatersrand goldfields for the period January 1985 to May 1988 30

Figure 4.1. Seismograph locations on the Klerksdorp-East Rand-Witbank and East Rand-OFS profiles. Post Witwatersrand Supergroup rocks have been stripped (from Tweedie, 1986) 32

Figure 4.2. Frequency response of EV17 and EV17H seismometers ... 35

Figure 4.3. Synchronisation of the master and internal clocks ... 39

Figure 4.4. Measured velocity amplitude response of the recording system (from Peberdy, 1986) 41

Figure 4.5. Filtration of a noisy seismogram 41

Figure 4.6. Flow diagram showing the process of producing a record section 43

Figure 5.1. Synthetic record sections for simple 1-D models of the seismic velocity structure of the Kaapvaal Craton 47

Figure 5.2A. Record section for Klerksdorp - East Rand - Witbank profile. Tremors from the Klerksdorp goldfield 56

Figure 5.2B. P-wave record section for Klerksdorp - East Rand - Witbank profile. Tremors from the Klerksdorp goldfield 57

Figure 5.2C. S-wave record section for Klerksdorp - East Rand - Witbank profile. Tremors from the Klerksdorp goldfield 58

Figure 5.3A. Record section for Klerksdorp - East Rand - Witbank profile. Tremors from the East Rand goldfield 61
Figure 5.3B. P-wave record section for Klerksdorp - East Rand - Witbank profile. Tremors from the East Rand goldfield 62
Figure 5.3C. S-wave record section for Klerksdorp - East Rand - Witbank profile. Tremors from the East Rand goldfield 63
Figure 5.4A. Record section for Klerksdorp - East Rand - Witbank profile. Tremors from the Far West Rand goldfield 65
Figure 5.4B. P-wave record section for Klerksdorp - East Rand - Witbank profile. Tremors from the Far West Rand goldfield 66
Figure 5.4C. S-wave record section for Klerksdorp - East Rand - Witbank profile. Tremors from the Far West Rand goldfield 67
Figure 5.5A. Record section for O. F. S. - East Rand - Witbank profile. Tremors from the East Rand goldfield 70
Figure 5.5B. P-wave record section for O. F. S. - East Rand - Witbank profile. Tremors from the East Rand goldfield 71
Figure 5.5C. S-wave record section for O. F. S. - East Rand - Witbank profile. Tremors from the East Rand goldfield 72
Figure 5.6A. Record section for O. F. S. - East Rand - Witbank profile. Tremors from the O. F. S. goldfield 75
Figure 5.6B. P-wave record section for O. F. S. - East Rand - Witbank profile. Tremors from the O. F. S. goldfield 76
Figure 5.6C. S-wave record section for O. F. S. - East Rand - Witbank profile. Tremors from the O. F. S. goldfield 77
Figure 5.7A. P-wave velocity model, raytrace diagram and synthetic record section for the Klerksdorp - East Rand - Witbank profile. Tremors from the Klerksdorp goldfield 88
Figure 5.7B. S-wave velocity model, raytrace diagram and synthetic record section for the Klerksdorp - East Rand - Witbank profile. Tremors from the Klerksdorp goldfield 89
Figure 5.8. P-wave velocity model, raytrace diagram and synthetic record section for the Klerksdorp - East Rand - Witbank profile. Tremors from the East Rand goldfield 91
Figure 5.9A. P-wave velocity model, raytrace diagram and synthetic record section for the Klerksdorp - East Rand - Witbank profile. Tremors from the Far West Rand goldfield 94

Figure 5.9B. S-wave velocity model, raytrace diagram and synthetic record section for the Klerksdorp - East Rand - Witbank profile. Tremors from the Far West Rand goldfield 95
Figure 5.10A. P-wave velocity model, raytrace diagram and synthetic record section for the O. F. S. - East Rand profile. Tremors from the East Rand goldfield 98
Figure 5.10B. P-wave velocity model, raytrace diagram and synthetic record section for the O. F. S. - East Rand profile. Tremors from the East Rand goldfield 99
Figure 5.11. P-wave velocity model, raytrace diagram and synthetic record section for the O. F. S. - East Rand profile. Tremors from the O. F. S. goldfield 101
Figure 5.12A. Synthetic record section for a 1-D seismic velocity model of the Kaapvaal Craton computed using the reflectivity method 103
Figure 5.12B. Detail of the P-wave arrivals on the synthetic record section for a 1-D seismic velocity model of the Kaapvaal Craton computed using the reflectivity method 104
Figure 6.1. Location of the deep reflection seismic profile 110
Figure 6.2. Interpretation of the trans-Witwatersrand Basin deep seismic reflection profile 116
Figure 6.3A. Unmigrated panel (CDP 900-1540) from the trans-Witwatersrand Basin deep seismic reflection profile. An interpretation of the upper 2 s TWT is shown above 117
Figure 6.3B. Migrated panel (CDP 1180-1300) from the trans-Witwatersrand Basin deep seismic reflection profile 118
Figure 6.3C. Unmigrated panel (CDP 2540-2700) from the trans-Witwatersrand Basin deep seismic reflection profile and interpretation 119
Figure 6.4. Panel (CDP 3540-4000) from the trans-Witwatersrand Basin deep seismic reflection profile showing the collar of the Vredefort Dome 120
Figure 6.5A. Migrated panel (CDP 160-290) from the trans-Witwatersrand Basin deep seismic reflection profile. This panel shows the reflective character of the Ventersdorp Dome . 122

Figure 6.5B. Collapse of a diffraction in the Ventersdorp Dome to a focus (CDP 200, 820 ms TWT) after finite difference migration using a migration velocity of 6000 m/s 123
Figure 7.1. 2-D model of the Bouguer gravity anomaly along the trans-Witwatersrand Basin deep seismic reflection profile 134
Figure 7.2. Velocity-depth models for Archaean Cratons 139
Figure 7.3. Velocity-depth models for southern Africa 146

LIST OF TABLES

Table 2.1. Compressional velocity and density of some of the major lithological units in the Witwatersrand Basin (from Campbell and Peace, 1984) 16

Table 3.1. Tonnes mined and seismic activity for South African gold fields for the nine year period 1971-1979 30

Table 4.1. Seismograph gain settings 33

Table 4.2. Routine allocation of tape tracks 34

Table 5.1. Two-layer crustal models for the Kaapvaal Craton. The model for the western Transvaal is from Willmore et al. (1952), and the two models for the eastern Transvaal are from Hales and Sacks (1959) 48

Table 5.2. Representative seismic velocity, density and maximum thickness of formations constituting the Kaapvaal Craton 52

Table 6.1. Acquisition parameters for the deep seismic reflection field trials conducted in the Kroonstad district 108

Table 6.2. Acquisition parameters for the trans-Witwatersrand Basin deep seismic reflection profile 109

Table 6.3. Data processing sequence applied to the trans-Witwatersrand Basin deep seismic reflection profile 114

1. INTRODUCTION

1.1 Seismology and the Earth's interior

It was shortly after the start of this century that reasonably accurate and complete sets of seismograms began to be recorded, and by 1936 it was established that the earth consisted of several approximately spherical shells (the inner and outer core, mantle and crust). Since then efforts have been devoted to the refinement of this model. Recent advances in seismology include the detailed mapping of the deep structure of continents using the reflection seismic technique, the tomographic imaging of seismic velocity variations within the mantle, and the mapping of the topography of the core-mantle boundary. This study describes the seismic imaging of the Kaapvaal Craton of South Africa using both the refraction and reflection techniques.

1.2 Aim and scope of this study

The Kaapvaal Craton has several characteristics which make it particularly interesting for seismic investigation.

(a) It is a well preserved fragment of the Archaean crust.

(b) Gold was discovered in late Archaean rocks of the Witwatersrand Basin, one of five Precambrian basins preserved on the Craton, near Johannesburg in 1886. Since then the basin has produced more than half the world's gold (Pretorius, 1976).

(c) The Craton has the world's greatest concentration of kimberlite intrusions (Dawson, 1980, p.10). Xenoliths contained within the kimberlite provide samples of the lower crust and mantle.

(d) The Craton also hosts the Bushveld Complex, an igneous intrusion with vast reserves of chromium and platinum group elements.

(e) The geology of the Craton has been well mapped because of these rich mineral deposits.

(f) A cryptoexplosion structure known as the Vredefort Dome is found in the centre of the Witwatersrand Basin. The origin of this structure is still debated, but it is thought to provide a transect of the Archaean crust.

(g) Deep-level mining for gold and uranium induces frequent earth

tremors, thereby providing a unique laboratory for the study of earthquake mechanisms and also a source of energy for deep seismic sounding.

During the 1950's several investigations utilized Witwatersrand mine tremors in order to study the seismic velocity structure of the Craton, resulting in simple one- or two-layered models (Willmore et al., 1952; Gane et al., 1956; Hales and Sacks., 1959). Knowledge of the deep structure of the crust constituting the Kaapvaal Craton has advanced little during the past three decades. Since the advent of semi-conductor electronics and digital computers in the 1960's there have been dramatic advances in seismograph design, signal processing and seismic interpretation techniques. In this study we make use of these technical advances to derive a substantially more detailed crustal model than hitherto available.

Seismometers have been deployed on two profiles joining the major mine tremor source areas (the East Rand, Far West Rand, Klerksdorp, and Orange Free State goldfields) recording seismograms on magnetic tape for subsequent digital processing. Modern interpretation methods have been used to interpret the travel-times and amplitudes of P and S body waves. A deep seismic reflection profile, about 112 km in length and intersecting both the refraction profiles, was surveyed by contractors for the National Geophysics Programme during August 1988. The author was part of the group which proposed the profile, and part of a four man team that supervised the acquisition and processing of the data.

The main aims of this study are listed below.

(a) Establish the seismic velocity structure of the central Kaapvaal Craton.

(b) Compare the P- and S-wave velocity structure and interpret any variation in Poisson's ratio.

(c) Describe any seismic velocity discontinuities (such as the Moho and Conrad) which may be detected.

(d) Integrate the seismic model with geological and other geophysical data.

(e) Compare the seismic structure of the Craton with adjacent terranes in southern Africa, and other Archaean shields.

(f) Interpret any evidence pertaining to the evolution of the Craton.

The data set acquired for this project is also suitable for several other studies which are beyond the scope of this thesis, but will be undertaken in the future. These include studies of attenuation, site effects, anisotropy, and higher mode surface waves.

This project was funded by the Foundation for Research Development for the period March 1986 to December 1988. It originally formed part of the "Tectonic and Structural Framework of South Africa" section of the National Geoscience Programme. In 1987 administration of the project was transferred to the National Geophysics Programme.

2. KAAPVAAL CRATON

In this chapter geological and geophysical information relevant to the interpretation of the seismic data is reviewed.

2.1 Geology

2.1.1 Tectonic evolution

The Kaapvaal Craton is one of the ancient nuclei around which the African continent is built (Figure 2.1). The crystalline rocks constituting the bulk of the Craton are generally referred to as "basement granites", although the term encompasses a range of compositions which may be of purely igneous origin, gneissic or migmatites. The bulk composition of the Archaean crust is dioritic, though diorites and andesites themselves are rare. The Archaean crystalline massifs have a characteristic bimodal composition, the most important rock types being tonalite and cogenetic trondhjemites (Tankard et al., 1982, p 21 & 34). The greatest ages obtained for these rocks is ca. 3.55 Ga, with the intrusion of granitoids continuing sporadically until about 2.6 Ga. (Tankard et al., 1982, p 6).

Within the crystalline rocks are relatively small fragments of intensely metamorphosed and structurally deformed rocks of Swazian age known as "greenstones", which are derived from sedimentary and volcanic strata. The basal Onverwacht Group of the Swaziland Group has yielded a Nd-Sm age of 3.51 Ga (Tankard et al., 1982, p 6). The suite of Archaean rocks comprising the Craton is known informally as the Basement Complex, of which the greenstone belts comprise less than 10% of the exposure (Tankard et al., 1982, p 21). A profound unconformity separates the Basement Complex from the relatively undisturbed cover rocks. The Basement Complex crops out over large areas to the east of the Transvaal escarpment, but over the remainder of the Craton it is covered by younger rocks except for a few isolated inliers such as the Johannesburg, Vredefort, and Ventersdorp Domes (Figure 2.2).

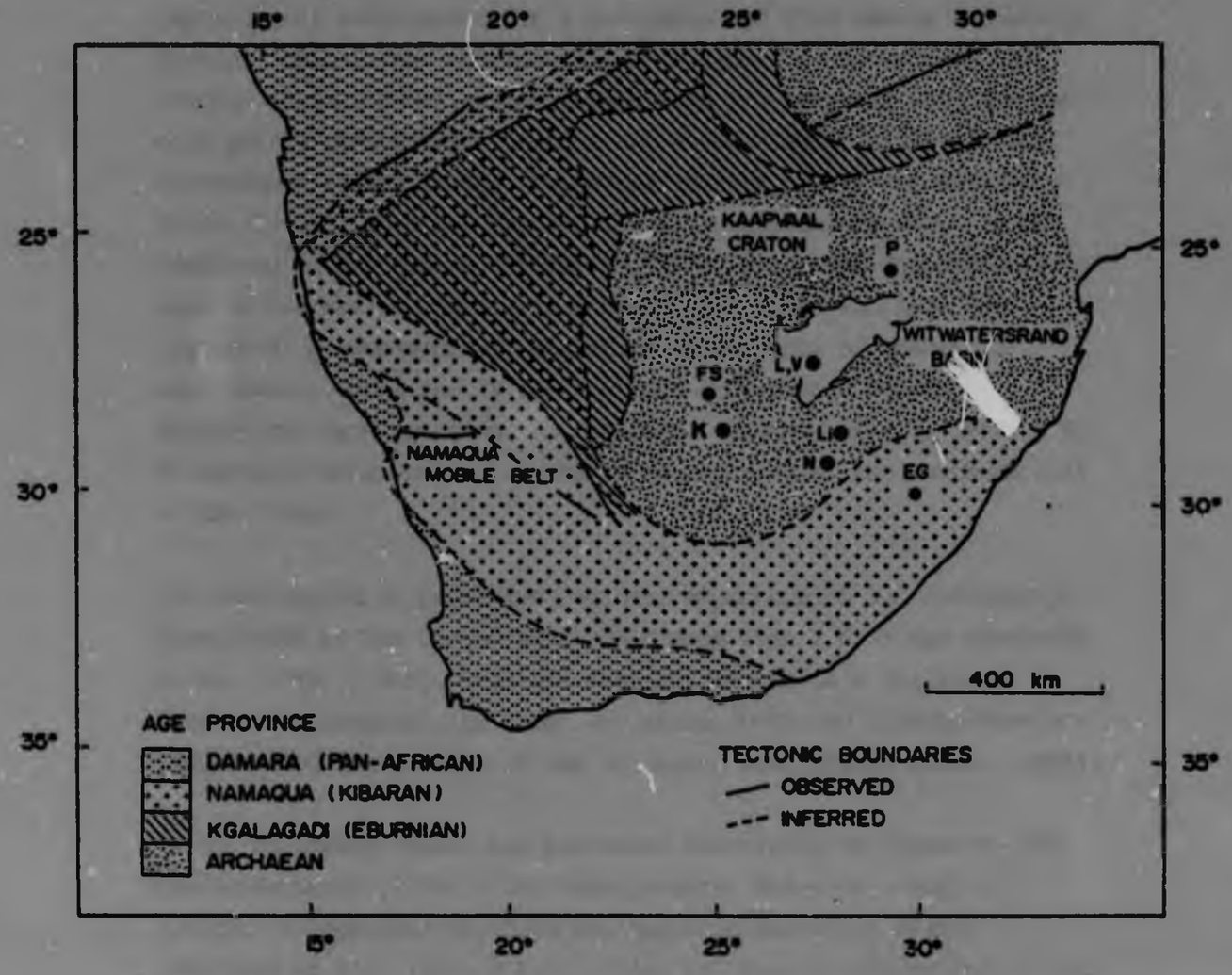


Figure 2.1. Generalized distribution of the major tectonic provinces in southern Africa (after Hartnady et al., 1985 and Jones, 1988). Kimberlite localities referred to in the text are Premier (P), Kimberley (K), Lace (L), Voorspoed (V), Ngopetsoeu (N), Lipelaneng (Li), Frank Smith (FS) and East Griqualand (EG).

The Archaean-Proterozoic boundary is conventionally drawn at the time of cratonic stabilization. Since 3.0 Ga the Kaapvaal Craton has been relatively stable, with tectonic movement providing the depositional environment for a succession of five basins exhibiting fluvial, deltaic and continental-shelf types of deposition: the Pongola (3.0-2.75 Ga), which formed when the Kaapvaal Province was only partly cratonized; Dominion and Witwatersrand (2.75-2.5 Ga); Ventersdorp (2.5-2.25 Ga); Transvaal (2.25-2.0 Ga); and Waterberg (2.0-1.75 Ga). No other Precambrian sedimentation is known to be preserved on the craton (Pretorius, 1976, p 3). The depositional axes of the basins migrated northward with time, and have been related to a complementary migration of the loci of granitoid emplacement. Consequently the Archaean-Proterozoic boundary is diachronous from southeast to northwest (Tankard et al., 1982, p 8). Phanerozoic sediments of the Karoo Sequence cover the southern half of the Craton.

The last period of pervasive regional metamorphism and deformation experienced by the Craton took place more than 2.6 Ga ago (Hartnady et al., 1985, p 237). This has been attributed to a collision between the Kaapvaal and Zimbabwe Craton, with the Limpopo Province representing the remains of the collision zone (Burke et al., 1986).

To the southwest, south and southeast the Craton is rimmed by the mid-Proterozoic (2.0-0.9 Ga) Namaqua-Natal Province, which is thought to represent multiple amalgamation-accretion events (Hartnady et al., 1985, p 241). This, in turn, is surrounded by the Pan-African (670-530 Ma) Damara Province. The last major tectonic episodes affecting southern Africa were the Cape Orogeny (280-230 Ma) which gave rise to the Cape Fold Belt, and the fragmentation of Gondwana (135-115 Ma).

2.1.2 Vredefort structure

The Vredefort Dome, located in the centre of the Witwatersrand Basin, is one of the earth's largest cryptoexplosion structures (Figure 2.2). The dome of basement granite is about 40 km in

diameter, and is surrounded by a collar of steeply dipping and overturned Dominion, Witwatersrand, Ventersdorp and Transvaal rocks. Strong geochemical gradients in the granitic basement rocks have been interpreted as evidence that the Archaean crust may be "turned on edge". A traverse from the collar to the centre of the structure is thought to be equivalent to a 14 km section through the Archaean crust (Hart et al., 1981).

The basement geology is divided into two roughly concentric zones. The Vredefort upper crust consists of massive granites or granitic-gneisses, and is known as the Outer Granite-gneiss (OGG). In the centre of the Vredefort Dome (10-15 km below the original cratonic surface) rocks of granitic composition, in granulite facies, predominate. This zone is termed the Inlandsee leucogranulite (ILG). Mafic granulites found in this zone are thought to be relics of supracrustal strata, which existed prior to a profound reconstitution of the middle crust (Hart et al., 1981). A serpentinised ultramafic body has been drilled in the centre of the Dome, and is interpreted to be a sample of mantle rock (R. J. Hart, University of the Witwatersrand, pers. comm., 1989). The OGG and ILG are separated by a narrow (ca. 10 m) zone of pseudotachylite and brecciated dolerite termed the Vredefort discontinuity. Associated with the discontinuity is a 2-3 km broad magnetite-rich charnockitic zone (Hart and Andreoli, 1986).

The basement granite and collar rocks exhibit well-developed shock deformation features such as the presence of coesite, emplacement of pseudotachylite veins, lamellar deformations in quartz, and widespread occurence of shatter cones (Nicolaysen and Reimold, 1985). Dietz (1961) interpreted the Vredefort Dome as a meteorite impact crater. Subsequent petrographic studies of the collar rocks has revealed two distinct shock events, the most recent being responsible for the shatter cones and pseudotachylite veins (Lilly, 1981). This evidence, together with the presence of unusual alkalic igneous bodies, has led other workers to favour an endogeneous origin. Nicolaysen and Ferguson (1981) propose that shock metamorphism resulted from carbonated fluids rising from lower crustal levels.

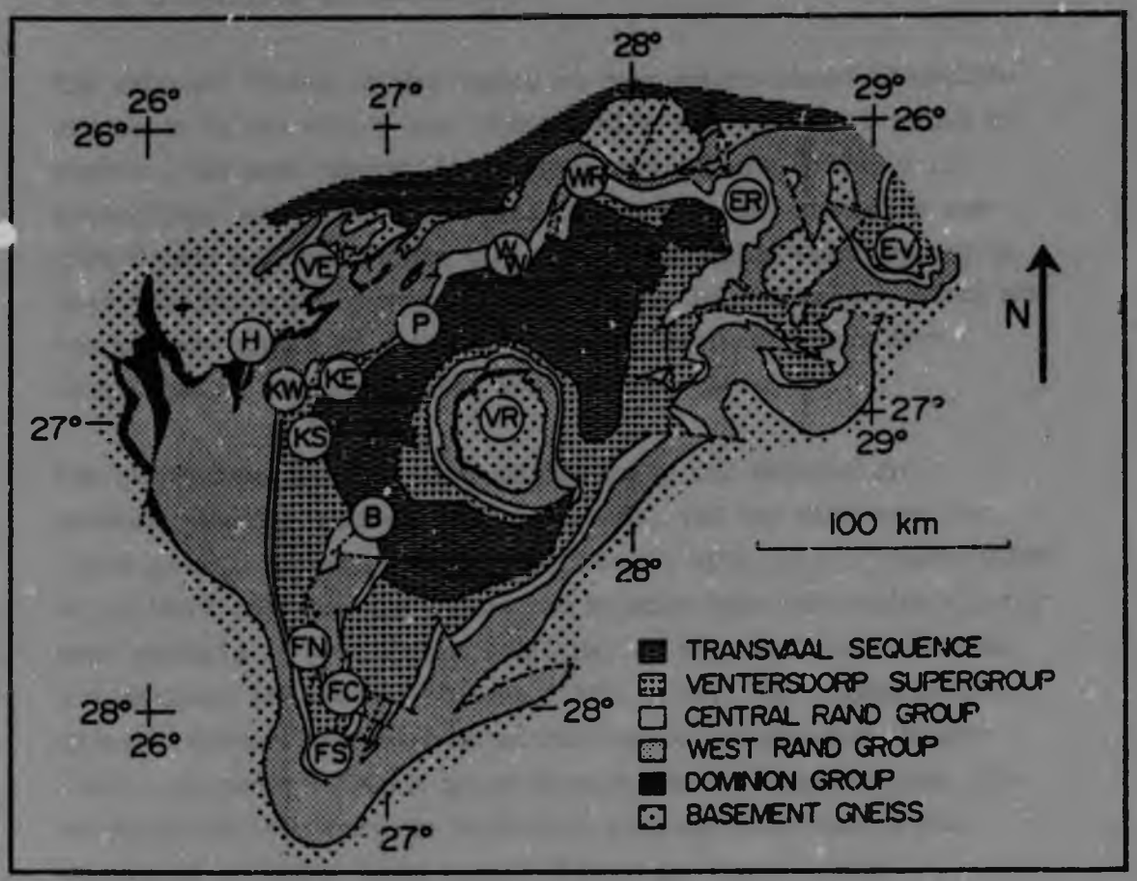


Figure 2.2. Geological map of the Witwatersrand basin with the Palaeozoic cover removed (after Borchers, 1964 and Jones, 1988). Approximate localities of goldfields and gaps between them are: EV, Evander; ER, East Rand; WR, West Rand; WW, Far West Rand; P, Potchefstroom gap; KE, Klerksdorp east; KW, Klerksdorp west; KS, Klerksdorp south; B, Bothaville; FN, Free State north; FC, Free State central; and FS, Free State south. Granite domes are: H, Hartebeesfontein; VE, Ventersdorp; and VR, Vredefort.

On the basis of palaeomagnetic measurements an age of approximately 2.0 Ga has been ascribed to the structure (Hargraves, 1970).

2.1.3 Kimberlites and xenoliths

The Kaapvaal Craton is the region of most concentrated kimberlite intrusion in the world, and together with the Yakutia province of Siberia, the most thoroughly investigated (Dawson, 1980, p 10). Kimberlites were first discovered on the Kaapvaal Craton in the 1870's, and are named after the town of Kimberley which sprang up near the rich diamond diggings. These rare igneous rocks, which are the primary source of diamonds, contain xenoliths which have originated in the lower crust and upper mantle.

The kimberlites tend to occur in clusters, for example the Kimberley-Barkly West and Virginia areas, and the diatremes are lined up on deep-seated fractures (Dawson, 1980, p 10). Kimberlites of at least two ages are known: the Premier mine kimberlite cluster near Pretoria is Precambrian (1250 Ma) in age; while most others are Mesozoic (140-80 Ma) (Dawson, 1980, p 16). The origin of the Mesozoic kimberlites has been attributed to large-scale shallow subduction under Gondwana prior to continental fragmentation. The volatiles derived from the subducted slab may have caused the succession of Karoo flood basalt volcanism, upper mantle metasomatism, and kimberlite magmatism (Helmstaedt and Gurney, 1984).

a) Lower crustal xenoliths

A suite of mafic to felsic garnet granulites have been collected from kimberlites in the Namaqua-Natal Province. These rocks record temperatures and pressures in the range 550-1000 ^{o}C and 4.5-20 GPa respectively, and may have surface equivalents in the Natal Province south of Durban. These xenoliths indicate that the lower crust is composed mainly of granulite-facies rocks, underlying the amphibolite and greenschist facies rocks and granites of the upper crust. The origin of the granulites is still a subject of debate:

one theory considers them to represent high-pressure equivalents of basaltic or gabbroic rocks; while another theory regards them as the residuum of rocks of more intermediate composition which have been subjected to an anatectic melting event during which the granitic constituents migrated into the upper crust (Dawson, 1980, p 210).

Lower crustal xenoliths are exceedingly rare at localities on the Kaapvaal Craton. Two examples from the Kimberley area recorded pressures less than 1 GPa, temperatures higher than in the Namaqua-Natal Province and do not contain garnet (Van Calsteren et al., 1986). Xenoliths from the Lace kimberlite near Kroonstad are also of granulite facies. Both sapphirine-bearing and sapphirine-free granulites were found, with quartz and garnet as the other abundant minerals. The Lace xenoliths are interpreted as indicating metamorphism of a sedimentary protolith at temperatures in the range 900-1000 °C and pressures >1 GPa. It is not known from where in the crustal section the specimens are derived (Dawson and Smith, 1987). Harris et al. (1987) also mention the recovery of two granulite xenoliths from the Voorspoed pipe near Kroonstad. Xenoliths from the Ngopetsoeu and Lipelaneng kimberlites in Lesotho have been interpreted as basaltic cumulates with a lower crustal origin. They have been divided into two classes: Group 1 consisting of Cr-spinel wherlites and lherzolites, and Group 2 consisting of Al-spinel lherzolites (Carswell et al., 1984).

There are several possible explanations for the scarcity of lower crustal xenoliths in kimberlites on the Craton: the lower crust was not sampled by the kimberlite; fragments of the lower crust were altered or assimilated; or lower-crustal xenoliths are so undistinguished in appearance that they have been overlooked by petrologists (Nixon, 1987, p 421).

b) Mantle xenoliths

Over 90% of all the mantle xenoliths recovered in southern Africa belong to the peridotite suite and are composed of olivine with lesser orthopyroxene and minor garnet and/or clinopyroxene. They are thus garnet (spinel) lherzolites and harzburgites (Nixon, 1987, p 218). The peridotite suite is comprised of a high temperature

(>1100°C) and low temperature (<1100°C) group. Other rock types include eclogites, pyroxenites, dunites and metasomites (Nixon, 1987, p 404 & 408). Xenoliths from the Kaapvaal Craton and Namaqua-Natal Province suggest that the mineralogy of the mantle is essentially similar (C B Smith, Witwatersrand University, pers comm, 1988).

In South Africa diamond-bearing kimberlites are restricted to the Kaapvaal Craton. The relatively cool equilibration temperatures estimated for inclusions within the diamonds are interpreted to indicate that the Craton had grown to its full areal extent and cooled to approximately the present thermal gradient at the time of diamond formation (Nixon, 1987, p 410).

2.2 Seismic investigations of crustal structure

2.2.1 Mine tremor studies

Seismological studies of mine tremors commenced in 1939 at the Bernard Price Institute of Geophysical Research, University of the Witwatersrand (Gane, 1939). On the basis of early observations, Gane et al. (1946) concluded that the Witwatersrand mine tremors were large enough, and occurred frequently enough to permit observations to be made at relatively large distances without it being necessary to occupy a station for an excessively long time.

Deep seismic sounding of the Craton by studies of the travel-times of elastic waves generated by Witwatersrand earth tremors began in 1948. In the first field programme seismometers were deployed at 29 sites in the western Transvaal (Willmore et al., 1952); and later also at 57 sites to the north, south and east of Johannesburg (Gane et al., 1956). Finally, a profile consisting of 18 stations was surveyed between Johannesburg and Kosi Bay in order to investigate the effect of the escarpment on travel times (Hales and Sacks, 1959).

The model deduced from these studies consists of a crust (V_p = 6.0–6.18 km/s, V_s = 3.6–3.68 km/s) with a thickness of 35.1–36.6 km overlying a mantle with P_n = 7.96–8.27 km/s. The seismic velocities were not found to differ significantly with azimuth (Hales and Sacks, 1959). Evidence for the existence of a layer in the lower crust with intermediate seismic velocities is equivocal. Willmore et al. (1952) were the first to identify intermediate velocity phases (6.83 km/s) on seismograms from the western Transvaal, but this interpretation was deemed unsatisfactory by Gane et al. (1956, p. 312). Subsequently Hales and Sacks (1959) reported evidence for an intermediate layer (6.7–7.2 km/s) within the crustal section for the eastern Transvaal. However, Bott (1971, p.42) suggested that this phase was in fact a supercritical Moho reflection and not a refraction from the lower crust. The velocity models are summarized in Figure 2.3.

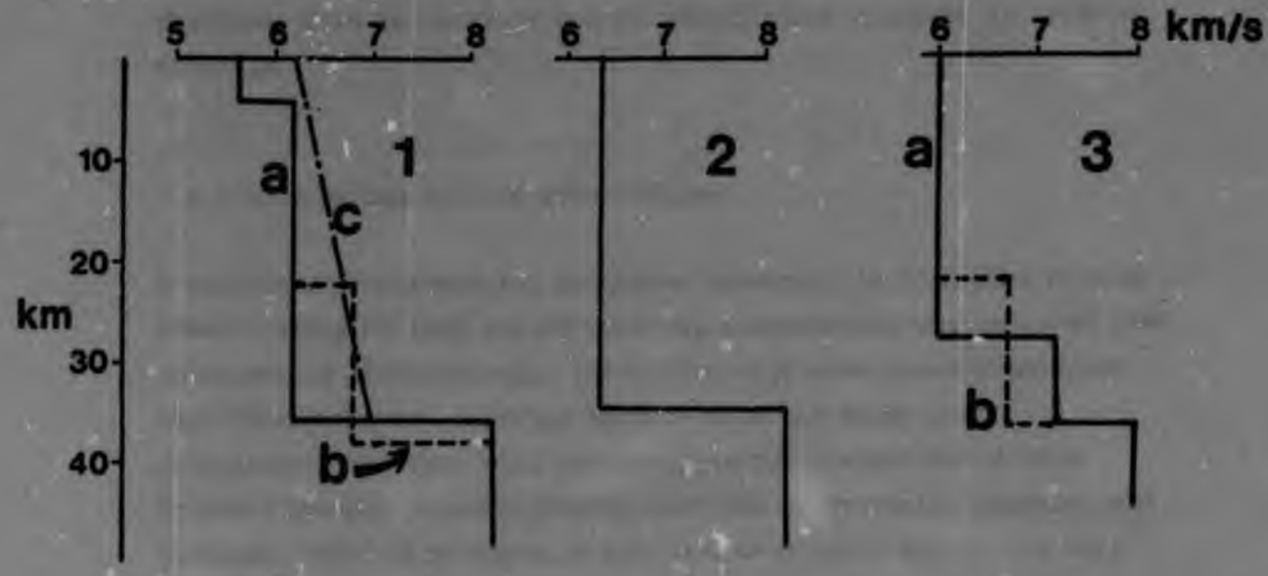


Figure 2.3. Seismic velocity models of the Kaapvaal Craton. (1) Willmore et al. (1952), (2) Gane et al. (1956), (3) Hales and Sacks (1959).

2.2.2 Refraction surveys using explosive sources

A 36 km seismic refraction profile, oriented north-south over the core of the Vredefort dome, was surveyed in 1978 as part of the South African Geodynamics Project (Green and Chetty, 1987). The outer granitoid-gneisses yielded velocities in the range 5.9-6.1 km/s. In the centre of the Dome velocities of 6.42-6.45 km/s were reliably defined, indicating rocks of an intermediate composition. Drill holes 20-30 m deep intersected complex gneisses of dioritic average composition. "Crust on edge" models of the Vredefort basement feature very steep dips, which were not seismically observed. This is possibly due to insufficient contrast in seismic velocity.

2.2.3 Long period surface wave studies

A surface wave observation programme commenced in 1965 when a five station array of long period vertical seismometers was deployed near Johannesburg (Bloch et al., 1969). Rayleigh wave phase velocities were determined by analysing records from the array near Johannesburg together with records from the nearest World Wide Standard Seismic Network (WWSSN) stations at Pretoria, Bulawayo and Windhoek. Multi-mode Rayleigh and Love wave group velocities were also computed from records of earthquakes originating near the Kariba Dam, and in southern Malawi. The phase velocities cover the period range 20-100 s; and the group velocities extend from 2-40 s for the fundamental mode, and 2-12 s for the higher modes.

Simultaneous inversion of the fundamental and first higher Rayleigh and Love group velocity modes for the Kariba-Pretoria path, and the Rayleigh phase velocities for the Pretoria-Bulawayo path yield the crustal shear velocity models shown in Figure 2.4. The common characteristic of all the inversion models is the presence of two crustal low-velocity channels beginning at depths of 12 and 24 km.

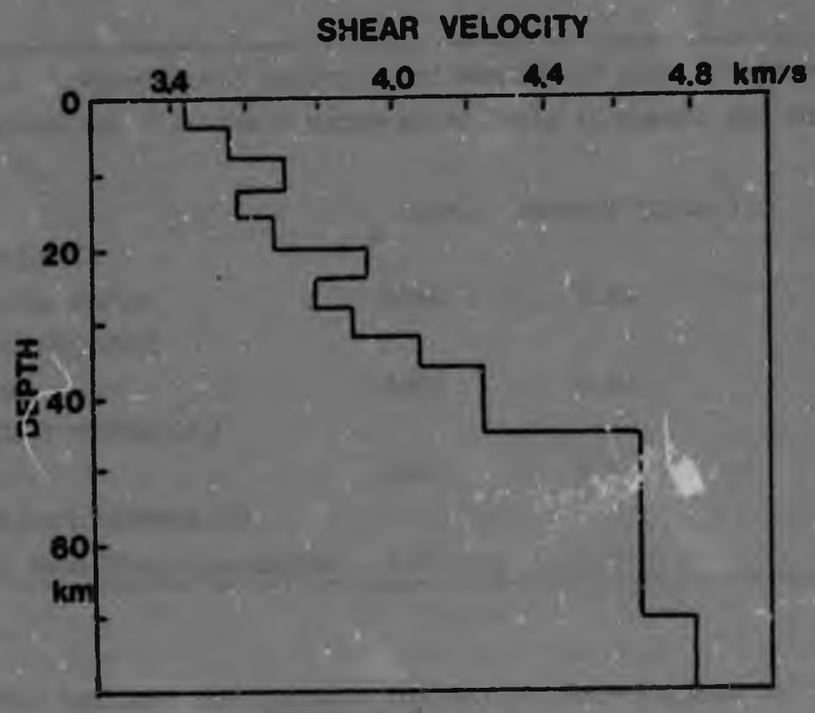


Figure 2.4. Shear wave velocity model for the Kariba-Pretoria path derived by Bloch et al. (1969).

The phase velocities for the array area confirm the high sub-crustal velocities previously determined from mine tremor studies. The phase and group velocity curves obtained for the Kariba-Pretoria path are similar to those for other shield areas.

2.2.4 Reflection seismics

Reflection seismology was introduced in 1982 for the exploration of the Witwatersrand Basin, enabling the deeply buried parts of the basin and the structurally complex basin margins to be mapped (Campbell and Peace, 1984). The seismic velocities of the major lithological units in the Witwatersrand Basin have been determined by means of vertical seismic profiles and velocity logging of boreholes (Table 2.1). Reflection coefficients of important geological contacts have been studied through an analysis of acoustic impedance profiles constructed from borehole density and velocity logs. The estimated reflection coefficients fall in the range 3% to 11%.

Table 2.1. Compressional velocity and density of some of the major lithological units in the Witwatersrand Basin (Campbell and Peace, 1984, p 7).

	v_p (m/s)	density (g/cm^3)
KAROO SEQUENCE		
sandstone, shale	3500	2.65
TRANSVAAL SEQUENCE		
dolomite	6800	2.88
VENTERSDORP SUPERGROUP		
lava	6400	2.85
WITWATERSRAND SUPERGROUP		
Central Rand Group quartzites	5700	2.65

In seismic sections the Basement Complex is characterised by numerous short reflecting segments, and a zone of particularly strong reflection has been identified some 7.5 km within the Archaean crust (Durrheim, 1986). Gravity and seismic refraction data from the Vredefort Dome also indicate an increase in acoustic impedance from upper to lower crust (assuming that the "crust on edge" model for the core of the Vredefort Dome is correct), the transition occuring some 10 km from the collar. Durrheim (1986) proposes that the zone of strong reflection corresponds to this boundary. Hart and Andreoli (1986) consider that they have successfully located this boundary in the field: they have identified the "Vredefort discontinuity", a 10 m wide zone of pseudotachylite and brecciated dolerite which forms an abrupt contact between the upper Outer Granite-gneiss (OGG), and the granulite facies rocks (LLG) in the core of the Dome. They further propose that this discontinuity may be comparable to the seismic discontinuity intersected in the Kola borehole on the Baltic shield at a depth of ca. 9 km below the surface, which coincides with a zone that is anomalously brecciated, hydrous and highly mineralized (Kozlovsky, 1984).

2.3 Other geophysical investigations

2.3.1 Gravity and magnetics

Compilations of gravity and aeromagnetic data covering the Witwatersrand basin and environs have been published by Durrheim et al. (1986) and Corner et al. (1986b).

The Bouguer gravity map (Figure 2.5) is compiled from some 13500 observations. The arc of gravity lows, convex to the north, is due to a ridge of basement granite which forms the perimeter of the main Witwatersrand basin. An inner concentric arc of gravity highs is due to the considerable thickness of dense West Rand shale, Ventersdorp lavas, and Transvaal dolomites filling the main basin. The roughly linear southeastern margin of the basin is marked by a steep gravity gradient. A gravity high, convex to the south, is found in the northeastern corner of the map. This coincides with the Bethal lobe of the Bushveld complex. The prominent northeast trending Bethlehem gravity high (B-B') lies to the southeast of the basin.

The gravity field of the Vredefort structure was studied in detail by Stepto (1979). The 30 mGal Bouguer anomaly found in the core of the Dome is attributed to an increase in density towards the centre, in accord with the "crust on edge" model. The densities used to model the anomaly range from 2.65 g/cm^3 for the Outer Granite-gneiss, to 2.84 g/cm^3 in the core, characteristic of rocks with a dioritic bulk composition.

A model of the regional structure of the Kaapvaal Craton was derived by simultaneous interpretation of the gravity and aeromagnetic data sets (Corner et al., 1986a). A feature of this model is the correlation of a highly magnetic layer within the basement granite of the Vredefort Dome, and prominent magnetic anomalies at the craton margin. It is proposed that this magnetic horizon is a continuous mid-crustal marker. A second feature of the model is the interpretation of the Bethlehem gravity high as the result of a crustal arch bringing denser rocks of the lower crust, as observed in the core of the Vredefort structure, towards the surface.

2.3 Other geophysical investigations

2.3.1 Gravity and magnetics

Compilations of gravity and aeromagnetic data covering the Witwatersrand basin and environs have been published by Durrheim et al. (1986) and Corner et al. (1986b).

The Bouguer gravity map (Figure 2.5) is compiled from some 13500 observations. The arc of gravity lows, convex to the north, is due to a ridge of basement granite which forms the perimeter of the main Witwatersrand basin. An inner concentric arc of gravity highs is due to the considerable thickness of dense West Rand shale, Ventersdorp lavas, and Transvaal dolomites filling the main basin. The roughly linear southeastern margin of the basin is marked by a steep gravity gradient. A gravity high, convex to the south, is found in the northeastern corner of the map. This coincides with the Bethal lobe of the Bushveld complex. The prominent northeast trending Bethlehem gravity high (B-B') lies to the southeast of the basin.

The gravity field of the Vredefort structure was studied in detail by Stepto (1979). The 30 mGal Bouguer anomaly found in the core of the Dome is attributed to an increase in density towards the centre, in accord with the "crust on edge" model. The densities used to model the anomaly range from 2.65 g/cm^3 for the Outer Granite-gneiss, to 2.84 g/cm^3 in the core, characteristic of rocks with a dioritic bulk composition.

A model of the regional structure of the Kaapvaal Craton was derived by simultaneous interpretation of the gravity and aeromagnetic data sets (Corner et al., 1986a). A feature of this model is the correlation of a highly magnetic layer within the basement granite of the Vredefort Dome, and prominent magnetic anomalies at the craton margin. It is proposed that this magnetic horizon is a continuous mid-crustal marker. A second feature of the model is the interpretation of the Bethlehem gravity high as the result of a crustal arch bringing denser rocks of the lower crust, as observed in the core of the Vredefort structure, towards the surface.

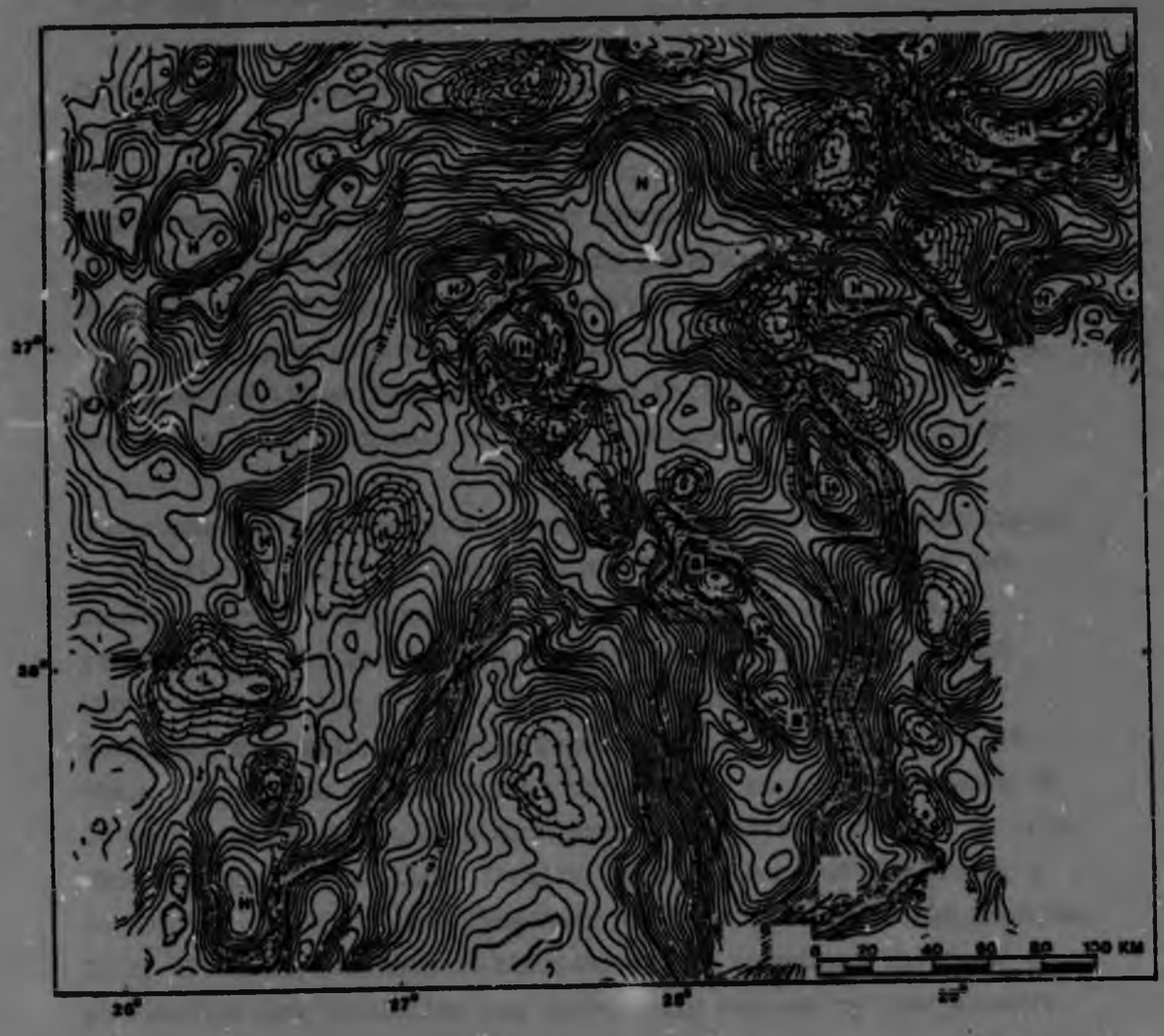


Figure 2.5. Bouguer gravity map of the Witwatersrand Basin and environs (Durrheim et al., 1986). The contour interval is 2 mGal.

2.3.2 Deep electrical soundings

Deep and ultra-deep Schlumberger soundings and magnetometer array studies show that the resistivity structure of southern Africa correlates very well with the tectonic structure (Van Zijl, 1978). Schlumberger sounding results have identified two kinds of terrain depending on the amount of fracturing present: massive terrains, which consist of vast amounts of massive, strongly consolidated, unfractured granitoid material in the form of granitic intrusions, gneisses and migmatites; and fractured terrains, which are associated with intensely deformed, fractured metamorphic rocks.

Two ultra-deep soundings have been conducted on the Kaapvaal Craton (Van Zijl, 1978). The Pietersburg and Dealesville soundings had maximum current electrode separations of 1200 km and 600 km respectively. The Pietersburg sounding showed that the Kaapvaal Craton is a massive terrain, and is characterized by a highly resistive zone which has an average resistivity of about 100 000 Ohm.m and extends downwards from the surface to a maximum depth of 10 km. It is underlain by a moderately resistive (5 000 Ohm.m) zone, which is some 25 km thick. Finally, near the base of the crust, a conductive (50 Ohm.m) zone has been detected (see Figure 14 from Van Zijl, 1978). In the case of the Dealesville sounding, the depth of penetration and resolution was drastically reduced by the presence of conductive Karoo sediments. The sounding showed a moderately resistive crust (3000 - 17 000 Ohm.m), beneath which an extremely conductive layer was found to exist (Van Zijl et al., 1976).

In contrast, the Limpopo and Damara Mobile Belts are fractured terrains. This is manifested by the presence of a moderately resistive zone with an average resistivity of 5000 Ohm.m extending from the surface to a depth of 25 to 30 km, with the conductive zone at the base of the crust. The Namaqua-Natal Mobile Belt exhibits the characteristics of a fractured terrain only in its central core.

Van Zijl (1978) considers the moderately resistive zone to be laterally continuous beneath massive and fractured terrains, and the

moderate resistivity to be indicative of free water. He attributes the conductive zone to hydration, suggesting that serpentinite (hydrated mantle rock) could account for its electrical properties.

2.3.3 Heat flow

Jones (1988) presents heat flow data from the central Kaapvaal Craton. The mean heat flow for the Witwatersrand Basin is 51 mW/m^2, which is higher than the mean heat flow for Archaean cratons. The extra heat (ca. 7.5 mW/m^2) is largely produced in the supracrustal rocks, resulting in a subsediment heat flow of ca. 43.5 mW/m^2. Measurements from the granitic basement exposed within the Vredefort Dome allow the contribution of the crust beneath the Basin to be estimated at ca. 26.5 mWm^{-2}. When combined with the contribution from the supracrustal rocks, a total crustal contribution of 34 mW/m^2 is indicated. The heat flux through the Moho is estimated to be 17 mW/m^2.

Measurements within the basement granites on the northwestern rim of the basin (Hartebeesfontein and Ventersdorp Domes) yield an abnormally low mean heat flow of 33 mW/m^2, probably indicating a smaller radiogenic contribution from the crust below the domes. If erosion was responsible for the removal of a radioactive layer, this must have occurred before the extrusion of the Dominion lavas (Jones, 1988, p 3255).

The lithospheric temperature profiles derived from the geothermal data are in concord with P-T regimes inferred from kimberlite inclusion studies. The correlation between crustal antiquity, low heat flow and distribution of diamondiferous kimberlites is best explained by differences in lithospheric structure: the lithosphere beneath the Craton lies in the stability field of diamond, thus kimberlites tapping it may be fertile; while the lithosphere in mobile belts lies within the graphite field, hence kimberlites are barren (Jones, 1988).

3. MINE TREMORS - THE SEISMIC ENERGY SOURCE

Explosives are used as the seismic energy source in most deep seismic sounding experiments. In this study I have made use of mine-tremors induced by deep-level mining. The use of tremors has several advantages: it is relatively cheap as no shot holes have to be drilled or explosives expended; a station may be occupied until an adequate number of tremors are recorded; and the large amount of shear energy produced in addition to compressive energy allows additional analyses to be performed. Unfortunately some difficulties also arise from the use of tremors: the source location and origin time are imperfectly known; the source is variable as tremors with a range of magnitudes and source mechanisms are recorded; the source region can be several hundred meters in extent; and the experiment takes a longer period to complete. In this chapter results of mine-tremor studies pertinent to the deep seismic sounding experiment are discussed.

3.1 Mining induced seismicity

A major hazard of deep-level gold mining in the Witwatersrand Basin is the violent failure of stressed rock in the vicinity of mining operations, leading to considerable loss of life and damage to mine workings (Malan, 1984). Mining induced seismic events range in magnitude from -6 to 5 on the Richter Scale. The term "mine tremor" is used to describe the larger events, and "rockburst" the violent disruption of rock due to a seismic event (Van den Heever, 1982, p 1).

The first seismological investigation of Witwatersrand mine tremors commenced in the 1930's using a surface network of seismic recorders (Gane, 1939). It was discovered that most tremors happened shortly after the time of underground blasting (Gane et al., 1946), and that the foci of most tremors were close to actively mined areas (Gane et al., 1952).

The first underground seismic network, comprising a three-dimensional array of seismometers, was installed in 1960 at the ERPM

mine near Boksburg with the aim of learning more about the relationships between rock mechanics and seismicity. It was shown that the majority of seismic events have their focus within tens of metres of advancing longwall mining faces (Cook, 1963). Since then networks have been installed in deep-level mines in all the major gold fields. The purpose of the seismic networks are: rapid and reliable location of the source of seismic events allowing inspection and/or rescue; identification of areas of anomalous seismicity as an aid to mine planning; and research so as to improve event locations and mine planning (Spottiswoode, 1986).

3.2 Location, origin time and local magnitude

A good knowledge of the location and origin time of the seismic event is important in the compilation of record sections. These were obtained either from the South African Seismological Network (SASN), or from mine networks.

(a) South African Seismological Network (SASN)

The SASN consists of 24 stations distributed throughout South Africa, and at Windhoek. Data are published monthly in the Seismological Bulletin produced by the S A Geological Survey (Fernandez et al., 1986, 1987, 1988). Regional events which produce good quality P-wave arrival times at a minimum of four stations are located using the "space-time" method of Lomnitz (1977), which involves iterative least-squares processing. All other regional events are evaluated for epicentral distance and local magnitude only. In reducing ground-motion values to local magnitudes, distance corrections are applied (Guzman, 1978). Raw data for distant events is presented without further processing.

The arrival times of the P- and S-waves are read with an accuracy of 0.1 s at best. Mine tremors with magnitudes greater than 2.0 are usually recorded at a sufficient number of stations for a location and origin time to be calculated. The focal depth of events from South African goldfields is fixed at 2 km in the calculation. The location, origin time and magnitude are reported in the Bulletin,

together with the standard deviations of each of these parameters. For a typical mine tremor, the standard deviations of the source parameters are: location ±5 km, origin time ±0.5 s, magnitude (M_L) ±0.15.

(b) Mine networks

The mine seismograph networks have the capability to locate hypocentres within an uncertainty of 35-50 m, reporting the location relative to the mine coordinate system (Spottiswoode and McGarr, 1975, p 93). Generally the mine networks do not run on absolute time. For this experiment accurate clocks were constructed and linked to the mine networks at Klerksdorp, ERPM and the Far West Rand.

3.3 Source parameters

The Fourier spectra of the displacement amplitudes of earthquakes, as measured in the far-field, are found to attain a constant low frequency value (S_0) which is proportional to the seismic moment (M_0). M_0 can be calculated using either the P or S body wave using the following equations:

$$M_0 = S_0 \frac{.4(\pi)\rho(v_p^3)R}{f(\theta,\phi)_p} 10^{-7} \quad \text{Nm} \qquad (3.1)$$

$$M_0 = S_0 \frac{.4(\pi)\rho(v_s^3)R}{g(\theta,\phi)_s} 10^{-7} \quad \text{Nm} \qquad (3.2)$$

where ρ = density (g/cm^3),

v_p, v_s = compressive and shear velocity (km/s)

S_0 = low frequency asymptote (cm.sec)

R = distance (km)

Median values for the radiation factors for a double-couple source were determined from 1000 values of $f(\theta,\phi)$ and $g(\theta,\phi)$ randomly distributed on the focal sphere. The median value of $f(\theta,\phi)$ is 0.39, and for $g(\theta,\phi)$ is 0.57 (Spottiswoode and McGarr, 1975, p. 103).

The best empirical fit of data from ERPM mine relating seismic moment M_0 to magnitude M_L is given by the following relationship

$$\log_{10} M_0 = 10.7 + 1.2\, M_L \qquad (3.3)$$

where M_0 is in Nm (Spottiswoode and McGarr, 1975, p 106).

The relationship of Gutenburg and Richter (1956) relating magnitude and energy

$$\log_{10} E = 4.8 + 1.5\, M_L \quad \text{Joule} \qquad (3.4)$$

was found to fit the ERPM data reasonably well (Spottiswoode and McGarr, 1975, p 101).

The corner frequency f_0 is defined by the intersection of the high- and low-frequency asymptotes of the displacement spectrum. At frequencies above the corner frequency, the spectra diminish as f^{-k}. Ground velocity rather than displacement is recorded by the seismometers used in this experiment. As velocity is simply the derivative of the displacement, the theoretical spectrum is transformed in a straightforward manner: instead of a flat low frequency spectrum, there is a 6 db per octave increase in amplitude up to the corner frequency, after which the spectrum decays at a rate of f^{-k-1} (Peberdy, 1986, p. 58). For the ERPM data the value of k was found to be 2 and 3 for the compressional and shear waves respectively (Spottiswoode and Mogarr, 1975, p 98). For ERPM events with M_L = 2-3 the corner frequency was found to be between 5 and 15 Hz (Spottiswoode and McGarr, 1975, p 110). This is in good agreement with the observation of Cook (1963) that the larger tremors radiated energy at about 10 Hz.

Figure 3.1 shows normalized velocity density spectra of four tremors, ranging in magnitude from 2.78 to 3.68, recorded at a station situated some 65 km southeast of the Klerksdorp goldfield source region. All events have a corner frequency of ca. 17 Hz, although the larger events have relatively more power at the lower frequencies. Although source parameters have not been extensively studied in this project, initial results confirm the conclusion reached by Peberdy (1986) that effects due to local geology dominate the shape of the velocity density spectrum.

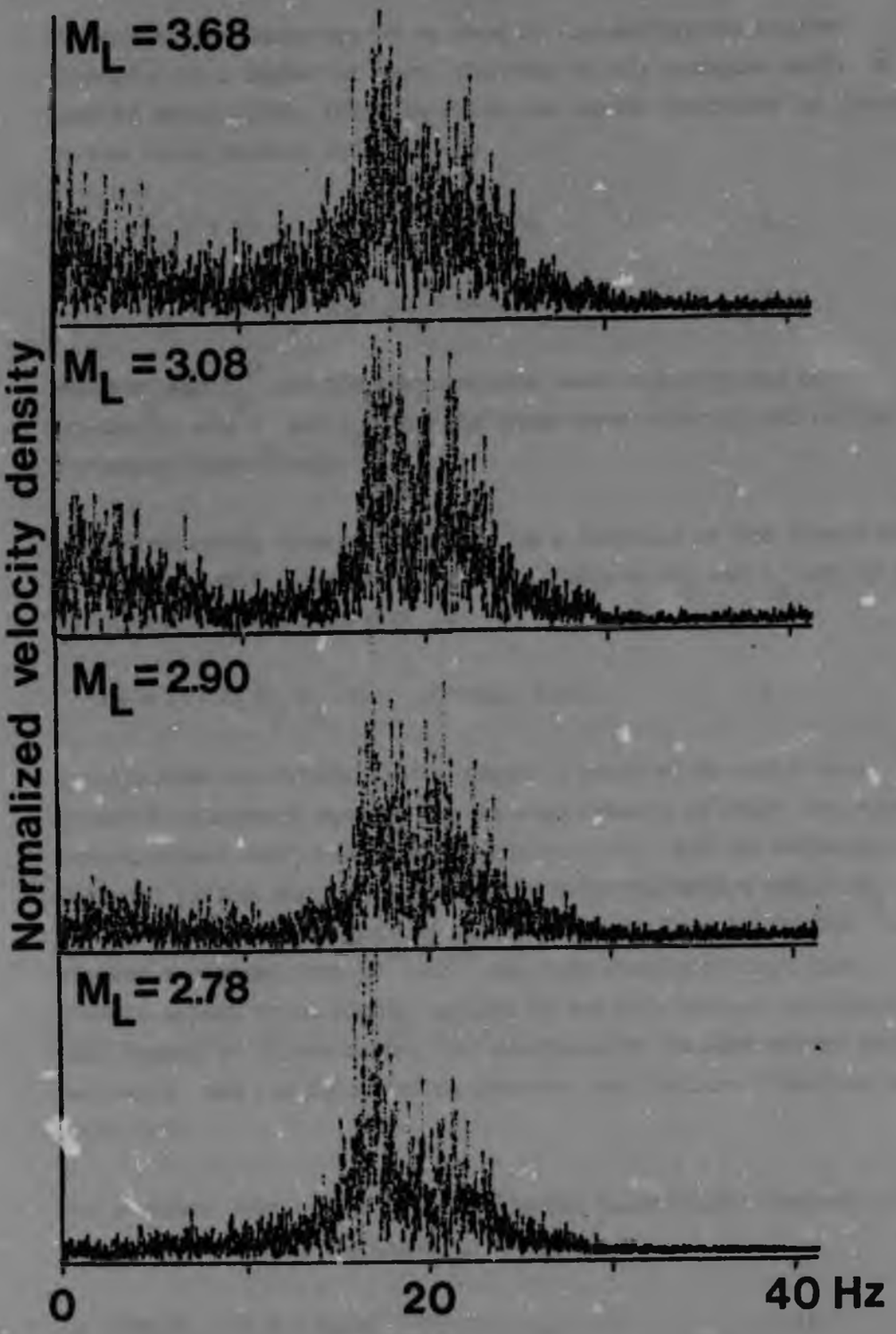


Figure 3.1. Normalized vertical component velocity density spectra of Klerksdorp goldfield tremors recorded at a station in the Vredefort Dome (about 65 km southeast of the source region).

The corner frequency may be related to the earthquake source dimension in a number of ways. The most widely accepted model is that of Brune (1970, 1971) in which the corner frequency is related to the fault surface radius r_0 by

$$r_0 = 1.97.v_p/(2.pi.f_0^p) \text{ meters} \quad (3.5)$$

$$r_0 = 2.34.v_s/(2.pi.f_0^s) \text{ meters} \quad (3.6)$$

where v_p and f_0^p are the compressional wave velocity and corner frequency, and v_s and f_0^s are the shear wave velocity and corner frequency respectively.

The relationship between M_0 and f_0 is a function of the stress drop across the fault plane at the time of rupture. M_0 and r_0 may be used to calculate the stress drop ds

$$ds = (7/16)\, M_0/r_0^3 \text{ Pa} \quad \text{(Brune, 1971).} \quad (3.7)$$

Spottiswoode and McGarr (1975) report a study of P- and S-wave ground displacement spectra for 24 mine tremors at ERPM. The spectra were analysed using the model of Brune (1971), and its extension by Tsifunic (1972). For the events (M_L = 0-3) the source radius r_0 ranged from 50-500 m, and the stress drops ds from 0.5-5 MPa. The moments M_0 ranged from 10^{11}-10^{14} Nm. They concluded that mine tremors appear to be highly similar to natural crustal earthquakes with regard to stress drops, the relationship between moment and magnitude, and the relationship between rock failure dimension and magnitude.

For a stress drop of 5 MPa the following relationship between corner frequency and local magnitude is obtained

$$\log_{10} f_0 = 2.3 - 0.5M_L \quad (3.8)$$

(Peberdy,1986).

The pulse duration T_d is approximately equal to the duration of the

rupture process, which is again proportional to the source dimension and corner frequency. This may be expressed by

$$T_d = k/f_0 \text{ s} \quad \text{where k is approximately 1} \qquad (3.9)$$

(Spottiswoode, 1984, p 31).

A source mechanism study of 11 mine tremors (M_L = 1·2) at Blyvooruitzicht Gold Mine in the Far W Rand was conducted by Spottiswoode (1984). The data were consistent with zero volume change, and were interpreted as shear failures. Fault-plane solutions suggested slip on shear zones striking parallel to the advancing face, or on either either of two dykes cutting across the face.

3.4 Source mechanism and radiation pattern

An explosive source will produce dominantly compressive waves with a radiation pattern concentric about the source (Evernden et al., 1986, p 145). In contrast, the seismic energy radiation pattern produced by an earthquake double-couple source mechanism (i.e. no rotation of the fault plane) produces both compressional and shear energy. One nodal plane of the P-wave pattern coincides with the fault plane; while the nodal planes of the S-wave pattern are at 45° to the fault plane. This implies that the maximum compressive displacement coincides with minimum shear displacement, and vica versa (Kasahara, 1981, p 36). In a study of 24 mine-tremors from ERPM the ratio of P- to S-wave energy was found have a median of 0.18 with a range 0.005 to 1.1 (Spottiswoode and McGarr, 1975, Table 1).

The radiation pattern for a tremor is clearly far more complicated than the concentric pattern produced by an explosive source. The variation of amplitude with distance from the source is not just a function of the raypath and site effect, but also of the orientation of the fault plane and the direction of slip of the particular tremor. However, in practice the radiation pattern is not generally

uniform for the entire rupture process of a tremor, and so the actual occurrence of nodal planes is unlikely (Spottiswoode and McGarr, 1975, p 103). Consequently an averaging of the amplitude of specific phases rather than a measurement of peak amplitude, or an averaging of many events, is considered likely to give more reliable results.

If a seismic event originates in a region with dimensions much less than the distance to the observation points, it may be represented as a point source. If it is considered to be due to slip on a fault, only four independent parameters are needed to describe the source: the strike and dip of the fault, the direction of slip within the fault, and the seismic moment M_0 (Spottiswoode, 1984, p 31).

3.5 Magnitude distribution

During the course of the deep seismic sounding experiment it was found that events with $M_L > 3$ were generally required to produce a satisfactory signal to noise ratio at distances greater than 200 km. In order to estimate the period each station would have to be occupied, the relationship between the magnitude and frequency of occurrence of tremors in the various mining regions was assessed.

The classic empirical relationship of Richter (1958)

$$\log_{10} N = a - bM$$

describes the frequency of earthquakes (N) with magnitude greater than or equal to M, where a and b are constants. The cumulative distribution of magnitudes for seismic events for various South African gold mining districts for the period January 1985 to May 1988 is shown in Figure 3.2. It is apparent that the Far W Rand is the most seismically active area. The Klerksdorp area releases almost as much seismic energy, but tends to have more large events. The Rand and O. F. S. gold fields have relatively low levels of seismic activity.

It has been established that the level of mine-tremor activity is

related to the volume of rock removed and the depth of mining (McGarr, 1976). The change in gravitational energy due to mining operations can be estimated by the product of tonnes mined and the mean rock-breaking depth. Calculations show that less than 1% of the total gravitational energy change due to mining is radiated in the form of seismic energy (McDonald, 1982, p 67; McGarr, 1976, p 1490). This suggests that most of the energy changes associated with mining are non-violent in nature.

The relationship between tonnes mined and seismic activity for the different gold fields for the period 1971-1979 is shown in Table 3.1. While seismic activity and tonnes mined are broadly related, it is also clear that this cannot completely explain the variation between the gold fields. For example, the O F S and Klerksdorp goldfields had similar levels of seismicity in spite of the fact that almost twice as much ore was mined in the O F S during the period under consideration.

There is evidence to suggest that the geological structure of a particular district plays a role. The Far West Rand has a very high level of seismic activity. It is possible that the dewatering of the overlying Transvaal dolomites during the early 1970's could explain the higher level of seismicity during this time (McDonald, 1982, p 87). Mining operations in the Klerksdorp and O. F. S. gold fields are carried out at similar depths, and the geological structure is also similar. The larger events tend to be associated with geological discontinuities such as faults and dykes (Arnot,1991; Potgieter and Roering, 1984; Gay et al, 1984; Lawrence, 1984). These large events release by far the greatest proportion of energy. At ERPM, the only mine of significance on the East Rand during this period, seismic events are recorded in back areas, stabilising pillars and geological discontinuities, the latter generally hosting most of the large events (McDonald, 1982, p 90).

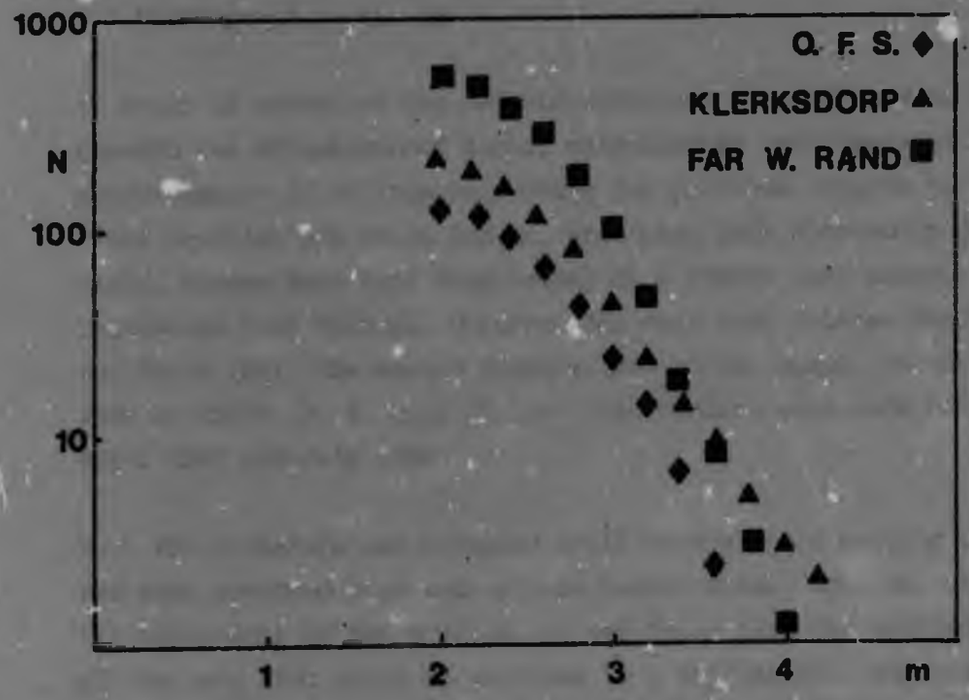


Figure 3.2. Magnitude-frequency distribution for mine tremors in Witwatersrand Basin gold fields for the period January 1985 to May 1988. N(m)=cumulative number of events of magnitude m per year. (Fernandez et al, 1988).

Table 3.1. Tonnes mined and seismic activity for South African gold fields for the nine year period 1971-1979. The tonnage and number of events are shown as an annual average. Data compiled from McDonald (1982).

Number of seismic events			Gold Field	Tonnes mined
M_L 2.0-2.9	3.0-3.9	> 4.0		
100	19	1	East Rand	7.20
541	113	7	Far W Rand	18.55
112	53	2	Klerksdorp	14.11
87	57	1	O F S	24.44

4. DATA ACQUISITION, PROCESSING AND DISPLAY

4.1 Seismograph locations

In order to establish the seismic structure of the Kaapvaal Craton beneath the Witwatersrand Basin, seismographs were deployed at approximately 10 km intervals along two profiles (Figure 4.1). The first profile, 260 km in length, stretches from Klerksdorp gold field, across East Rand Proprietary Mine (ERPM) near Boksburg, and terminates near Witbank. Observations were made between March 1986 and March 1987. The second profile, 230 km in length, stretches from ERPM to the O. F. S. gold fields. Observations were made between April 1987 and July 1988.

Each field station was occupied until several good quality events had been recorded from each of the source areas, most importantly the end-points of the profile. It was found that the maximum number of stations that could be serviced in a day was six, especially when the stations were distant from Johannesburg. The data recovered from six stations also took the best part of a week to replay and digitize. The duration of the experiment was far longer than initially anticipated due to chronic unreliablity of the old recording systems. The tape transport was particularly prone to malfunction, resulting in entanglement of the tape. Stations had to be occupied for up to three months because of the poor data return.

The station locations were plotted on 1:50 000 scale topographic maps. The accuracy of the station coordinates and elevations are estimated to be better than 100 and 10 meters respectively. The bed rock geology was determined from 1:250 000 scale geology maps, and by inspection in the field. The station coordinates are listed in Appendix A.

4.2 Seismometers

At each station one vertical and two horizontal component seismometers, orientated north-south and east-west, were buried in a

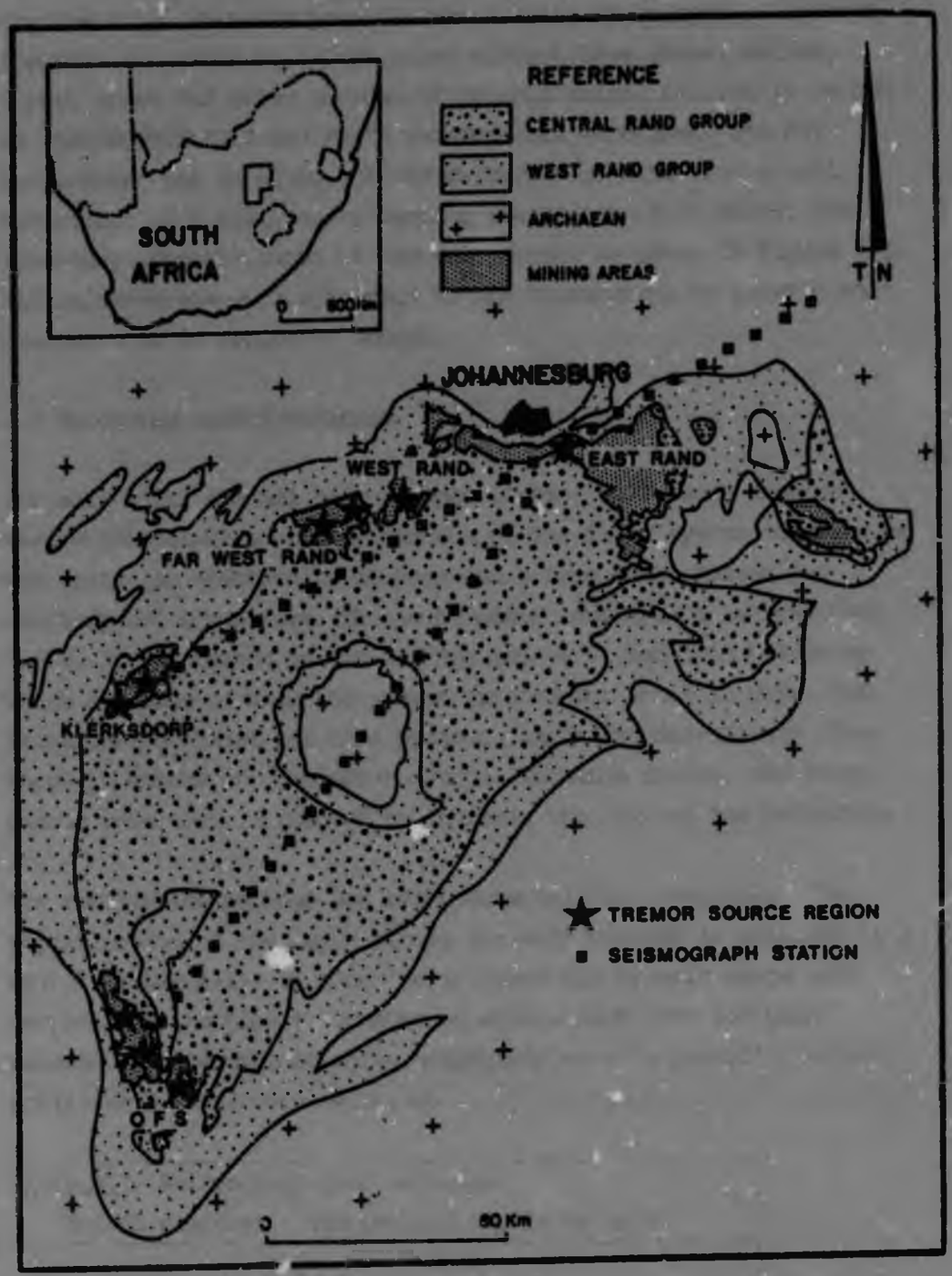


Figure 4.1. Seismograph locations on the Klerksdorp - East Rand - Witbank and East Rand - O F S profiles. Post Witwatersrand Supergroup rocks have been stripped (from Tweedie, 1986).

shallow hole. Wherever possible the station was placed on bedrock. Due care was taken to select sites distant from roads, railway lines, trees and other sources of seismic noise. Critically damped 1 Hz ELECTROTECH EV17 and EV17B seismometers were used. The EV17 seismometer has an output of 347 mV/mm/sec at 2 Hz (for a coil resistance of 5 kOhm, and a damping resistance of 13 kOhm). The frequency response curve of the seismometer is shown in Figure 4.2. The seismometers were connected to the seismograph by twisted pair cables about 20 meters in length.

4.3 Recording instrumentation

Portable multi-channel seismographs (Green, 1973) were used to record the output of the seismometers. The field system consists of two units (an electronics package and a tape deck) housed in weatherproof containers. The total power consumption is less than 7.5 W. It is powered by two 140 Amp.hour 6 V lead-acid batteries, which are able to keep the system running for about 10 days. The batteries purchased for this project started to deteriorate after about 18 months of continuous charge-discharge cycles, and solar panels were then introduced to increase the life of the batteries.

The electronics package has eight external input channels. The amplification of the input signal for each channel is selected by a switch (Table 4.1). In order to increase the dynamic range each geophone was routinely recorded on both a high- and low-gain channel. If the ambient noise conditions made it possible, switch positions 3 and 7 were selected.

Table 4.1. Seismograph gain settings

Switch position	Theoretical amplifier gain
1	1.00
2	1.45
3	4.17
4	17.99
5	54.95
6	177.83
7	457.09

The time for the system is obtained from both a radio and an internal clock. During daylight hours the 10 MHz WWV/ZUO radio signal is recorded whereas the 5 MHz is utilized during the night. The changeover is achieved automatically using the internal clock. The internal clock utilizes a 1 MHz primary frequency which has a stability of 2×10^{-9} s per day, and the clock output is a standard VELA 100 time code. A portable master clock, which is synchronised in the laboratory with the radio time, was also used to provide an absolute time reference. The master clock signal was routinely input on a seismograph channel whenever a station was serviced. The lead or lag of the internal clock could then be determined by digitization and comparison of the master and internal clock signals.

The tape recorder employs a locked loop transport system and a dc motor. With a tape speed of 2.5 mm/s and 35.3 cm tape reels containing 2 800 meters of 12.5 mm tape, the unit runs for 12 days. There are ten tracks on the tape. The outer tracks were generally not used as they are most prone to damage. The routine allocation of the tracks is listed in Table 4.2.

Table 4.2. Routine allocation of tape tracks

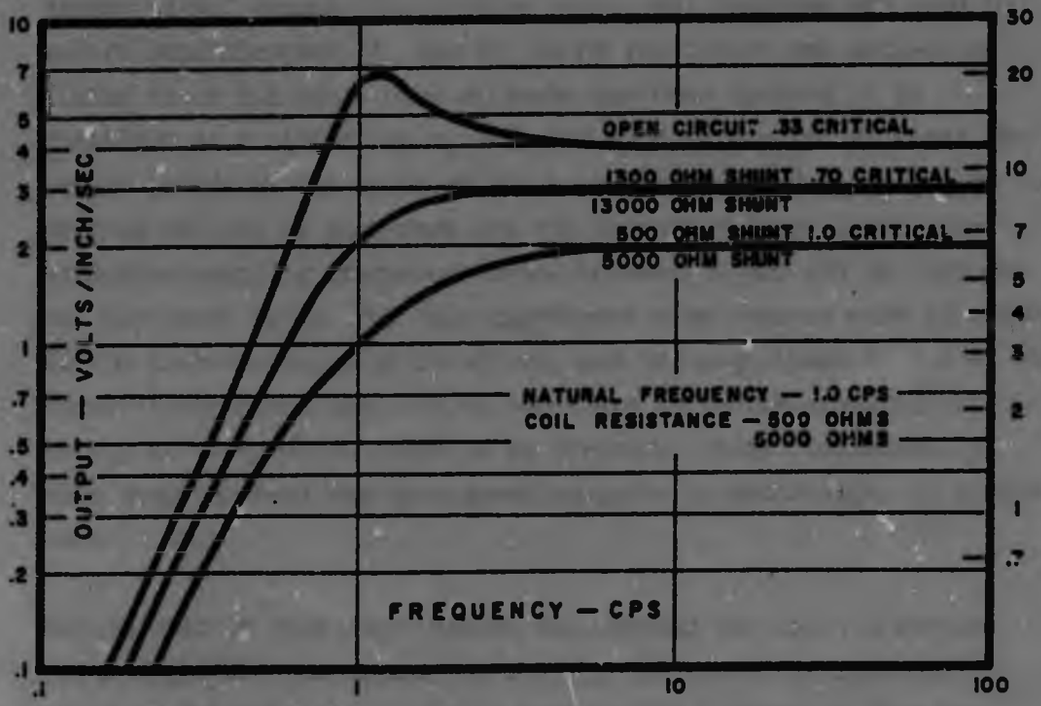
Track	Channel	Gain
1	-	-
2	vertical	low
3	vertical	high
4	N - S	low
5	clock	-
6	radio	-
7	N - S	high
8	E - W	low
9	E - W	low
10	-	-

Visits were made, usually on a weekly basis, to each station. The magnetic tape and batteries were replaced, faulty components repaired or replaced, and a master clock signal recorded on a geophone track to enable later synchronisation of the internal

SPECIFICATIONS

Sensitivity	4.8 volts/inch/second (1.89 volts/cm/sec.) 200 ohm coil (open circuit)
	19.2 volts/inch/second (7.6 volts/cm/sec.) 5000 ohm coil (open circuit)
	.72 volts/inch/second (.28 volts/cm/sec.) 500,000 ohm coil (open circuit)
Available Coil Resistances	200 ohms coil and lower are standard, higher coil resistance values up to 10 megohms available upon special order; exact values being determined in accordance with the preferred damping curves. Consult us for your special requirements.
Damping	Any damping from .35 (open circuit) to 1.0 may be obtained with the 2 shunt damping resistors, the values of which will be largely from the resistance of the coil in all cases.
Tilt Angle	±2° all directions, using leveling screw.
Natural Frequency	1.0 cps ± .025 cycles (calibrated level)
Coil Excursion	.62 cms or more
Mass of Suspension	2700 grams
Size	3½" x 3" x 5½"
Weight	17½ pounds

RESPONSE CURVES



ELECTRO-TECHNICAL LABS DIVISION
MANDREL INDUSTRIES, INC.
A SUBSIDIARY OF AMPEX CORPORATION

Figure 4.2. Frequency response of EV17 and EV17H seismometers.

clock. A log was kept of each visit, noting details of station performance, seismometer channel gain settings and calibration settings.

4.4 Digitization

The field tapes were replayed and digitized in the laboratory. The replay search mode speed is 38 cm/sec, or about 150 times the record speed. At this speed the frequencies of a seismic event are raised to audio frequencies. The signal is monitored both audibly through a loudspeaker, and on an oscilloscope. At the high replay speed a tremor signal sounds like a sharp explosion. Switches are used to select amplification (5, 10, 20, 50 or 100 times) and anti-alias filter (1 or 2.5 kHz). Once an event has been located it is digitized at a slower replay speed of 6.25 cm/sec, or 25 times the record speed. As the speed of the tape decks varied depending on the precise setting of each deck and the battery voltage level, the effective sampling frequency varied between 60 and 100 Hz, but was usually about 80 Hz. For this experiment mine tremors were recorded in the distance range of 20-360 km, and had magnitudes M_L = 2-4. The corner frequencies are 5-15 Hz and there is little significant energy at frequencies above 20 Hz (Peberdy, 1986). Consequently, this sampling rate was considered adequate to avoid aliasing of the data.

During most of 1986 digitization was carried out using a system which digitizes one channel at a time, and wrote the data on standard 9 track tape in IBM360 format with 2 bytes of data per sample and 1024 samples per block. The number of samples and digitization rate were selected by means of switches. An ultra-violet recorder was triggered at the instant replay commenced, with digitization commencing a selected time (usually 0.6 sec) later. The seismometer and clock channels, as well as a signal indicating the start and end of digitization were recorded on the UV-paper. This enabled the time at which digitization commenced, as well as the sampling rate, to be established. A typical record consisted of either 4800, 5600 or 6400 samples, with a record time sampling rate

of 75-85 Hz. The start and end of digitization could be determined to better than 40 ms.

A PC-based analogue to digital conversion system was introduced toward the end of 1986. A PC-26™ A-D board was installed in an CW16XT™ microcomputer. Three seismometer channels and the clock could be digitized concurrently. Generally a real time sampling rate of 2kHz per channel was selected. As the replay speed while digitizing is about 25 times the record speed, this typically yielded an effective sampling rate of about 80 Hz and record length of 80 s. The digitized signal is written in binary format onto the hard disk. Subsequently the data was transferred to 360 kbyte floppy disks.

The master clock and calibration signal were recorded on tape each time a station was serviced. These were digitized, together with all tremors with a reasonable signal to noise ratio. The total amount of clock, calibrate and seismic data recorded on floppy disk during this experiment is in excess of 120 Mbytes. In order to process and plot the digital records, the binary data is converted to ASCII format.

The phase difference between the internal seismograph clock and the master clock was determined by examining the ASCII file. The initiation of a time pulse was easy to detect in the series of digitized voltages. Usually the seismograph internal clock was triggered with a delay of about 0.1 s, this being the operators reaction time (Figure 4.3). The time at which the digitization of a particular record commenced, and the digitization rate were also determined by inspection of the ASCII file using a text processing programme such as PcWrite™. The digitization rate was determined by counting the number of samples in the first 10 s of the record.

The accuracy of timing is estimated to be equal to about twice the sampling interval i.e. about 25 ms for a record sampled at 80 Hz. This is far smaller than the errors due to uncertainties in the origin time and epicentre of the mine tremors.

4.5 Calibration and system response

In order to be able to calculate the seismometer output and hence the ground velocity, it was important to establish the effect on the input signal of the seismograph amplifiers, the magnetic tape (several types were in use), the replay amplifiers and the digitization process. The calibration procedure consists of feeding a signal of known amplitude and frequency into the seismograph in place of a seismometer. The seismograph generates its own high- and low-level calibration signal. The internal calibrator generated a 10 Hz signal with peak-to-peak double amplitudes of 5mV and 500 mV. These were recorded on each seismometer channel at both a high and low gain setting. As the level of the internal calibration signal could be affected by the battery voltage, an external calibration signal was also sometimes recorded.

Calibration of the identical system has been carried out by Spottiswoode and McGarr (1975, Fig 2) and Peberdy (1986). The recording system has a fairly flat response in the frequency range of interest (1-20 Hz). The system response is shown in Figure 4.4.

4.6 Noise removal

Standard Fourier frequency domain band-pass filters were used to remove noise from the data. All the signal processing was carried out on a CW16AT microcomputer. A time series analysis programme was written in Fortran using the Fast Fourier Transform subroutine NLOGN from Robinson (1967, p 63).

The seismograms displayed in the record sections have all been filtered using a passband that rises from zero at 0.5 Hz to unity at 2 Hz, remains at unity to 8 Hz and decays to zero again at 12 Hz. The flanks of the frequency domain filter have the shape of a cosine function (between 0 and pi). A data window of 4096 samples was filtered. The effect of the bandpass filter on a noisy seismogram is shown in Figure 4.5.

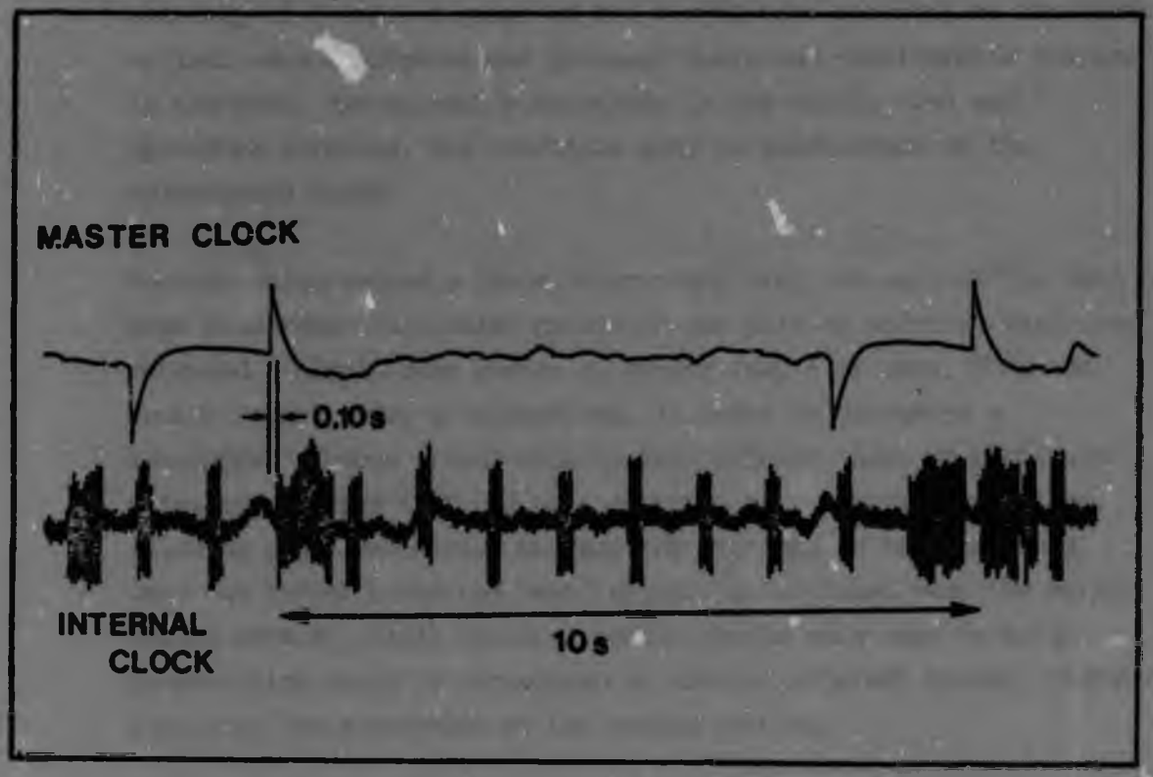


Figure 4.3. Synchronisation of the master and internal clocks.

4.7 Compilation and display of record sections

For a particular profile each source region was considered in turn. The reduced travel-time for each event for which a origin time and epicentre location was available was calculated using a reduction velocity of 6 km/s. A graph of the travel-time residual of the first arrival versus distance was plotted. There was considerable scatter in the data, due primarily to errors in the origin time and epicentre location, but sometimes also to malfunction of the seismograph clock.

Records which showed a large discrepancy with the bulk of the data were discarded. Particular attention was paid to stations which had recorded a significant number of events (say 6 or more) from the source region under consideration, in order to determine a meaningful average travel-time to this station. Also of particular value were events that had been recorded at two or more stations, allowing phase velocities between the stations to be determined. Once the travel times had been reliably established over the entire record section, small residual static shifts were made to align phases which could be correlated on several adjacent traces, thereby enhancing the appearance of the record section.

Records with good signal to noise ratios and showing good definition of the various phases were selected for display. Where possible, the vertical component was used. In order to avoid cluttering the record section, seismograms were chosen for plotting at regular distance increments. The seismograms were bandpass filtered, and each trace normalized.

Computer programmes were written to display the record sections. The seismograms were plotted using either a Hewlett-Packard 7475A pen plotter, driven by a programme written in GW-Basic and HPGL (Hewlett Packard Graphics Language); or on a Versatec electrostatic plotter driven by a Fortran programme using the Uniras graphics package.

Each record section was produced at three time scales: a 50 s window showing the entire seismogram using a reduction velocity of 6 km/s;

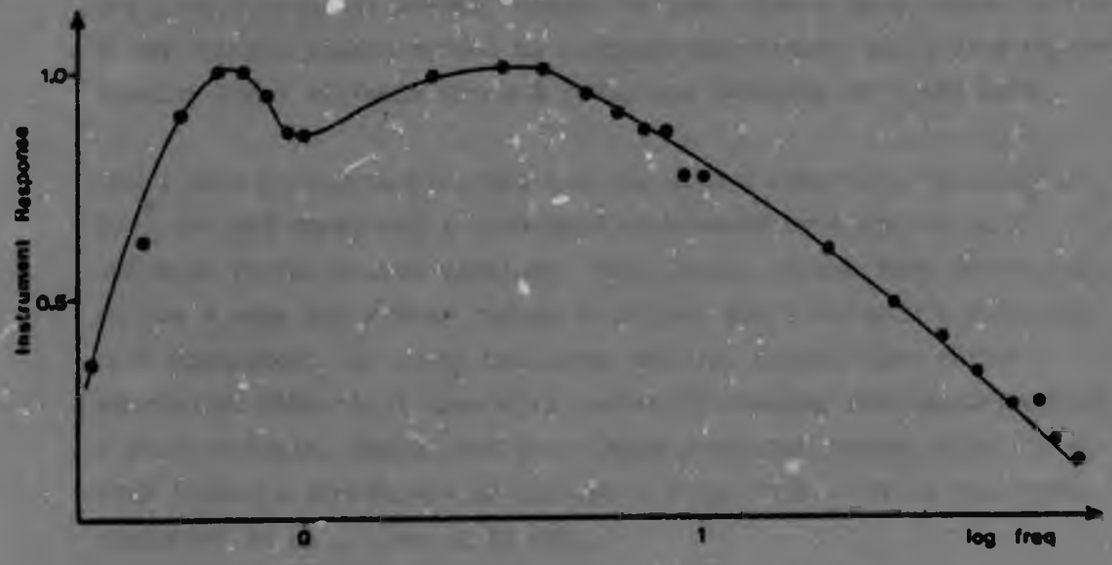


Figure 4.4. Measured velocity amplitude response of the recording system (from Peberdy, 1986).

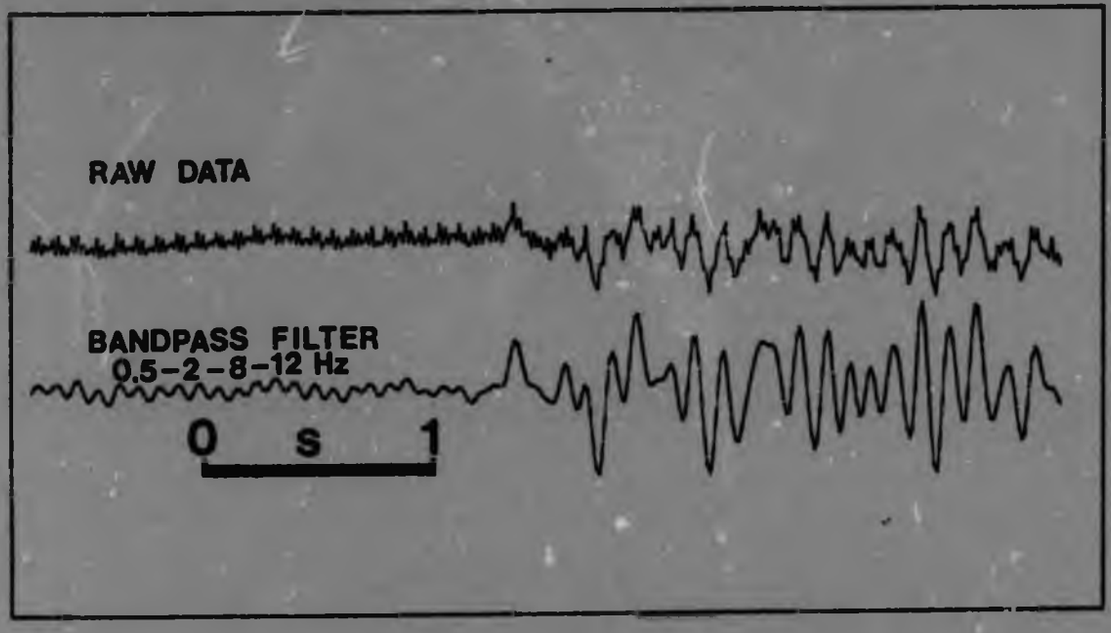


Figure 4.5. Filtration of a noisy seismogram. In this case the bandpass filter has removed high and low frequency noise, but not a noise component in the passband. The filtered trace is plotted with an expanded amplitude scale.

a 12 s window showing the P arrivals using a reduction velocity of 6 km/s, with arrivals having velocities less than 4 km/s muted, as the S and surface phases tended to dominate the trace; and a 24 s window showing the S arrivals using a reduction velocity of 3.464 km/s.

The S wave record section was plotted with a reduction velocity of $6/3^{\frac{1}{2}}$ (=3.464 km/s) and a time axis compressed by a factor of $3^{\frac{1}{2}}$ relative to the P wave sections. This format allows easy comparison of the S wave and P wave record sections: for a Poisson's ratio of 0.25 throughout the crust and upper mantle, travel-time curves calculated from the P wave will perfectly overlay the corresponding S wave arrivals. Deviations from these predicted travel time curves thus indicate deviations of Poisson's ratio from 0.25 in the crust (Holbrook et al., 1988, p 12 088).

The entire route followed from transducer to record section is summarized in Figure 4.6.

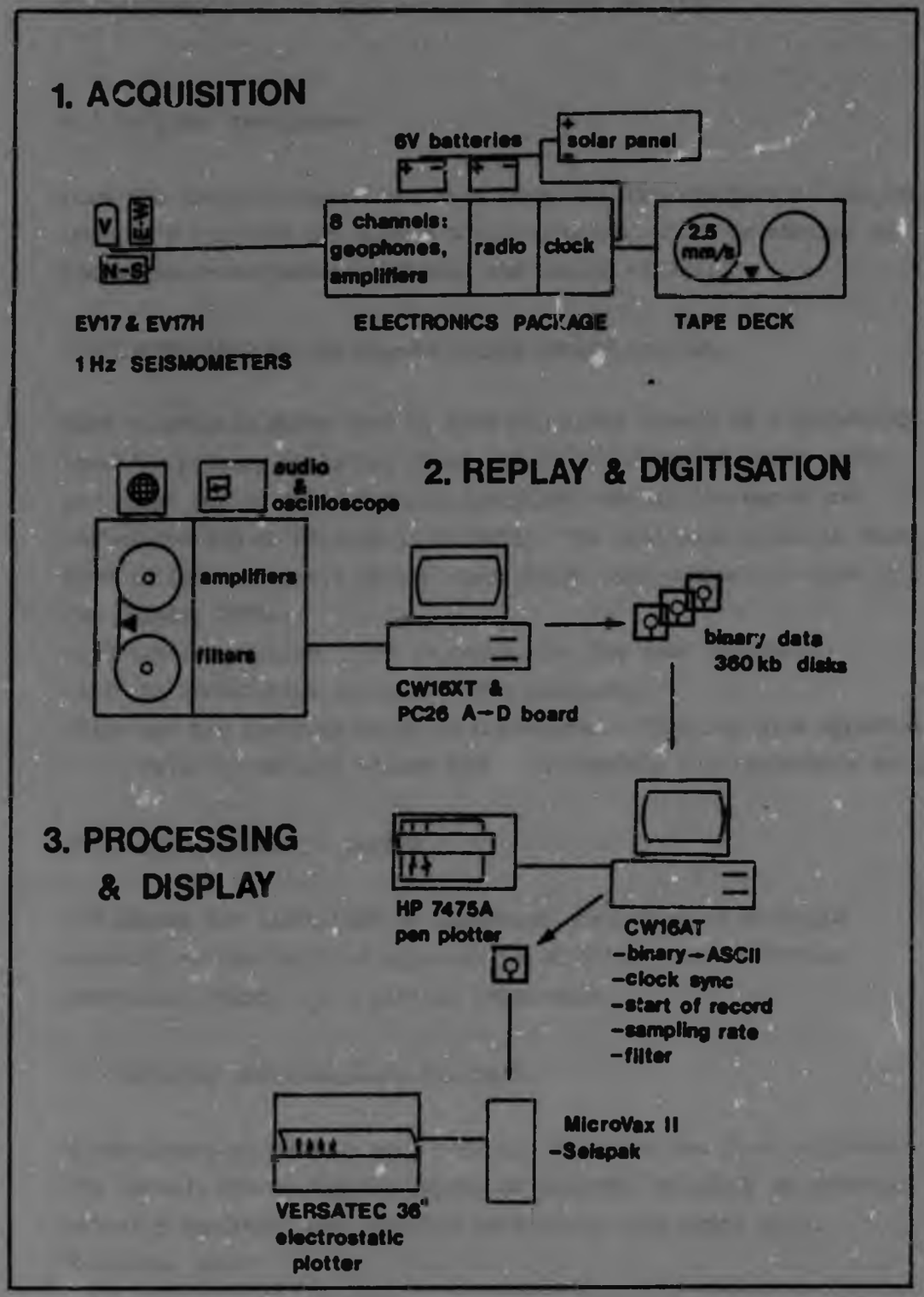


Figure 4.6. Flow diagram showing the process of producing a record section.

5. INTERPRETATION OF DEEP SEISMIC SOUNDING PROFILES

5.1 Analysis techniques

Once the record sections had been compiled, the analysis of the data generally followed the scheme outlined below, which is similar to the sequence suggested by Mooney and Walter (1987).

(a) Correlation of the phases in the record section.

Each seismogram shows more or less prominent onsets of a number of specific pulses, including those due to the direct P and S waves, and those due to reflection at interfaces within the earth and refraction due to changes in velocity. The following criteria were used to identify "wave groups" associated with a specific type of ray (Giese, 1976a):

(i) the travel-time curve is continuous for some distance;
(ii) the travel-time increases with distance;
(iii) and the quantity dx/dt is a continuous function with apparent velocity showing values within a possible and reasonable range.

(b) Identification of phases

The phases are identified as refracted, reflected or multiple arrivals on the basis of apparent parallelism with an earlier traveltime branch, or a similar observation.

(c) Interpretation of first arrivals

Slope-intercept methods were used to interpret the first arrivals. The methods assume dipping layers of constant velocity or constant velocity gradient, and velocity increasing with depth (e.g. Slotnick, 1958)

(d) One-dimensional model

One-dimensional (1-D) interpretation of first and secondary arrivals using the Herglotz-Wiechert approach and methods described by Slichter (1932) and Giese (1976b). These methods are used to interpret reflected as well as refracted arrivals, and can incorporate velocity gradients and inversions. The album of synthetic seismograms calculated for a range of velocity transitions by Braile and Smith (1975) also proved very useful in interpreting the nature of seismic transition zones.

1-D ray tracing was used to produce synthetic record sections for previously proposed models of the seismic velocity structure of the Craton. In this study a 2-D Raytracing/Synthetic seismogram computer programme was used to carry out forward modelling. The programme RAYAMP-PC was written by D. Crossley of the Geophysics Laboratory, McGill University and implemented on a CW16AT™ microcomputer. It is based on the programme RAYAMP written at the University of British Columbia (Spence et al., 1984). The velocity structure is represented by large polygonal blocks, within which the velocity gradient is uniform and of arbitrary orientation. Amplitudes of reflected and refracted waves are determined using zero-order asymptotic ray theory; and head wave amplitudes by means of first-order asymptotic ray theory.

A reduction velocity of 6 km/s has been used to produce the synthetic record sections. Each trace has been normalized to the largest amplitude event on it. The following notation is used to refer to prominent branches of the traveltime curves:

P_1 - direct wave travelling in upper layer
P_I - head wave arising at the top of the second layer
$P_I P$ - reflection from top of second layer
P_n - head wave arising at the Moho
$P_m P$ - reflection from Moho

(i) Single-layer crust

Gane et al. (1956) recorded tremors on profiles radiating to the

north, south, east and west of the Central Rand goldfield, and did not find any evidence for a systematic variation of velocity with azimuth. Their best mean value for v_P in the crust is 6.18 km/s, with Moho at a depth of 35.1 km and a sub-Moho velocity of 8.27 km/s. They regard the occasional appearance of second phases as being due to energy following paths of low attenuation or having fortuitous focusing properties (Gane et al., 1956, p. 312).

A linear increase in velocity according to

$$v_P = 6.18 + 0.003z$$

with z in km takes into account the experimentally predicted increase in velocity with depth for granitic rocks (Birch, 1958) and was incorporated into the model. This predicts a velocity of 6.29 km/s at at a depth of 35 km. The synthetic record section for this model is shown in Figure 5.1A. The critical distance is ca. 90 km, and the cross-over distance is ca. 185 km. The large velocity discontinuity at the Moho gives rise to strong sub- and super-critical $P_m P$ reflections.

(ii) Two-layer crust

The identification of a mid- or lower-crustal layer with an intermediate seismic velocity presents difficulties, as the intermediate layer rarely produces a first arrival for a plausible range of models (Hales and Sacks, 1959, p. 32).

Willmore et al. (1952, p. 68) observed tremors in the western Transvaal, and regarded the second P phases at offsets of 200-290 km to be too early to be due to the direct arrival. They suggested the existence of a lower-crustal layer with an intermediate seismic velocity (see Table 5.1). Their model corresponds closely to a crust consisting of layers of granite and gabbro (Birch, 1958, p. 168). A profile stretching east of Johannesburg to the Indian Ocean also provided evidence for an intermediate layer (Hales and Sacks, 1959). The second arrivals recorded at offsets of 180-300 km were regarded as arriving too early to be ascribed to the direct arrival, and were interpreted as coming from a layer with a velocity of about 7km/s. Two possible models proposed by Hales and Sacks (1959, p. 28) are tabulated below (Table 5.1).

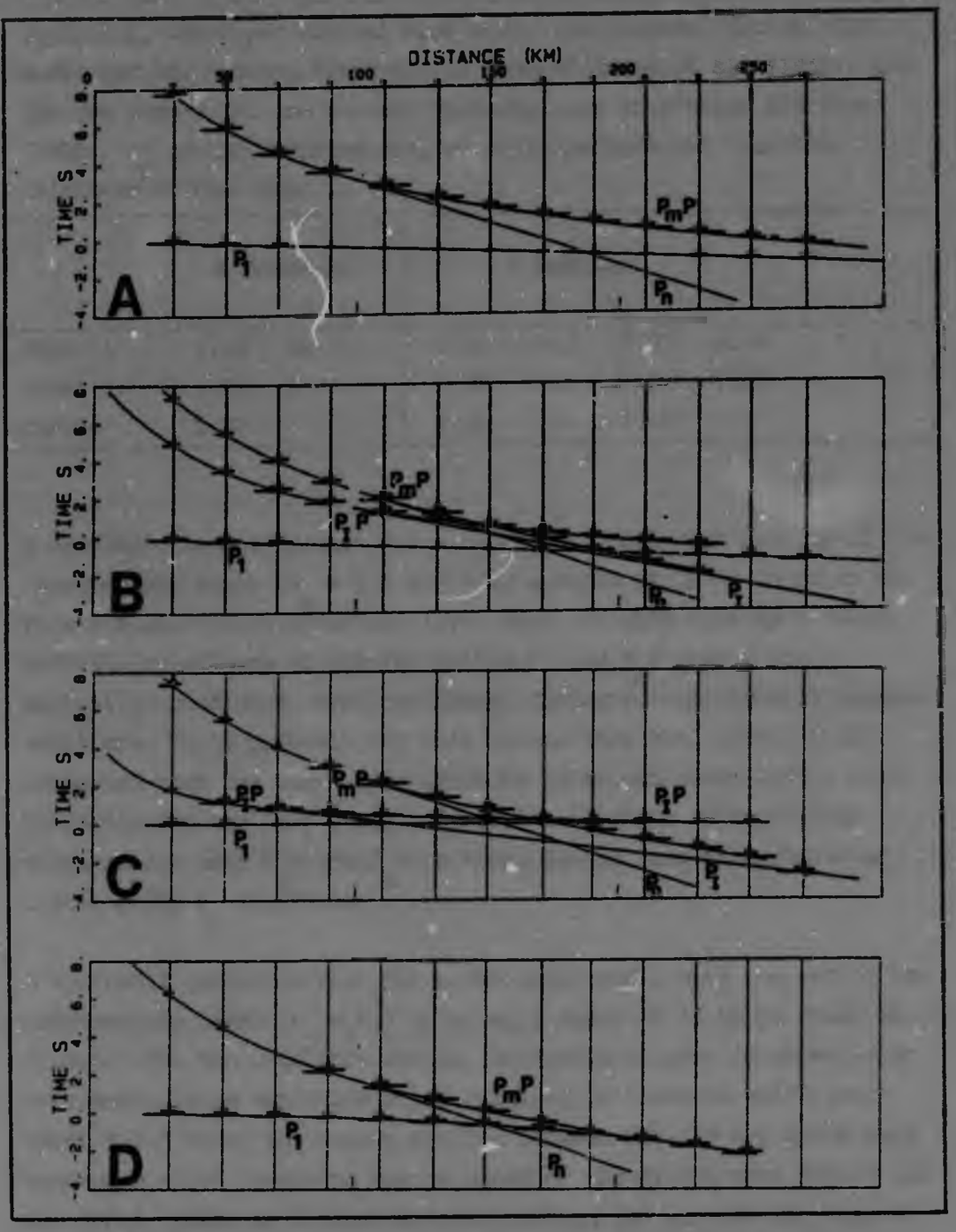


Figure 5.1 Synthetic record sections for simple 1-D models of the seismic velocity structure of the Kaapvaal Craton. (A) single-layer crust, (B) two-layer crust with layer 2 at 28 km, (C) two-layer crust with layer 2 at 14 km, (D) velocity gradient.

Table 5.1. Two-layer crustal models for the Kaapvaal Craton. The model for the western Transvaal is from Willmore et al. (1952), and the two models for the eastern Transvaal are from Hales and Sacks (1959). v_p is the compressional velocity in km/s and h is the thickness of the layer in km.

	W Transvaal		E Transvaal			
	v_p	h	v_p	h	v_p	h
layer 1	6.09	22.7	6.03	28.2	6.03	21.9
layer 2	6.83	15.5	7.19	8.4	6.71	14.7
mantle	8.27		7.96		7.96	

A synthetic record section for a two-layer model with the top of the intermediate layer (v_p = 7.2 km/s) at a depth of 23 km is shown in Figure 5.1B. The intermediate layer does not give rise to a first arrival. At offsets of 200-240 km the P_I and $P_m P$ phases are virtually coincident, with the latter having a significantly greater amplitude. It is probably for this reason that Bott (1971, p 42) suggested that the phase identified by Hales and Sacks (1959) as a refraction was in fact a supercritical reflection. The critical distance for both $P_I P$ and $P_m P$ is about 100 km, and the cross-over distance for P_n is 170 km.

A synthetic record section for a two-layer model with the top of the intermediate layer (v_p = 6.7 km/s) at a depth of 14 km is shown in Figure 5.1C. The existence of the intermediate layer is revealed by reasonably large amplitude super-critical reflections which occur about 0.5 s after the direct arrival between 110-170 km; and a weak head wave which starts to emerge ahead of the direct wave beyond 110 km. The P_I phase is a first arrival between 110 and 180 km, beyond which the P_n phase arrives first. The $P_m P$ phase is prominent due to the velocity discontinuity at the Moho.

(iii) Velocity gradient within crust

Willmore et al. (1952, p. 68) consider the large amplitudes of the

second P phase, and its sharp decrease in amplitude between 280 and 300 km, to be best accounted for by a single-layer crust with velocity increasing with depth. Their velocity model has a near surface velocity of 6.09 km/s and a velocity gradient of 0.026 km/s/km. This is consistent with a simple increase in the basic component of the rock from something close to average granite near the surface to gabbro or nearly gabbro at the base (Birch, 1958, p. 168).

Hales and Sacks (1959) comment on the large amplitudes associated with the second P phase observed in the eastern Transvaal at offsets of 170-250 km, and suggest that this might indicate an increase in velocity with depth within the intermediate layer. However, they refrain from any firm interpretation because of possible complications due to the escarpment.

The synthetic record section due to a model with a near surface velocity of 6 km/s, a velocity gradient of 0.025 km/s/km, and Moho at a depth of 38 km is shown in Figure 5.1D. The direct and super-critical P P arrivals are similar in amplitude, while the sub-critical $P_m P$ phase is significantly smaller in amplitude than the direct P_m wave. The apparent velocity of the refracted direct arrivals increases to virtually 7 km/s until they are terminated at an offset of 270 km. At 250 km this phase has a reduced travel time of -2 s.

(e) Two-dimensional model

Two-dimensional (2-D) models were created by joining adjacent 1-D models and constrained by geological information. The synthetic record section produced by the 2-D model was compared with the observed record sections and refined on a trial-and-error basis. The P-wave velocities of the rocks constituting the Kaapvaal Craton and the supracrustal formations are listed in Table 5.2. Where actual seismic velocity measurements are unavailable, the density-velocity function

$$d = 0.252 + 0.3778v_p \quad \text{(Birch, 1964, p. 4380)}$$

(where d = density in g/cm^3, v_p = compressional velocity in km/s) and the non-linear density-velocity function graphed in Dooley and

Moss (1988, p. 242) were used to estimate the P-wave velocity.

Table 5.2. Representative seismic velocity, density and maximum thickness of formations constituting the Kaapvaal Craton. It is important to note that the values may vary considerably between regions, and within formations. Source of data: 1-Roux (1970), 2-Campbell and Peace (1984), 3-Green and Chetty (1987), 4-Stepto (1979), 5-calculated using formula from Birch (1964). The tabulated maximum thicknesses are rough estimates gleaned from a variety of sources.

	maximum thickness (km)	density (g/cm^3)	v_p (km/s)
KAROO SEQUENCE			
sandstone, shale	1	2.65[2]	3.5[2]
TRANSVAAL SEQUENCE			
Pretoria Group			
shale, ferruginous qtz			
lava	4	2.85[1]	6.8[5]
Chuniespoort Group			
dolomite	2	2.88[2]	6.8[2]
VENTERSDORP SUPERGROUP			
lava	4	2.85[2]	6.4[2]
WITWATERSRAND SUPERGROUP			
Central Rand Group			
quartzite	3	2.65[2]	5.7[2]
West Rand Group			
ferruginous shales	7	2.80[1]	6.7[5]
DOMINION GROUP			
lava	3		
BASEMENT COMPLEX			
Outer Granite-gneiss		2.65[4]	6.0[3]
Inlandsee leucogranofels		2.84[4]	6.4[3]

(f) Shear wave model

Initial S wave models were constructed by assuming a constant

Poisson's ratio of 0.25 (which implies a constant $v_p/v_s = 3^{\frac{1}{2}}$). The S-wave velocities were first varied in order to improve the match between the synthetic record sections produced by ray-tracing and the observed arrivals. The position of the interfaces between the layers was only changed as a last resort.

The relationship between Poisson's ratio and the P- and S-wave velocities is given by

$$\text{Poisson's ratio} = 0.5\ [1 - (v_p^2/v_s^2 - 1)^{-1}]$$

(Holbrook et al., 1988, p 12 088).

(g) Reflectivity method computation of complete synthetic seismogram

The 2-D raytrace method (Spence et al., 1984) does not produce a complete synthetic seismogram. It only considers the wavegroups specified by the interpreter; is limited to body waves; cannot consider P- and S-waves simultaneously; and does not incorporate mode conversion or attenuation. Nevertheless, it is extremely useful for forward modelling, as the computations are very rapid, even on a personal computer.

The reflectivity method (Fuchs and Müller, 1971; Kind, 1985; Müller, 1985) is able to compute the complete theoretical seismogram for a layered earth, incorporating effects such as multiples, mode-conversions, attenuation, surface waves, and even different models of the seismic energy source. It is based on the Haskell matrix formalism for the propagation of plane waves through plane-layered media. The transformation from monochromatic plane waves into impulsive spherical waves due to a point source is carried out by double numerical integration over frequency and wavenumber. The reflectivity method is limited by the very long computation times required (over 30 hours CPU on a VAX780 computer for a simple crustal model), and the restriction to laterally homogeneous models. In particular, the reflectivity method was used to evaluate the effect of attenuation and velocity gradients in the mid-crust, crust-mantle transition and beneath the Moho on the amplitude and dominant frequency of the arrivals

(h) Synthesis with reflection seismic data

Once the trans-Witwatersrand Basin deep seismic reflection profile became available the initial 2-D velocity model was adjusted for consistency with the seismic reflection section. The seismic refraction 2-D velocity model was evaluated by comparing the vertical-incidence synthetic seismograms produced by this model with the observed reflection record section.

(i) Error estimates

Error estimates in refraction modeling are extremely difficult to make, because quantifiable uncertainties (e.g. from scatter in travel time data and misfits between calculated and observed travel times) are usually much smaller than the uncertainties introduced by the interpretive step of phase correlation (Holbrook et al., 1988, p 12 090). This uncertainty is well illustrated by the range of interpretations produced by workers analysing the same data set (the 1978 Saudi Arabian refraction profile), but using different interpretation methods (Mooney and Prodehl, 1984). Major features - such as the depth to Moho, velocities in the lower crust and upper mantle - are consistently determined. More subtle intracrustal features, such as low-velocity layers and velocity gradients, give rise to a greater variation in interpretation.

In the models produced in this study I consider the determination of the velocities and the depths of the interfaces to be better than 0.2 km/s and 2 km respectively. Greater changes in the model noticeably degrade the fit of the synthetic record section to the observed data.

5.2 Description of record sections

In order to carry out forward modelling the main wave groups occurring on the record section are identified. The travel-time curves are superimposed on the record sections, and the apparent velocity (in km/s) and interpreted identity of each curve indicated. The objective of raytrace modelling is to reproduce these features of the record section. In the discussion it is often necessary to refer to particular wave groups on the record sections. The trace number and reduced travel-time are used to specify the feature.

5.2 Klerksdorp - East Rand - Witbank profile

This 260 km profile commences at Klerksdorp, runs roughly parallel to the axis of the Potchefstroom syncline (which contains virtually the full succession of Dominion, Witwatersrand, Ventersdorp and Transvaal rocks), crosses the Rand anticline in the East Rand, and proceeds as far east as Witbank. Record sections are compiled for the Klerksdorp, East Rand and Far West Rand mine-tremor source regions.

1. Klerksdorp source region

A record section produced using a reduction velocity of 6 km/s, and with the seismograms 48 s in length is shown in Figure 5.2A. The 8.2, 4.7 and 3.6 km/s travel-time curve are superimposed to enable easy recognition of the P_n, S_n and S-wave arrivals respectively. The P- and S-wave arrivals are discussed with reference to more detailed record sections (Figures 5.2B and 5.2C). The most important features of the record sections are noted below.

a) Surface waves are not readily identified in Figure 5.2A, despite the broad bandwidth recordings. An indication of a low-frequency dispersed wave group is found at +7 s on trace #2 indicating a group velocity of ca. 3.2 km/s.

b) Virtually no $P_m S$ or $S_m P$ arrivals are evident on the record section. A possible exception is the arrival at +8 sec on trace #15 on Figure 5.2A, which has a dominant frequency of 2.5 Hz.

c) At distances less than 60 km, the first arrival is a strong impulsive phase with a reduced travel-time between between -0.2 and -0.1 s (see Figure 5.2B).

d) Between 60 and 120 km the first arrival is an emergent phase with a velocity approaching 6.3 km/s. At ca. 120 km this phase is extinguished.

e) A distinct second arrival observed between 60 and 120 km has a reduced travel time of ca. +0.5 s, and is more impulsive than the first arrival. This is attributed to the sP phase.

f) A step back in reduced travel-time is observed at a distance of about 130 km (traces #9 and #10).

g) Between 150 and 180 km the first arrival is a strong, impulsive low-frequency wave group with a velocity of ca. 6.2 km/s and a reduced travel-time of -0.5 s. This phase is denoted P_2.

h) Beyond 200 km a clear first arrival with a phase velocity of 8.1 km/s and dominant frequency of 15 Hz is developed, and is identified as the P_n phase. The large amplitude arrivals between +1 and +2 s on traces #6-10 are considered to be due to refractions and reflections close to the critical point, and are also used to constrain the travel-time curve. The P_n phase cannot be definitely identified on seismograms between 170 and 200 km, even where the travel-time curve indicates that it should be a first arrival.

i) The P_n phase is succeeded by a wave group which has the following characteristics:

(i) relatively large amplitude horizontal components - seismograms #17-21 are all horizontal component, the ratio of the vertical to radial component has been calculated for these records and found to be about 0.4, which is similar to that theoretically predicted for reflections at this wide angle;

(ii) low frequencies - dominant frequency between 3 and 8 Hz;

(iii) a long duration which increases with offset - at 250 km the duration of the wavegroup is about 3 s, with the onset at a reduced travel-time of -1.8 s and a phase velocity of ca. 6.6 km/s.

The wavegroup can be traced back to an offset of 120 km (seismogram #9). This wave group is interpreted to be due to energy penetrating the lower crust, and turned by a velocity gradient at the crust-mantle transition (diving waves) or reflected at the Moho. This phase is termed $P_m P$. Analysis of these arrivals using the T^2-X^2

method (Giese, 1976b, p. 151) yields a mean crustal velocity of 6.44 km/s and depth to the reflector of 33.2 km.

j) The direct S-wave has a velocity 3.7 km/s, and can be traced to an offset of 100 km (Figure 5.2C).

k) From 200-250 km, a distinct wave group with a velocity of 4.7 km/s is observed, and identified as the S_n phase. It is clearest on traces #19 and #20. The large amplitude events at +4 s on trace #6 and at +2.2 s on trace #9 are considered to represent a reflection or refraction close to the critical point, and are also used to constrain the travel-time curve.

l) A wavegroup characterised by a high amplitude and relatively low frequency is observed at offsets greater than 120 km. Prominent arrivals are at -2 s on trace #18 and -3 s on trace #21. It can be traced back along a curved line to the large amplitude arrival at +4 s at 100 km (trace #6). This branch is interpreted to be the $S_m S_m$ reflection. Analysis by the T^2-X^2 method indicates a mean velocity above the reflector of 3.76 km/s and a depth to the reflector of 35.2 km. The low dominant frequency (ca. 3 Hz) of the $S_m S_m$ phase is probably due to attenuation in the lower crust. Inspection of traces #19-20 show a marked increase in high frequency energy (>10 Hz) about 2 s after the onset of the low-frequency phase.

m) An event midway between the $S_m S_m$ and S_n phases is observed on several traces, notably on #17-18. The apparent velocity of the wave group is 4.3 km/s. It is interpreted to be a phase refracted by an interface marking a velocity increase in the lower crust.

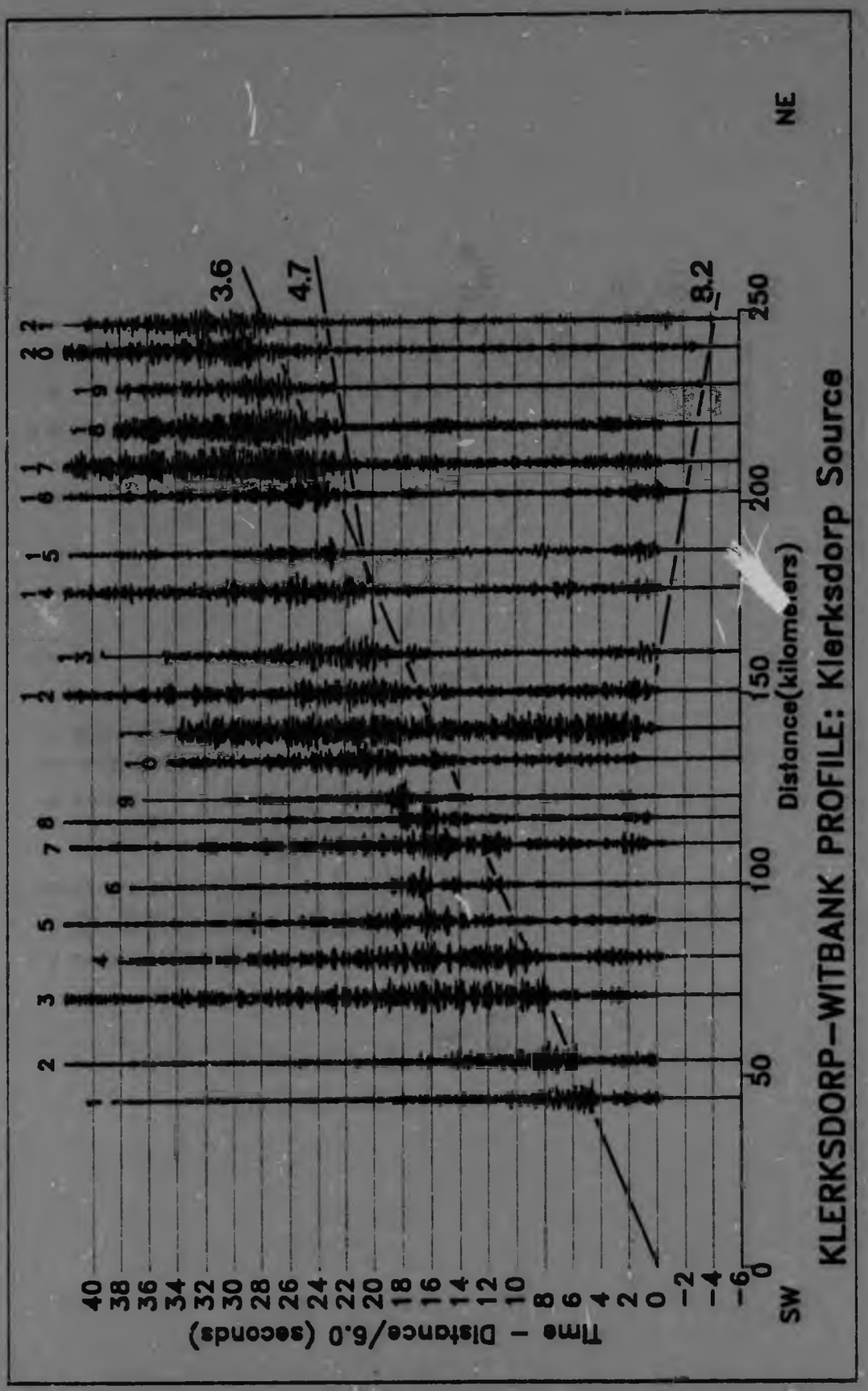


Figure 5.2A. Record section for Klerksdorp - East Rand - Witbank profile. Tremors from the Klerksdorp goldfield.

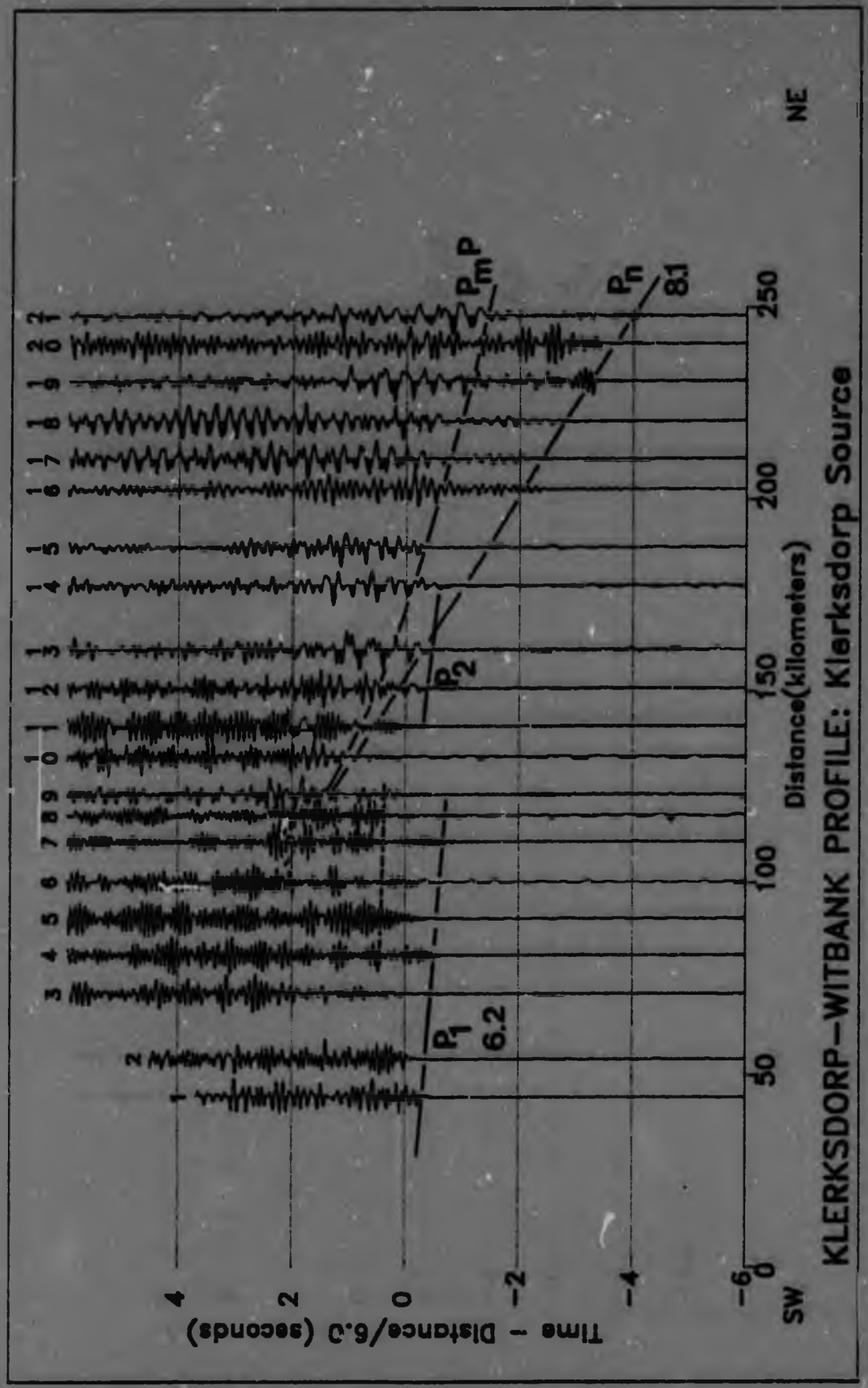


Figure 5.2B. P-wave record section for Klerksdorp - East Rand - Witbank profile. Tremors from the Klerksdorp goldfield.

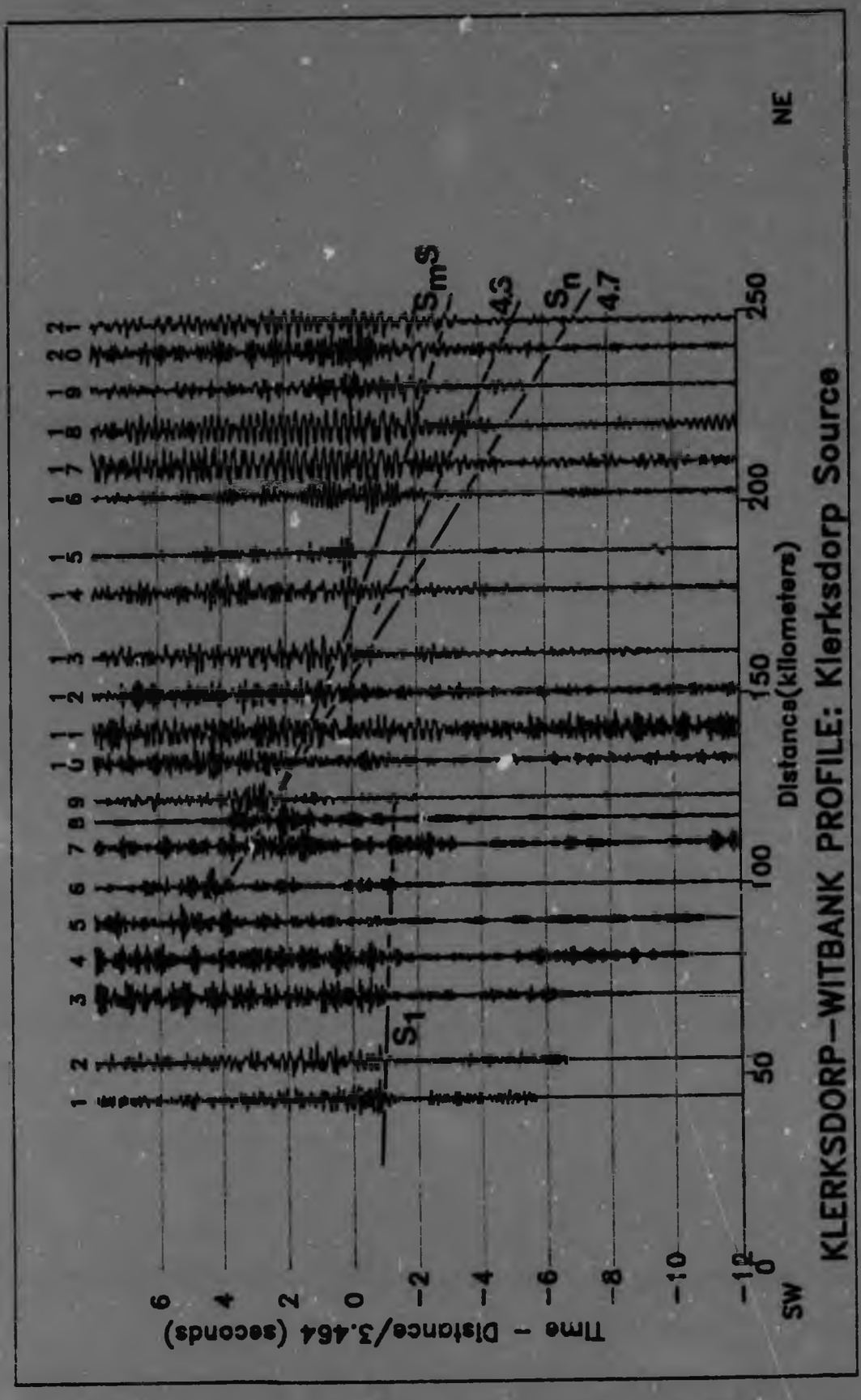


Figure 5.2C. S-wave record section for Klerksdorp - East Rand - Witbank profile. Tremors from the Klerksdorp goldfield.

2. East Rand source region

The key features of the record sections obtained for the East Rand source region are noted below. The 3.6 km/s travel-time curves have been drawn on Figure 5.3A to assist identification of the S-wave arrivals.

a) Surface waves are not obvious on Figure 5.3A, with the exception of the arrival evident at +15 s on trace #4 which has a propagation velocity of 3.0 km/s and has a dominant frequency of 1.4 Hz. Inspection of Figure 5.3C reveals that considerable seismic energy with a propagation velocity of 3.0-3.2 km/s is present on the traces, but the characteristic low-frequency dispersed waveform of the R_g phase is obscured by considerable high frequency energy. An example is the arrival at +2.5 s on trace #8.

b) No $S_m P$ or $P_m S$ arrivals are identified.

c) To the northeast of ERPM the first arrival is a strong impulsive phase as far as ca. 35 km, after which there is a drastic reduction in amplitude (Figure 5.3B).

d) Beyond 35 km a distinct second arrival is observed with reduced travel-times between +0.8 and +0.5 s. This is attributed to a reflection from a mid-crustal interface. The phase is denoted $P_I P$.

e) To the southeast of ERPM the waveform of the first arrival is emergent, probably due to reverberations within the thick sequence of high velocity supracrustal strata contained within the Potchefstroom syncline.

f) A distinct difference in frequency content exists between traces #1-3 (dominant frequency 6-8 Hz) and traces #5-8 (dominant frequency 12 Hz). The tremors which produced these sets of seismograms were of similar magnitude (M_L = 2.62 and 2.42 respectively). Inspection of many other seismograms recorded at these stations rules out the possibility of that site effects have caused the difference in frequency. The reduction in high-frequency energy in the traces observed beyond 100 km is attributed to attenuation experienced within the upper crystalline crust.

g) The S-wave arrivals recorded to the northeast of ERPM are strong and impulsive at distances less than 35 km (Figure 5.3C). Beyond this offset the phase disappears. There is evidence for a

phase at 0 s on traces #16-18.

h) To the southwest of ERPM the S-wave arrivals have a velocity of 3.7 km/s as far as 50 km. Between 50-100 km a phase with a velocity of 3.9 km/s becomes prominent. These phases are interpreted as energy propagated in the supracrustal strata contained within the Potchefstroom syncline. Beyond 100 km the first S-wave arrival is difficult to identify.

i) The large amplitude arrivals on traces #1-2 between +1 and +3 s have a high apparent velocity and are interpreted as $S_m S$ reflections.

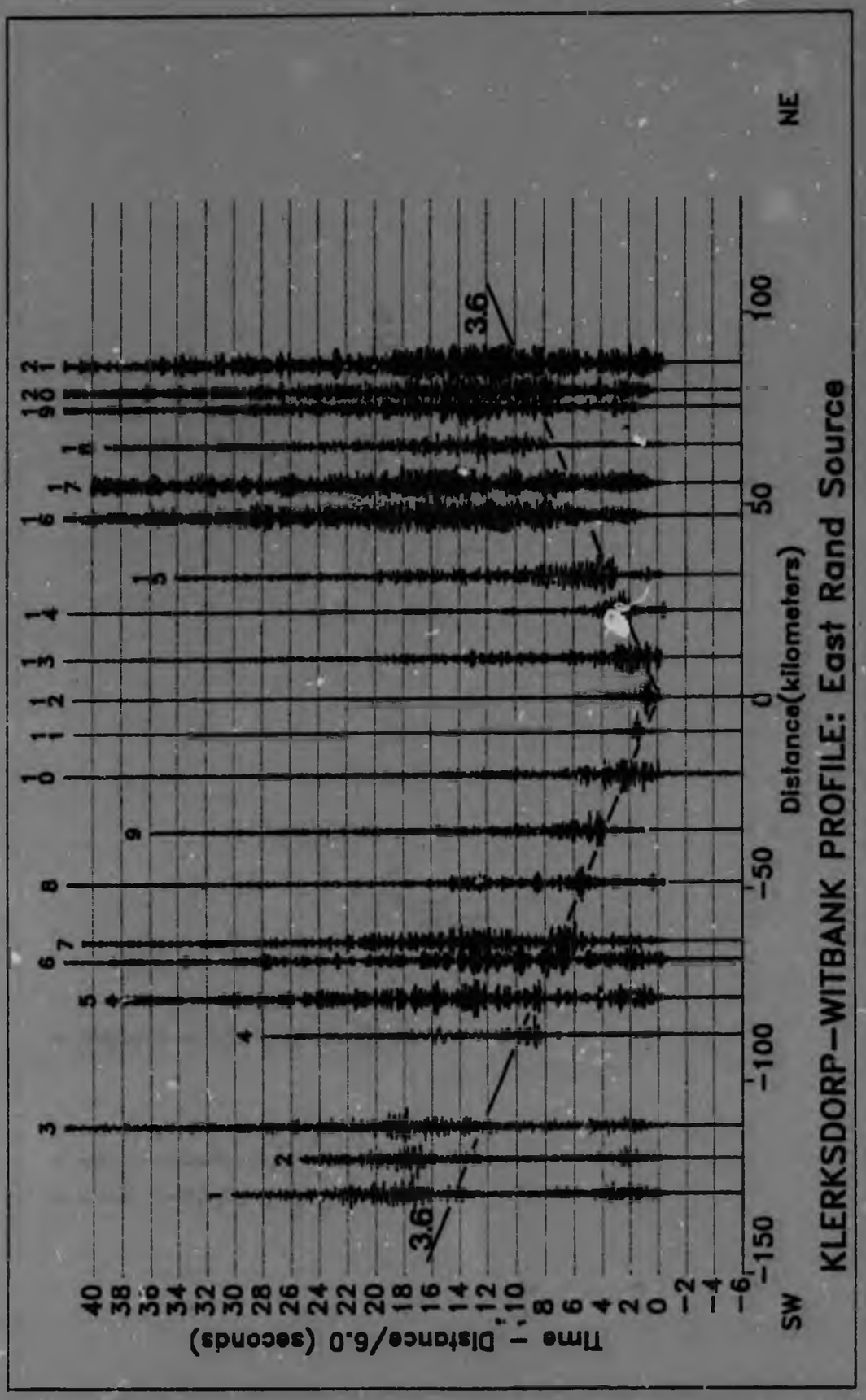


Figure 5.3A. Record section for Klerksdorp - East Rand - Witbank profile. Tremors from the East Rand goldfield.

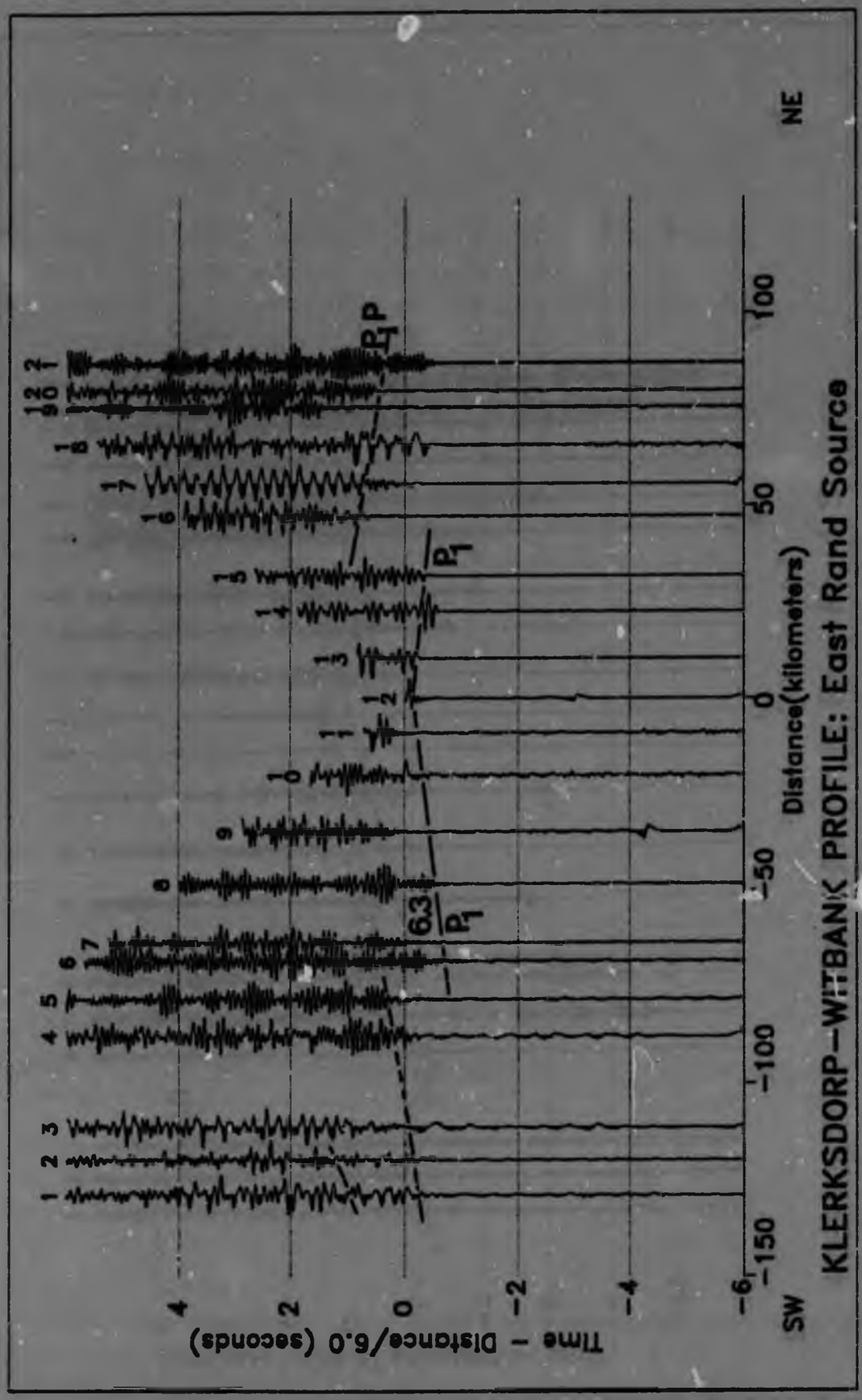


Figure 5.3B. P-wave record section for Klerksdorp - East Rand - Witbank profile. Tremors from the East Rand goldfield.

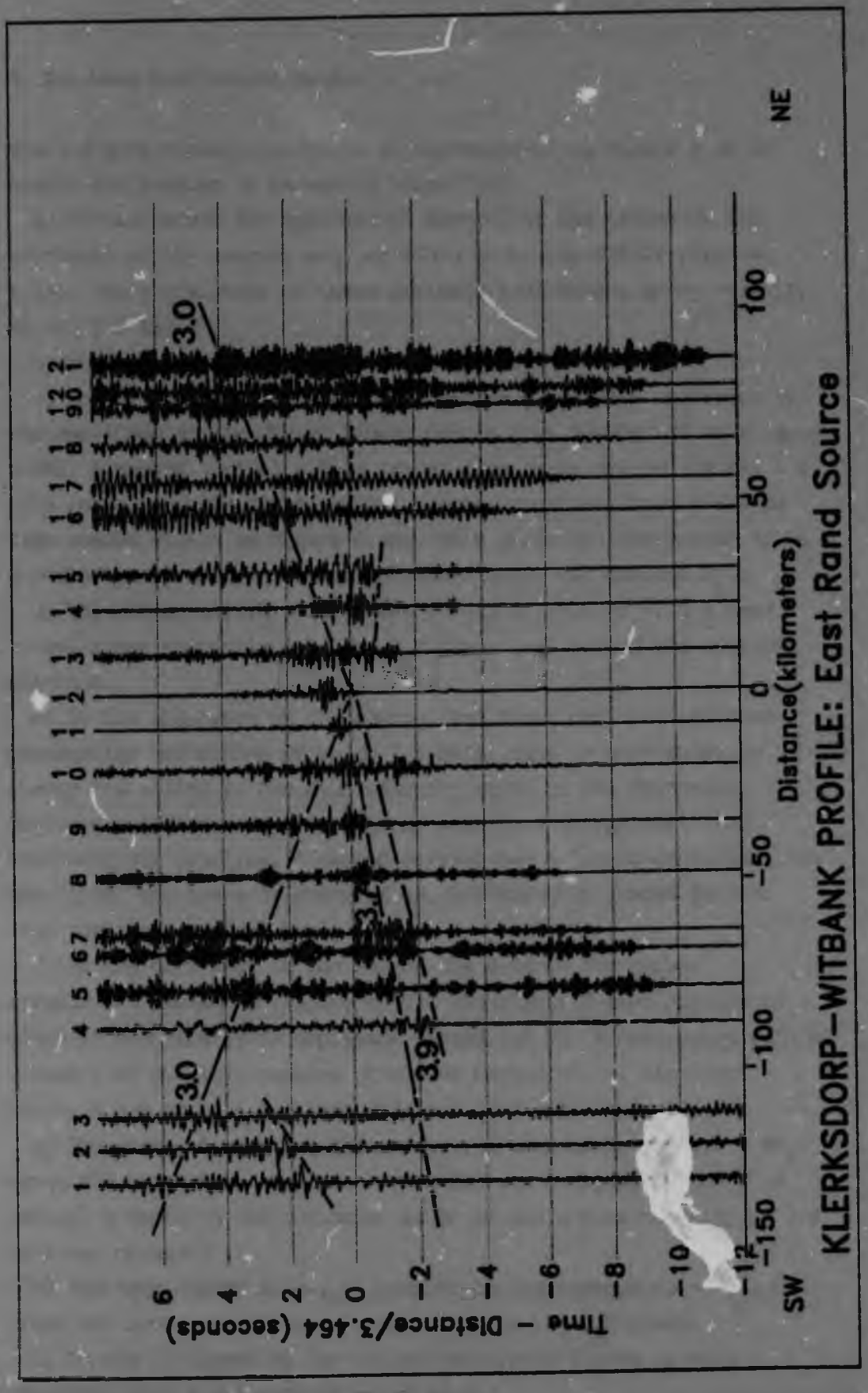


Figure 5.3C. S-wave record section for Klerksdorp - East Rand - Witbank profile. Tremors from the East Rand goldfield.

3. Far West Rand source region

The 3.6 km/s travel-time curve is superimposed on Figure 5.4A to enable the S-waves to be easily identified.

a) Surface waves are apparent on several of the traces to the northeast of the source, e.g. at +33 s on traces #23-24 (Figure 5.4A). The travel-time of these arrivals indicates a group velocity of ca. 2.7 km/s.

b) No $S_m P$ or $P_m S$ arrivals are identified.

c) To the northeast of the source region a dramatic reduction in the amplitude of the direct P-wave occurs just beyond 100 km (Figure 5.4B). A second arrival with a travel-time curve delayed by ca. 1 s with respect to the first arrival becomes prominent beyond 100 km (see traces #18-24 on Figure 5.4B). This phase is interpreted to be a reflection from a midcrustal discontinuity, and denoted $P_I P$.

d) The strong arrivals on traces #17-22 at +3.5 to +1.5 s have travel-times appropriate to the $P_m P$ phase just beyond the critical distance.

e) To the southwest of the source, the first arrivals indicate propagation velocities of up to 7.1 km/s. This is attributed to energy travelling in the high velocity rocks of the Transvaal Sequence and Ventersdorp Supergroup contained within the Potchefstroom syncline. A second arrival has a larger amplitude than the first, and has a velocity of ca. 6.4 km/s. On traces #4-7 it lags the first arrival by ca. 0.6 s.

f) To the northeast of the source the S-waves are rather erratically developed (Figure 5.4C). The direct S-wave appears to diminish drastically in amplitude beyond 100 km. A wave group with a velocity of 3.8 km/s becomes prominent beyond 80 km. Distinct arrivals are at -2 s on trace #15, and -4.5 s on trace #24.

g) The travel-time curve defined by the wave group at +0.8 s on trace #20 through to -0.8 s on trace #23 was analysed by the T^2-X^2 method. A depth to the reflector of 30 km and a mean velocity of 3.8 km/s was obtained.

h) The wave groups at ca. +4 s on trace #19 through to +0.8 s on trace #24 have arrival times appropriate to the $S_m S$ phase.

i) To the southwest of the source the direct S-wave is well developed with a velocity of ca. 4 km/s.

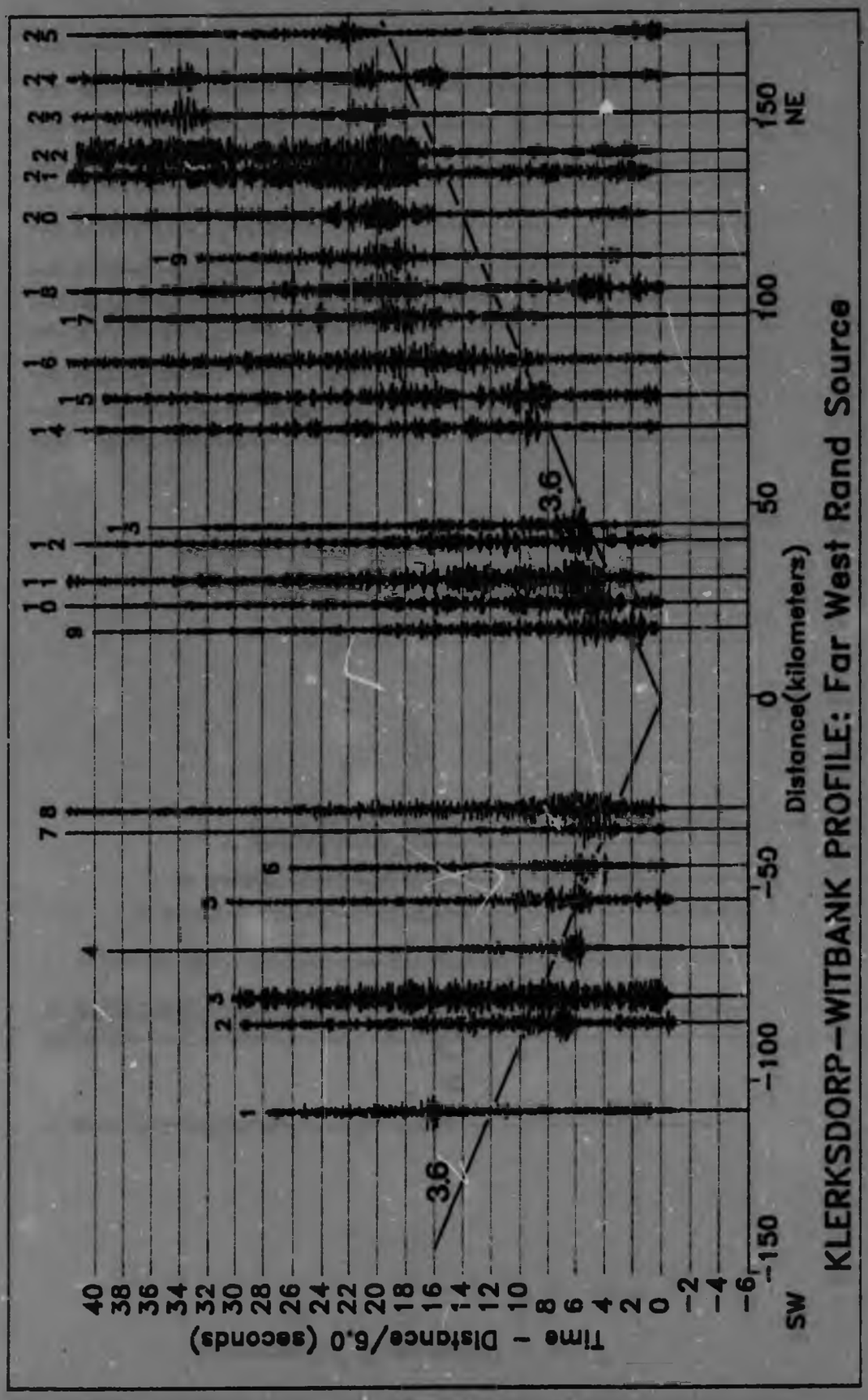


Figure 5.4A. Record section for Klerksdorp - East Rand - Witbank profile. Tremors from the Far West Rand goldfield.

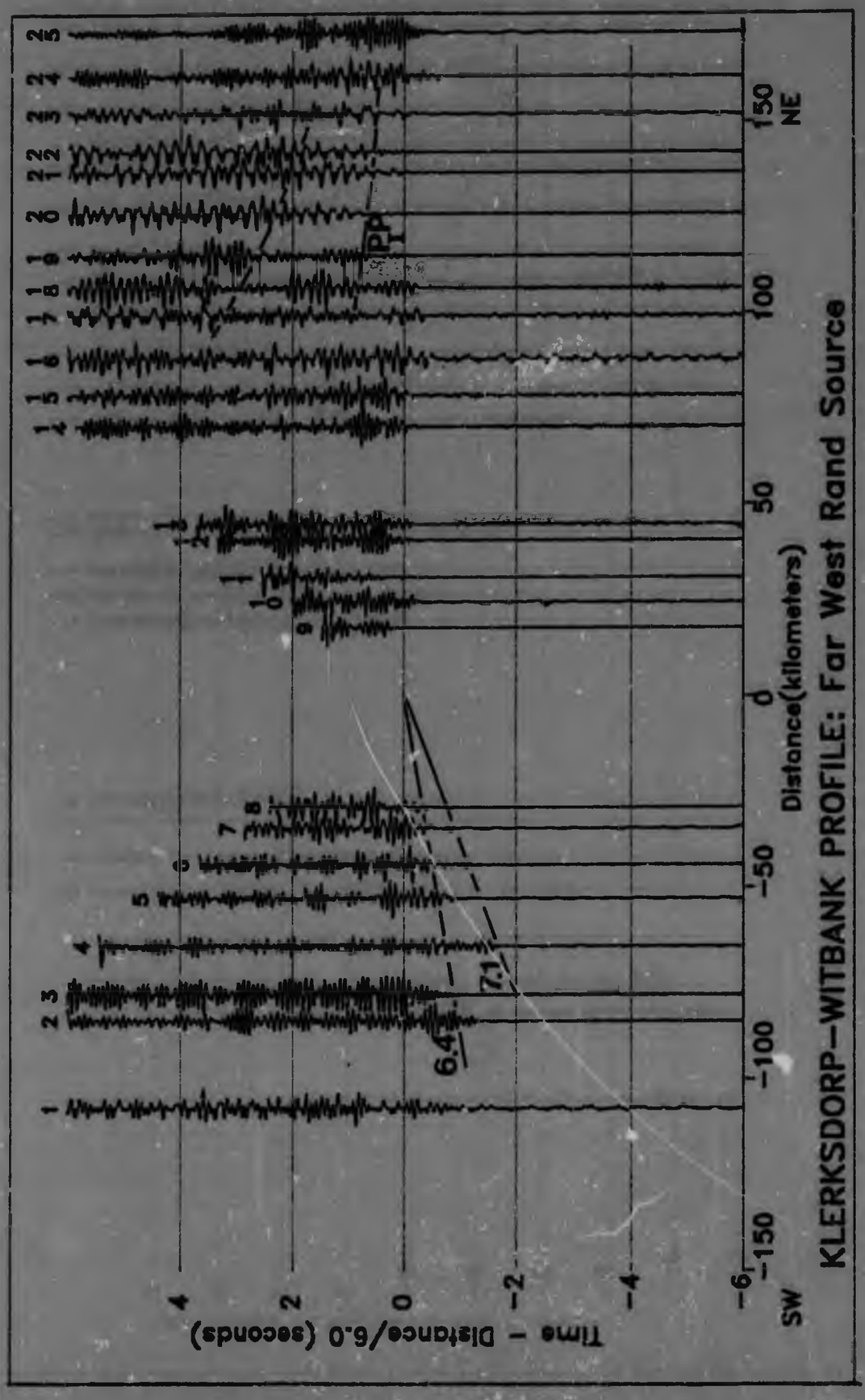


Figure 5.4B. P-wave record section for Klerksdorp - East Rand - Witbank profile. Tremors from the Far West Rand goldfield.

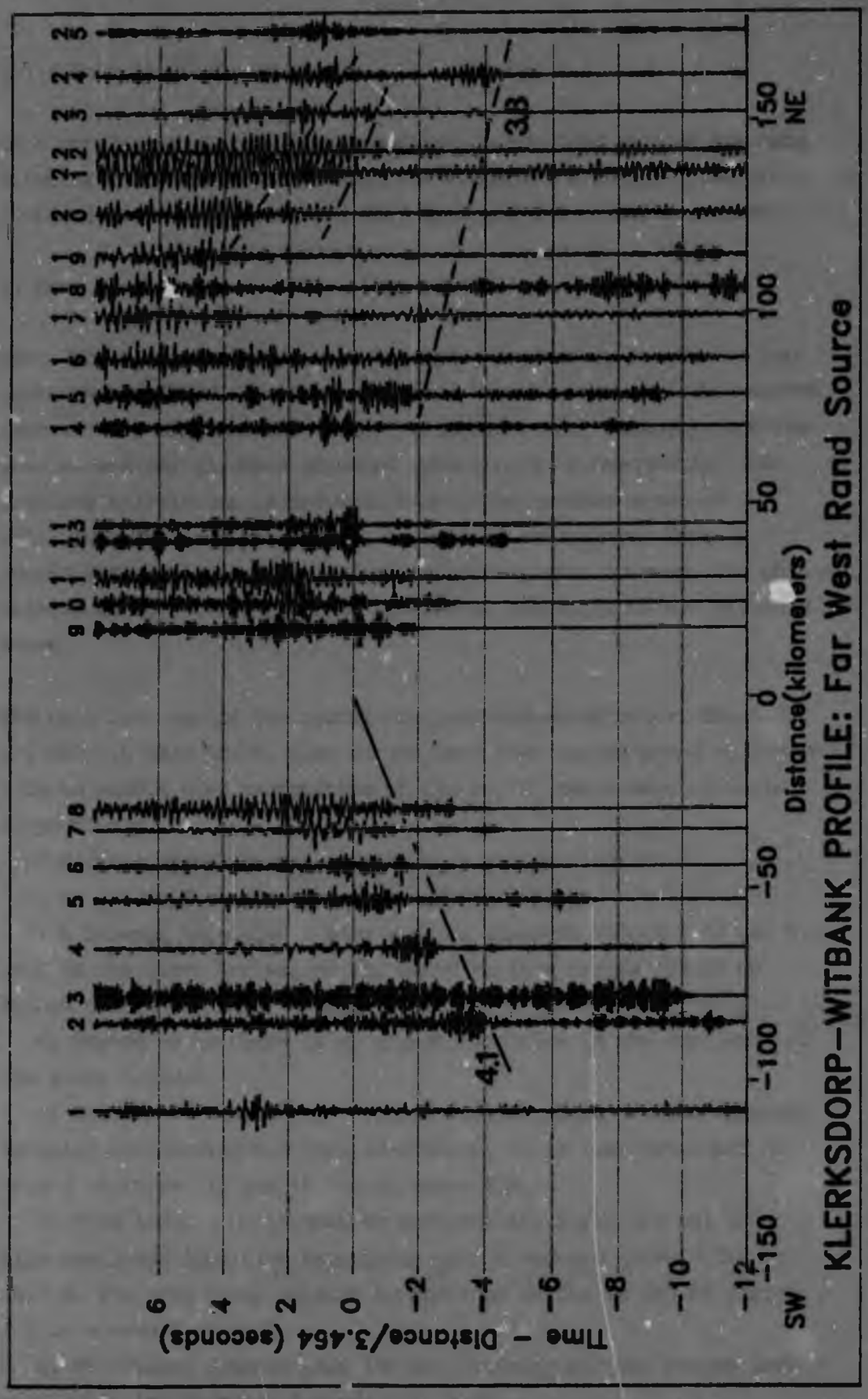


Figure 5.4C. S-wave record section for Klerksdorp - East Rand - Witbank profile. Tremors from the Far West Rand goldfield.

5.2.2 East Rand - O F S profile

This profile is approximately parallel to the long axis of the main Witwatersrand Basin, and crosses the Vredefort structure. Record sections are compiled for the East Rand and O F S source regions.

1. East Rand source

East Rand mine tremors are are located consistently too far to the north by the SASSN. Locations obtained from the mine seismic network were used to pinpoint the area of greatest tremor activity, and the source-receiver distance adjusted accordingly. Consequently, the absolute travel-time is not well known. The maximum error is believed to be less than 0.5 s, as some 50 seismograms from 20 events were considered in making the adjustments. However, the phase velocities for events recorded at several seismographs are reliably known.

The main features of the record sections are noted below. The 8.2, 4.7 and 3.6 km/s travel-time curves have been superimposed on Figure 5.5A to enable easy recognition of the P_n, S_n and S-wave arrivals respectively.

a) Surface waves are not prominent on the seismograms.

b) No P S or S P reflections are identified.

c) A strong, impulsive P-wave with an apparent velocity of ca. 6.4 km/s is the first arrival as far as 50 km (see traces #23-26 on Figure 5.5B).

d) Beyond 60 km there is an abrupt reduction in the amplitude of the first arrival.

e) Between 60 and 120 km a second arrival phase with an apparent velocity approaching 6.6 km/s is evident. It is best developed at +0.4 s on trace #12 and +0.9 s on trace #14.

f) From 145-155 km (traces #9 and #10) the first arrival is a high amplitude impulsive wave group with a reduced travel-time of -0.2 s. The wave group appears to continue as far as 205 km (trace #4) as a second arrival.

g) At offsets greater than 130 km virtually all the traces have a relatively low dominant frequency (< 5 Hz).

h) The P_n phase appears as a first arrival beyond 160 km. It has a velocity of ca. 8.2 km/s. A fair degree of scatter occurs in the P_n arrival times. Trace #1 is also noisy, making it difficult to pick the arrival time precisely. The high amplitude arrivals at +2 s on traces #11-13, as well as the reciprocal time on the reversed profile were used to constrain the travel-time curve.

i) The direct S-wave gives rise to a prominent arrival as far as 50 km (Figure 5.5C). This wave group has a velocity of 3.7 km/s.

j) Between 55 and 70 km (traces #15 and #16) a second S-wave group is identified, with a reduced travel-time of ca. +1 s.

k) The travel-time curve of the S_n phase is based on the arrivals at -7 s on trace #1, -3.5 s on trace #5, and the events at +2 s on traces #11 and #12. A velocity of 4.7 km/s is obtained.

l) The large amplitude arrivals succeeding the S_n phase are identified as Moho reflections ($S_m S$). An example is the arrival at -3.5 s on trace #1. The start of the S_m wavegroup is often difficult to recognise, making it difficult to trace the travel-time curve accurately.

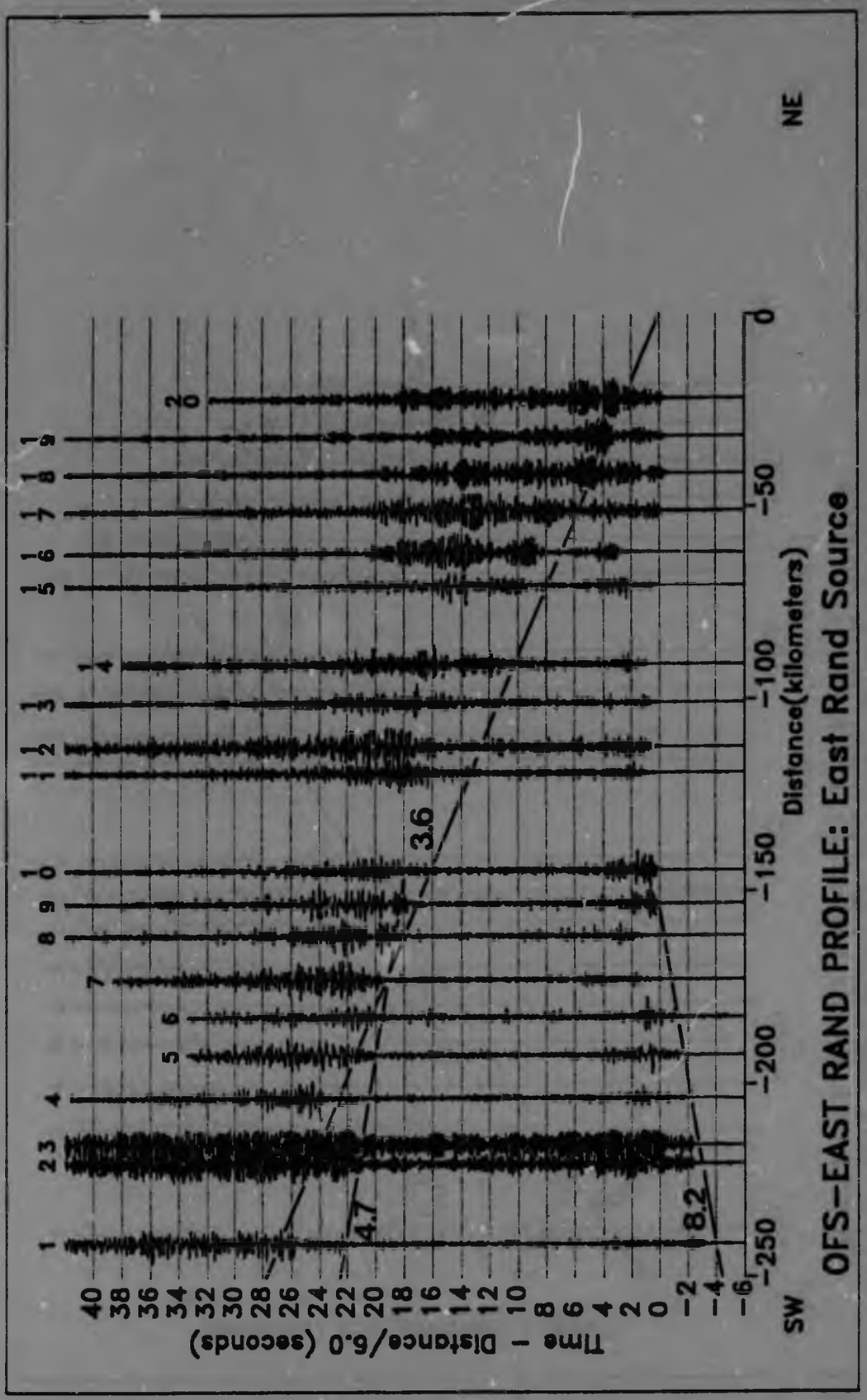


Figure 5.5A. Record section for O. F. S. - East Rand - Witbank profile. Tremors from the East Rand goldfield.

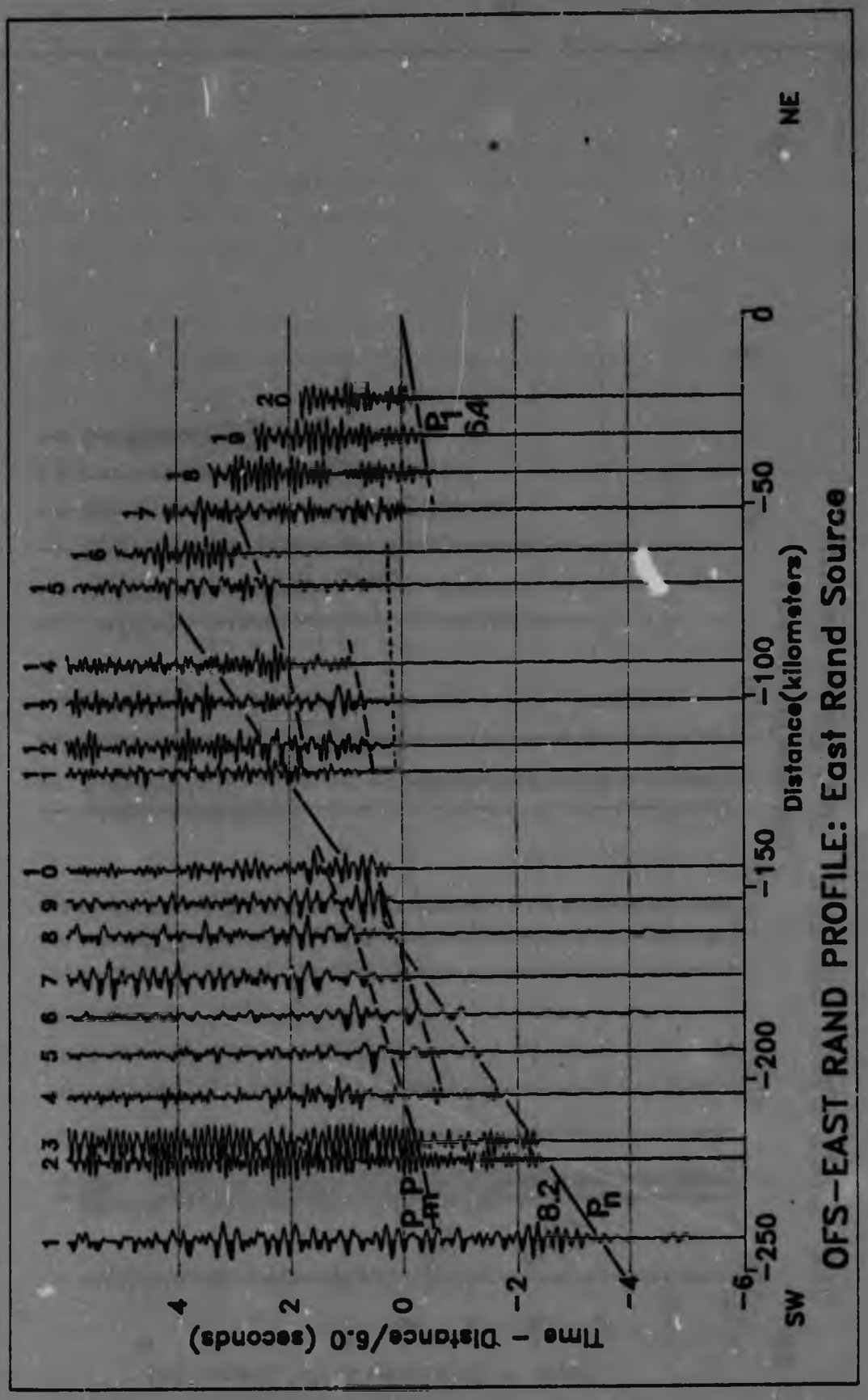


Figure 5.5B. P-wave record section for O. F. S. - East Rand - Witbank profile. Tremors from the East Rand goldfield.

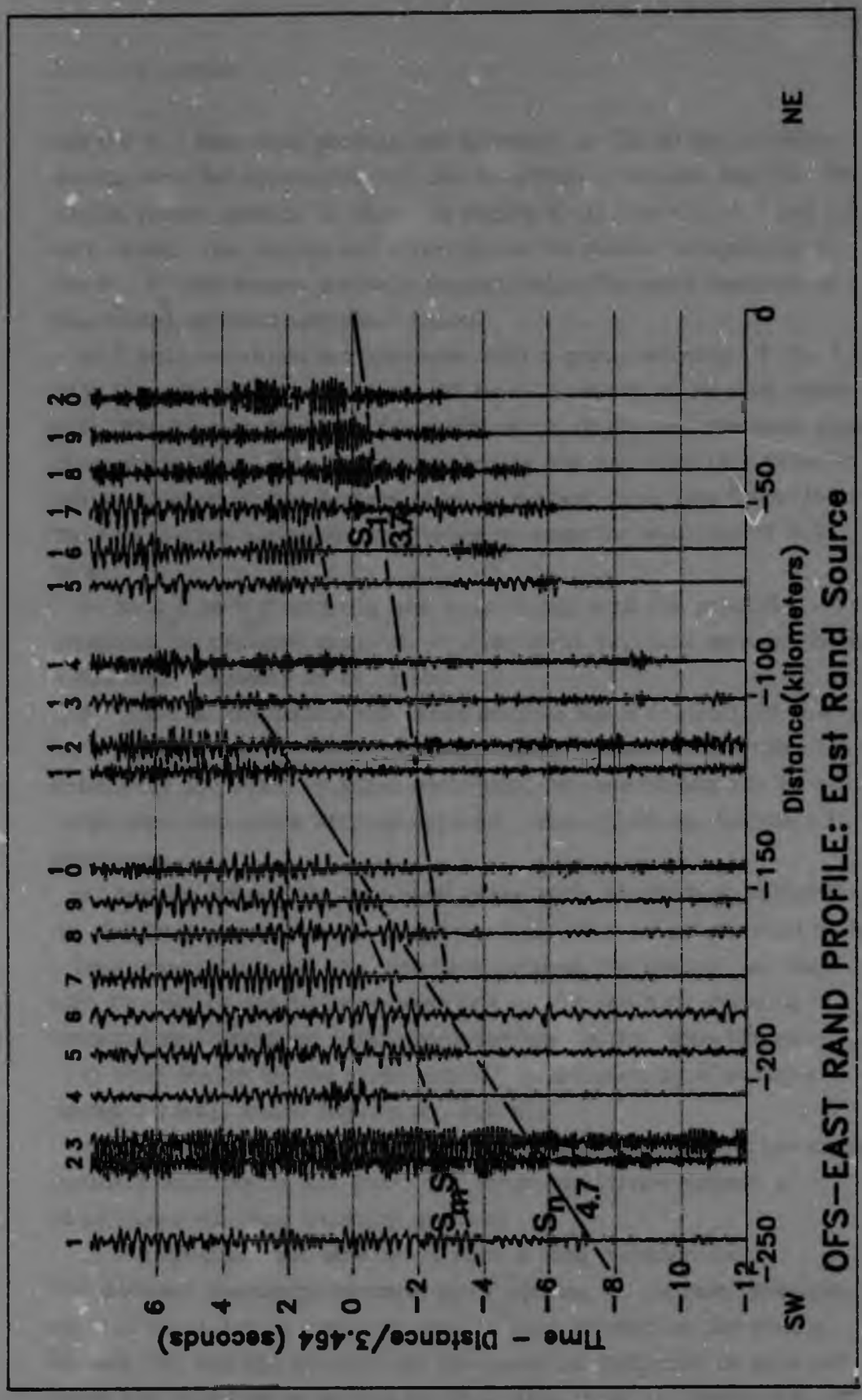


Figure 5.5C. S-wave record section for O. F. S. - East Rand - Witbank profile. Tremors from the East Rand goldfield.

2. O F S source

The O F S - East Rand profile was extended to 320 km by including events recorded by stations on the East Rand - Witbank segment. The entire record section is shown in Figure 5.6A. The 8.2, 4.7 and 3.6 km/s travel-time curves are superimposed to enable recognition of the P_n, S_n and S-wave arrivals respectively. The main features of the record sections are noted below.

a) A well-developed surface wave with a group velocity of ca. 3.0 km/s is recorded between 40 and 60 km (e.g. event at +8 s on trace #23). The Airy phase has a frequency of ca. 2 Hz, and the wave shows clear dispersion. This is interpreted as the Rayleigh (R_g) wave. At 235 km another strong surface wave is evident (+34 s on trace #5). The travel-time indicates an average propagation velocity of 3.2 km/s.

b) No $S_m P$ or $P_m S$ arrivals are identified, with the possible exception of the wave group at +7 s on trace #2. This wave group has a dominant frequency of ca. 2 Hz.

d) Close to the source the first arrival has a velocity of 5.8 km/s (Figure 5.6B). This is probably due to the effect of the relatively low velocity Karoo sediments. Between 50 and 150 km a large amplitude phase with an apparent velocity of ca. 6.1 km/s is prominent.

e) Between 95 and 130 km a weak phase with an apparent velocity of ca. 6.2 km/s appears as the first arrival. This is interpreted to be a head wave arising at the interface between the Central and West Rand Groups, or due to reverberations within the high velocity Ventersdorp Supergroup lavas overlying the Central Rand Group.

f) From 90-130 km the first arrival is followed by a stronger second arrival, which lags by ca. 0.6 s.

g) The P_n phase is prominent beyond 235 km. The travel-time curve yields a velocity of 8.2 km/s. The large amplitudes suggest a significant sub-Moho velocity gradient.

i) A high-amplitude wave group with a long duration and low dominant frequency succeeds the P_n phase. It is best developed at -1.0 to +1.3 s on trace #5, but is also evident on the traces between 250 and 320 km although the onset is difficult to pick and hence the velocity is uncertain. This wave group is interpreted to

be due to waves turned by a velocity gradient in the lower crust, or reflected at the Moho. The phase is denoted $P_m P$. The reduction in amplitude of this phase beyond 270 km was confirmed by careful examination of the three component seismograms. The large amplitude wave groups at +1.5 s and +2.2 s on traces #18 and #29 respectively are interpreted to be reflections or refractions near the critical distance.

k) The direct S-wave at distances less than 50 km has a velocity of 3.2 km/s, and is interpreted to be due to energy propagated within the Karoo Sequence (Figure 5.6C)

l) Beyond 50 km a phase with a velocity of 3.7 s is erratically developed. It is attributed to energy transmitted in the supracrustal rocks. The wave group appearing at -4 s on traces #8 and #9 is attributed to energy fortuitously focused in these strata. To be due to reflections or refractions within the crystalline basement would require unrealistically high velocities.

m) Beyond 250 km the S_n phase appears as a large amplitude arrival. The travel-time curve was constructed to be tangential to a curve marking the onsets of several large amplitude wave groups on traces #10-16 with reduced travel-times between -1 and +2 s. It is estimated that the S_n phase has a velocity of 4.7 km/s.

n) The $S_n S_m$ phase gives rise to high amplitude wave-groups as far as 250 km. Beyond this distance the amplitude is drastically diminished.

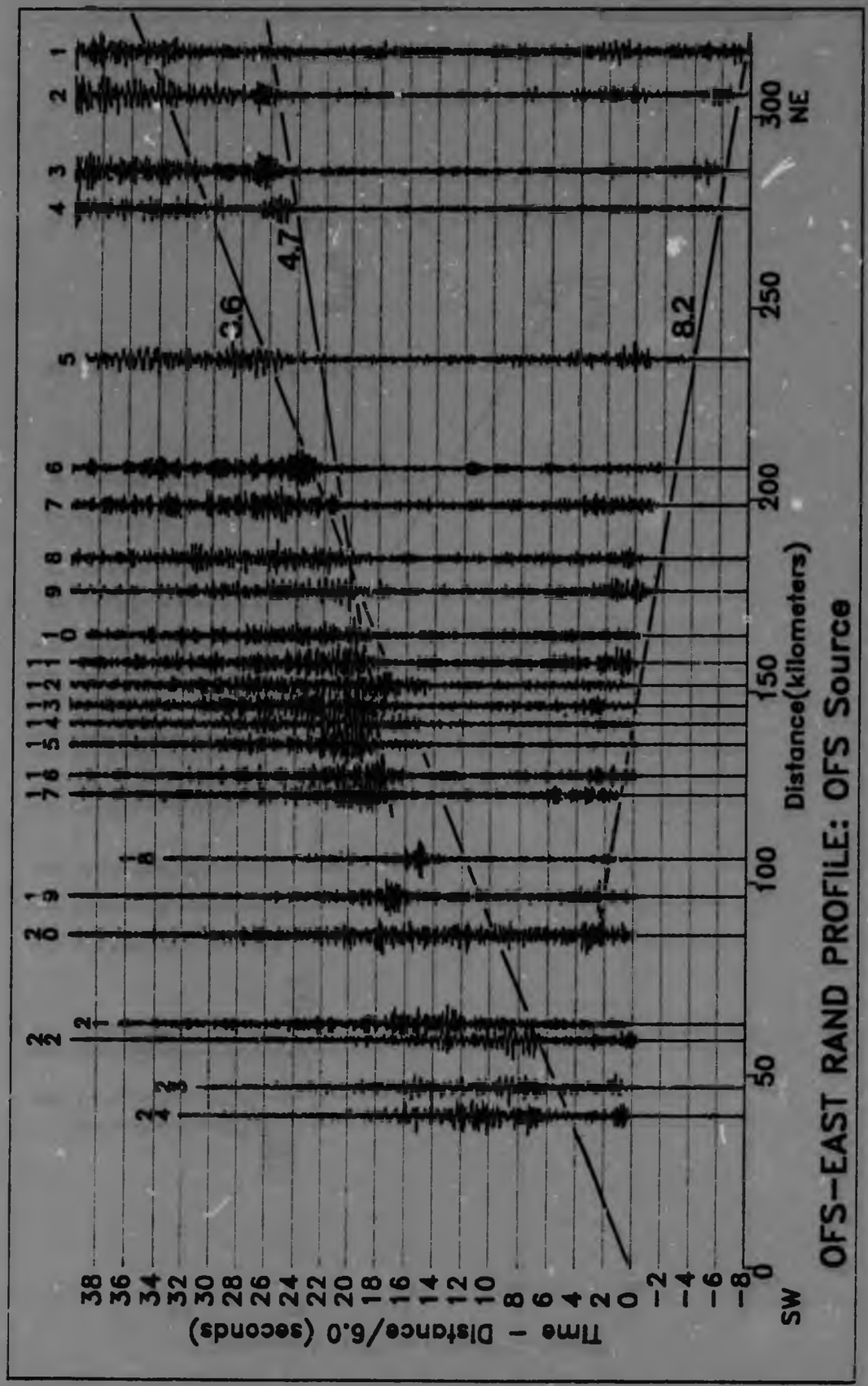


Figure 5.6A. Record section for O. F. S. - East Rand - Witbank profile. Tremors from the O. F. S. goldfield.

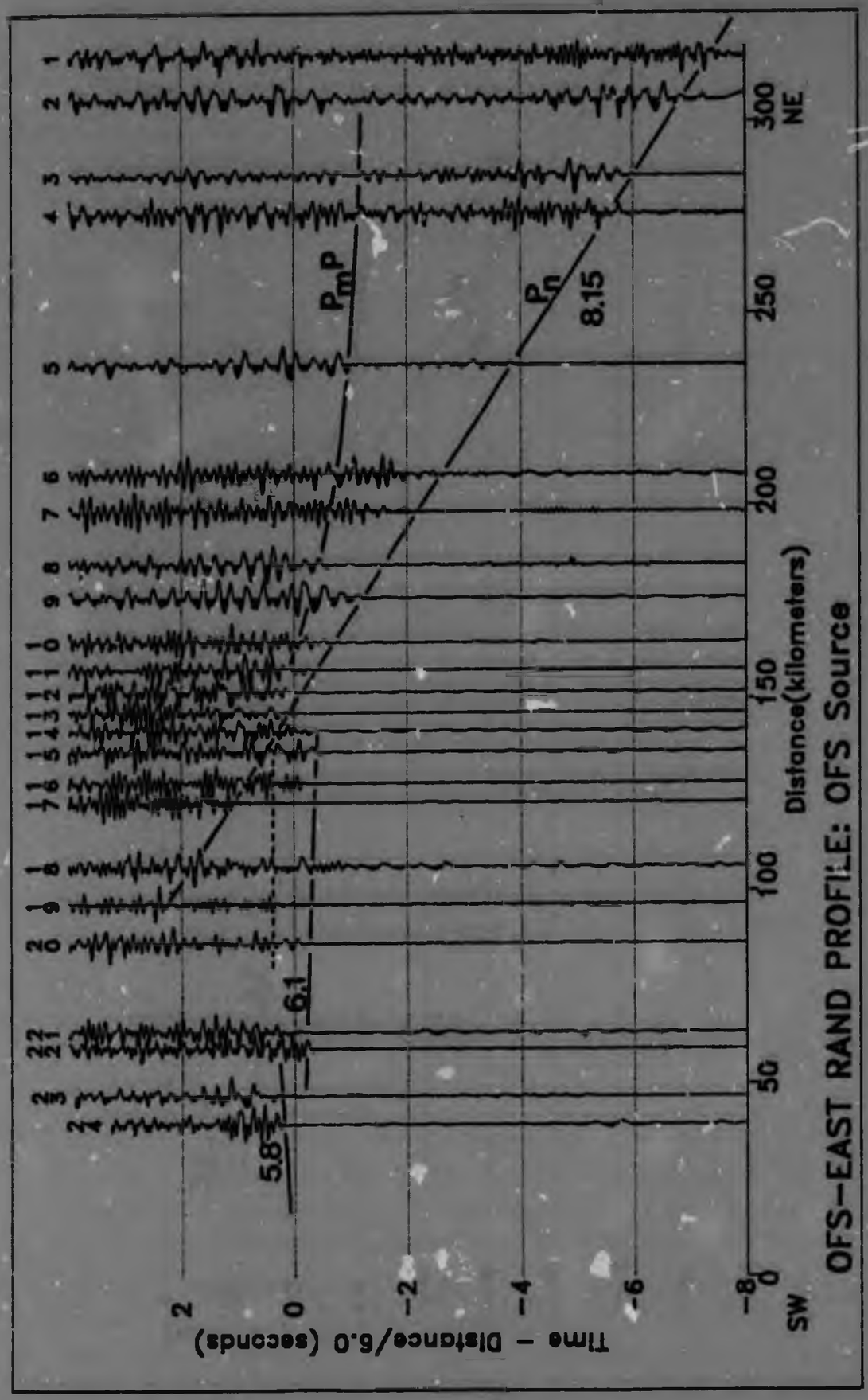


Figure 5.6B. P-wave record section for O. F. S. - East Rand - Witbank profile. Tremors from the O. F. S. goldfield.

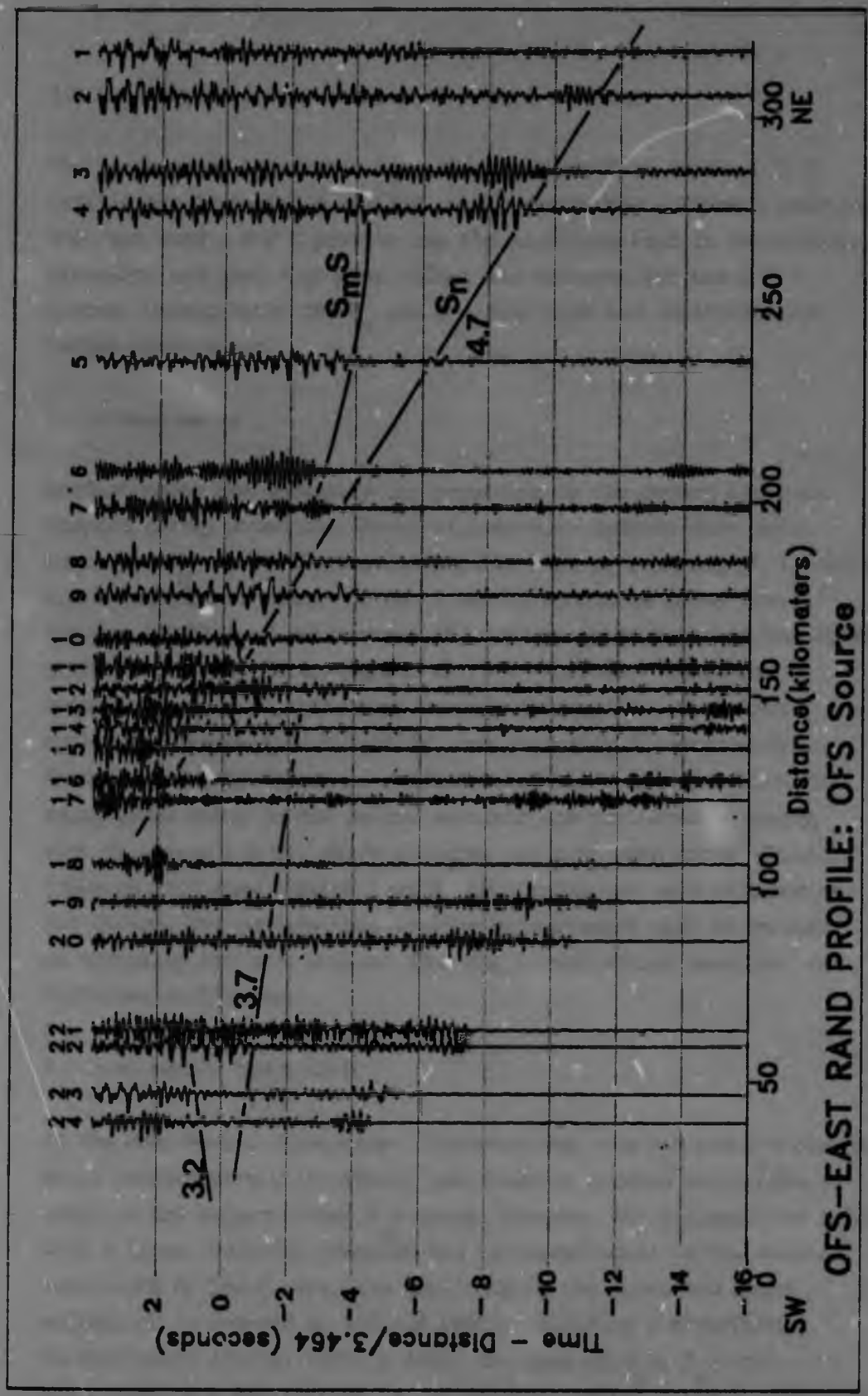


Figure 5.6C. S-wave record section for O. F. S. - East Rand - Witbank profile. Tremors from the O. F. S. goldfield.

5.3 Qualitative interpretation of record sections

The features of the record sections along the East Rand - O F S profile are essentially similar to the Klerksdorp - Witbank profile. The East Rand - O F S profile has the advantage that it is properly reversed, and that a greater offset was achieved for the O F S source. Consequently the P_n and S_n velocities and amplitudes are better constrained.

1. Surface waves

Surface waves are generally not prominent on the record sections. Shapira (1988) noted that South African mine tremors show well-developed R_g waves with the fundamental mode propagating at 3.1 km/s and a dominant frequency of ca. 1 Hz. It should be noted that Shapira (1988) used seismograms recorded on instruments of the SASSN which have a very narrow bandwidth (0.5 - 2.5 Hz), while the seismograms used in this study were recorded with a bandwidth typically ranging from 0.5-40 Hz, and digitally filtered with a bandwidth of 1-12 Hz before production of the record sections. The seismograms shown on the record sections are dominated by energy with frequency > 5 Hz, which obscures the 1 Hz wave group. Shapira (1988, p 270) does comment that R_g amplitudes are very variable on the Craton, and reports that similar seismographs only 50 km apart on virtually the same azimuth from the tremor source recorded very different amplitudes.

2. Crust-mantle transition

If the Moho were a first-order discontinuity, the $S_m P$ and $P_m S$ phases would constructively interfere, and together produce amplitudes as large as the supercritical $P_m P$ phase. However, for a transition zone with a linear velocity gradient and thickness equal to the dominant wavelength of the P wave, the amplitude of the converted phase reflection is reduced to 1/10 of that produced by a first-order discontinuity (Fuchs, 1975, p 454). The lack of $S_m P$, $P_m S$ and subcritical $P_m P$ reflections in the Kaapvaal Craton reveals something of the nature of the crust-mantle transition. The few events

identified as $S_m P$ phases have a dominant frequency of ca. 2 Hz.

Gupta (1966a) calculated reflection coefficients for a model that simulated a linear gradient zone above the Moho. Inspection of the theoretical curves (Gupta, 1966a, p 523) shows that the gradient zone indeed acts as a low-pass filter: as either frequency or layer thickness increase, the reflection coefficient tends to decrease. Reflection coefficients were read from the graph for a range of frequencies (1-32 Hz) and gradient zone thicknesses (0.1-6.4 km) for the incident angle required to produce the rays detected at offsets > 200 km. A seismic velocity increase across the gradient zone of 6.6 to 8.2 km/s was considered. The reflection coefficient is about 0.26 when the layer thickness is much smaller than the seismic wavelength. As the wavelength decreases or the layer thickness increases, the reflection coefficient is reduced to an asymptotic value of about 0.10, a reduction of some 60%. For a frequency of 8 Hz this reduction of the reflection coefficient is reached for a gradient zone 400 m in thickness, while at 2 Hz it is only reached for a gradient zone 1.6 km thick. Hence the absence of the converted phase reflections with frequencies > 3 Hz indicates that the crust-mantle transition zone is probably 1 to 2 km thick.

3. Change in character and extinction of the first arrival.

It is observed that the first arrival phase is impulsive as far as 30-50 km. Thereafter it has an emergent character. At a distance of 50-140 km, depending on the profile, the phase disappears. Two factors may be responsible for this observation.

(i) It may be due to a velocity inversion in the upper crust. The granitic upper crust has a lower seismic velocity (6.0-6.2 km/s) than the overlying shales of the West Rand Group (calculated to be ca. 6.7 km/s from the average density of 2.80 g/cm^3, although the results from a few reported sonic log measurements indicate a velocity of 6.2 km/s).

(ii) The Central Rand Group, in which the foci of most tremors is situated, has a considerably lower velocity than the overlying Ventersdorp lavas (5.7-6.0 and 6.4 km/s respectively). Direct rays striking this interface with an angle of incidence greater than 70° will be totally reflected. The foci of most tremors are within 2 km

of this interface. This implies that only rays striking the interface within a radius of about 6 km from the source will be transmitted directly to the layer above. As the overlying layer has a greater velocity, the transmitted rays will be refracted away from the normal, and a direct wave may be detected up to distances of 60 km from the source. Energy will be transmitted to larger distances by reverberations within the supercrustal strata.

In this study I have not attempted to determine the relative importance of these factors.

4. Second P-wave arrival

On all the record sections a second P-wave arrival is observed between 30-120 km. It lags the first arrival by 0.6-1.0 s, and has a velocity of ca. 6 km/s, except to the southwest of the Far West Rand where the velocity is ca. 6.4 km/s (see Figure 5.2B, 5.3B, 5.4B).

Tremors typically radiate ca. 80% of their energy as shear waves (Spottiswoode and McGarr, 1975, Table 1). The SV wave will be totally converted to a P-wave when reflected at the free surface at angles of incidence greater than 35° (Ewing et al., 1957, p. 31). Tremors typically occur near the level of mining, which is generally between 2 and 4 km depth. Consequently a sP phase with a large amplitude and lagging the direct P phase by ca. 0.8 s is likely to be generated. S to P mode conversions are also likely at other interfaces such as the Central Rand - West Rand and Central Rand - Ventersdorp contacts.

5. Transition from upper to lower crust.

A phase with a high amplitude, low dominant frequency, short travel-time curve, and early reduced travel-time is recorded as a first arrival at distances of 150-180 km on the Klerksdorp - Witbank record section (Figure 5.2B). These features are best explained by a mid-crustal velocity gradient. The frequency dependence of reflection coefficients in a velocity gradient zone is well known. Only if the depth range of gradient zones approaches that of the dominant wavelength can reflections originate within a gradient

zone, giving rise to a low-pass filter effect (Meissner, 1986, p 60; Gupta, 1966a, 1966b; Hron and Chapman, 1974). A second possible explanation for the low dominant frequency is attenuation. A study of attenuation of seismic waves produced by tremors in the Far West Rand using the single-scattering coda-Q model was conducted by Peberdy (1986). Observations were made along two profiles, one of which stretched southwards across the Potchefstroom syncline. Coda-Q was calculated for both the P- and S-waves for stations at distances up to 50 km. The results indicate a coda-Q value less than 250. This observation of a relatively low value for Q in crystalline basement is supported by Shapira (1988), who obtained a value for Q of 195 from measurements of the attenuation of the R_g phase in the central Kaapvaal Craton. These results suggest that attenuation within the upper crust of the Kaapvaal Craton could also contribute to the low dominant frequency of the phase.

On the record sections to the northeast and southwest of the East Rand source region (Figures 5.3B and 5.5B respectively), as well as to the northeast of the Far West Rand source region (Figure 5.4B), there is a clear second arrival phase, substantially retarded relative to the first arrival, which appears beyond 50 km. This phase is most simply interpreted in terms of a mid-crustal velocity discontinuity. T^2-X^2 analysis indicated that the reflector is in the depth range of 14-18 km. The phase is denoted P_IP on the record sections. Modelling indicates that a substantial velocity contrast (e.g. an increase from 6.2 to 6.6 km/s, is required to achieve a critical distance of ca. 60 km. If this phase were due to S to P mode conversions, no corresponding phase would occur on the S-wave record sections. However, the existence of the mid-crustal reflector is substantiated by corresponding S-wave phases (see Figures 5.3C, 5.4C and 5.5C).

It is concluded that the nature of the transition from upper (6.0-6.3 km/s) to lower (6.5-6.7 km/s) crust is abrupt in the vicinity of the Rand anticline (where it could be termed the Conrad discontinuity), but beneath the Potchefstroom syncline it appears to be gradational. The head wave generated by the discontinuity is not identified. Raytracing indicates that it would arrive simultaneously with reverberations in the high velocity supercrustal strata.

6. Attenuation of the $P_m P$ and $S_m S$ phases

The low dominant frequency of the $P_m P$ phase relative to the P_n phase and the long duration of the wave group is observed on all the record sections, but most prominently on the Klerksdorp - Witbank profile (Figure 5.2B). These features indicate that the $P_m P$ phase has experienced greater attenuation than the P_n phase. Pulse broadening is a consequence of intrinsic attenuation. When considered in the frequency domain, different frequency components will propagate with different phase and group velocities (Toksöz and Johnstone, 1981, p 352). Several mechanisms have been suggested to explain the attenuation of seismic waves:

(i) absorption of seismic energy by anelastic processes in rocks, including frictional dissipation due to relative motions at grain boundaries and across crack surfaces, flow and "squirting" in fluid-filled pores, and relaxation due to shear motions at pore-fluid boundaries;

(ii) scattering of seismic energy by heterogeneities within the rock;

(iii) and reflection in a velocity gradient zone or by multiple reflection between thin beds

(Toksöz and Johnstone, 1981, p 136; Meissner, 1986, p 60; Schoenberger and Levine, 1974).

The attenuation effects due to absorption and scattering are approximately additive. Several diagnostics have been proposed which would enable the dominant mechanism to be determined, the most applicable in this case being that the coda of a wave which has been scattered will contain relatively higher frequencies than the initial pulse (Richards and Menke, 1983). Inspection of the frequency spectra of traces #17-21 does not reveal any systematic increase of frequency with time in the $P_m P$ wave group (Figure 5.2B). In contrast, the $S_m S$ wave group does show a marked increase in high frequency energy (>10 Hz) about 2 s after the onset of the low-frequency phase (see especially traces #19-20 on Figure 5.2C). This could indicate scattering by heterogeneities in the lower crust. In order to roughly estimate the scale length of these heterogeneities we may use the result of Raynaud (1988, p. 227) that scattering is

peaked at the frequency for which the seismic wavelength is approximately six times greater than the scale-length of the elastic variations. Thus for the S-wave with a velocity of 3.8 km/s and frequency of scattering of 10 Hz, the seismic wavelength is 380 m and the correlation length of the seismic variations is about 60 m. The backscattering model of Wu and Aki (1985, p. 10270) yields a similar result. The absence of P-wave scattering may be due to its inherently longer wavelength.

Most field measurement of attenuation in the continental crust have used surface waves to obtain estimates of S-wave attenuation (Q_s). Relatively few measurements of P-wave attenuation (Q_p) have been made. Attenuation coefficients obtained for stable regions of North America and Eurasia are nearly identical within the limits of observation: the uppermost 15-20 km of the crust have values of Q_s in the range 250-1000, while greater depths have Q_s and show little regional variation (Mitchell et al., 1). The exceptionally high values of Q obtained in the lower crust has been attributed to the absence of water. Laboratory measurements show an increase in the Q of low-porosity olivine basalt from 100 to 2000 when outgassed (Tittman, 1977, p 197). Consequently, should the lower crust contain a significant amount of fluid in pores, this could cause a decrease in Q. The unusually low electrical resistivity observed at the base of the crust of the Kaapvaal Craton (Van Zijl, 1978) has been attributed to the presence of hydrated minerals or saline pore water at high fluid pressures (Van Zijl, 1978; Percival and Berry, 1987, p 40), and could also explain the existence of a layer with a low Q_p and Q_s.

It is concluded that anelastic absorption in the lower crust (possibly due to the presence of water-filled pores), together with the low-pass filter effect of a velocity gradient, are probably the dominant mechanisms giving rise to the attenuation of the $P_m P$ phase. Scattering due to heterogeneities with a relativly small spatial dimension has also contributed to the attenuation of the $S_m S$ phase.

7. Sub-Moho velocity

The absence of the P_n phase as a first arrival between 170 and 200

km may be explained by a velocity gradient below the Moho. This produces head waves with an amplitude minimum at some distance after the critical point, followed by a maximum, and then decreasing again (Cerveny et al., 1977, p 148). The precise position of the minimum and maximum depends on the model. Strong P_n and S_n head waves are observed beyond 200 km. This suggests the existence of an appreciable sub-Moho velocity gradient.

5.4 Raytrace modelling

Two-dimensional raytracing was carried out using the computer programme RAYAMP-PC. The objective of the modelling is to reproduce the major features of the observed record sections. The geometric symbols on the synthetic record sections represent observed travel-times used to constrain the modelling. The wavelets on the synthetic record section are normalised to the maximum amplitude on each trace. The same scaling method is applied to the observed record sections. On each model the velocity (km/s) and velocity gradient (km/s/km), except when it is less than 0.01 km/s/km, is indicated.

The scaling of the reduced travel-time axes of the record sections has been designed to facilitate comparison of the P- and S-wave record sections. If Poisson's ration is 0.25 for all the layers in the model, the travel-time curves will be exactly superimposed.

5.4.1 Klerksdorp - East Rand - Witbank profile

1. Klerksdorp source region

A 2-D model of the P-wave velocity structure between Klerksdorp and Witbank is shown in Figure 5.7A. The seismic energy source is located at a depth of 2.5 km, within a layer assigned a seismic velocity of 6 km/s. This layer represents the quartzites of the Central Rand Group. The overlying lavas of the Ventersdorp Supergroup and dolomitic rocks of the Transvaal Sequence have been assigned a uniform P-wave velocity of 6.3 km/s; and the underlying dense shales of the West Rand Group a velocity of 6.4 km/s. Horizontal layers have been used to represent these strata, although it is known that there is considerable faulting and folding within the Potchefstroom syncline. The wide (10 km) spacing of the seismographs, as well as the considerable size of the source region (about 25 km along the azimuth of the profile), make it impractical to resolve the structure of the supracrustal strata with the data acquired in this experiment.

Direct waves from the source are detected to an offset of ca. 50 km. At greater offsets direct waves are not detected, as the incident angle to the Central Rand/Ventersdorp contact exceeds the critical angle (about 70°), and the energy becomes trapped within the low velocity layer. Energy propagates within the Ventersdorp and Transvaal strata by multiple reflection, giving rise to a weak, emergent first arrivals at distances of 50-150 km.

The upper crystalline crust has a lower P-wave velocity than the West Rand Group rocks, giving rise to a shadow zone. In order to produce a wave group with a large amplitude and a short travel-time curve between 150 and 180 km, a velocity gradient of ca. 0.045 km/s/km is required in the upper crystalline basement. The velocity gradient zone commences at a depth of ca. 8 km, and is about 10 km thick. The lower crust (18-33 km) has a uniform velocity of ca. 6.6 km/s.

Moho is modelled at a depth of ca. 35 km. The crust-mantle transition is modelled by a gradient zone 2 km thick in which the velocity increases linearly from 6.8 km/s with a gradient of 0.5 km/s/km. This zone produces $P_m P$ reflections, with the critical distance at ca. 100 km. The low dominant frequency and long duration observed for this wave group cannot be reproduced by the raytracing programme. The P_n phase is observed to have large amplitudes at offsets greater than 200 km. In order to produce this feature, a zone 10 km thick and with a gradient of 0.01 km/s/km was introduced below the Moho.

The S-wave model is shown in Figure 5.7B. Calculation of the S-wave velocities from the P-wave model, assuming a Poisson's ratio of 0.25, does not completely satisfy the observed data.

The most prominent wave group on the observed record section (Figure 5.2C) is the $S_m S$ phase. Keeping the reflector at a depth of 35 km, an average crustal velocity of 3.8 km/s is required to match the observed travel-time curve. In order to maintain consistency with the better constrained P-wave model, the upper crystalline crust was assigned a velocity of 3.66 km/s at a depth of 6 km, increasing gradually (0.015 km/s/km) with depth. There is no evidence for a S-

Direct waves from the source are detected to an offset of ca. 50 km. At greater offsets direct waves are not detected, as the incident angle to the Central Rand/Ventersdorp contact exceeds the critical angle (about 70°), and the energy becomes trapped within the low velocity layer. Energy propagates within the Ventersdorp and Transvaal strata by multiple reflection, giving rise to a weak, emergent first arrivals at distances of 50-150 km.

The upper crystalline crust has a lower P-wave velocity than the West Rand Group rocks, giving rise to a shadow zone. In order to produce a wave group with a large amplitude and a short travel-time curve between 150 and 180 km, a velocity gradient of ca. 0.045 km/s/km is required in the upper crystalline basement. The velocity gradient zone commences at a depth of ca. 8 km, and is about 10 km thick. The lower crust (18-33 km) has a uniform velocity of ca. 6.6 km/s.

Moho is modelled at a depth of ca. 35 km. The crust-mantle transition is modelled by a gradient zone 2 km thick in which the velocity increases linearly from 6.8 km/s with a gradient of 0.5 km/s/km. This zone produces $P_m P$ reflections, with the critical distance at ca. 100 km. The low dominant frequency and long duration observed for this wave group cannot be reproduced by the raytracing programme. The P_n phase is observed to have large amplitudes at offsets greater than 200 km. In order to produce this feature, a zone 10 km thick and with a gradient of 0.01 km/s/km was introduced below the Moho.

The S-wave model is shown in Figure 5.7B. Calculation of the S-wave velocities from the P-wave model, assuming a Poisson's ratio of 0.25, does not completely satisfy the observed data.

The most prominent wave group on the observed record section (Figure 5.2C) is the $S_m S$ phase. Keeping the reflector at a depth of 35 km, an average crustal velocity of 3.8 km/s is required to match the observed travel-time curve. In order to maintain consistency with the better constrained P-wave model, the upper crystalline crust was assigned a velocity of 3.66 km/s at a depth of 6 km, increasing gradually (0.015 km/s/km) with depth. There is no evidence for a S-

wave caustic due to a steep velocity gradient. A velocity of 3.86 km/s was assigned to the lower crust (18-35 km). If the Moho is fixed at a depth of 35 km, the S_n phase is best modelled using a velocity of ca. 4.5 km/s. However, the observed S_n velocities are somewhat higher (4.7 km/s). In order to match the observed S_n travel-time curve it is necessary to increase the Moho depth to 39 km. A discontinuity at a depth of 33 km, marking an increase in S-wave velocity to 4.3 km/s, produces both the $S_m S$ phase and the arrivals mid-way between the S_n and $S_m S$ phases. Consequently the S-wave crust-mantle transition appears to take place over ca. 4 km. The rather weak amplitudes of the S_n phase are modelled by a low Moho velocity gradient.

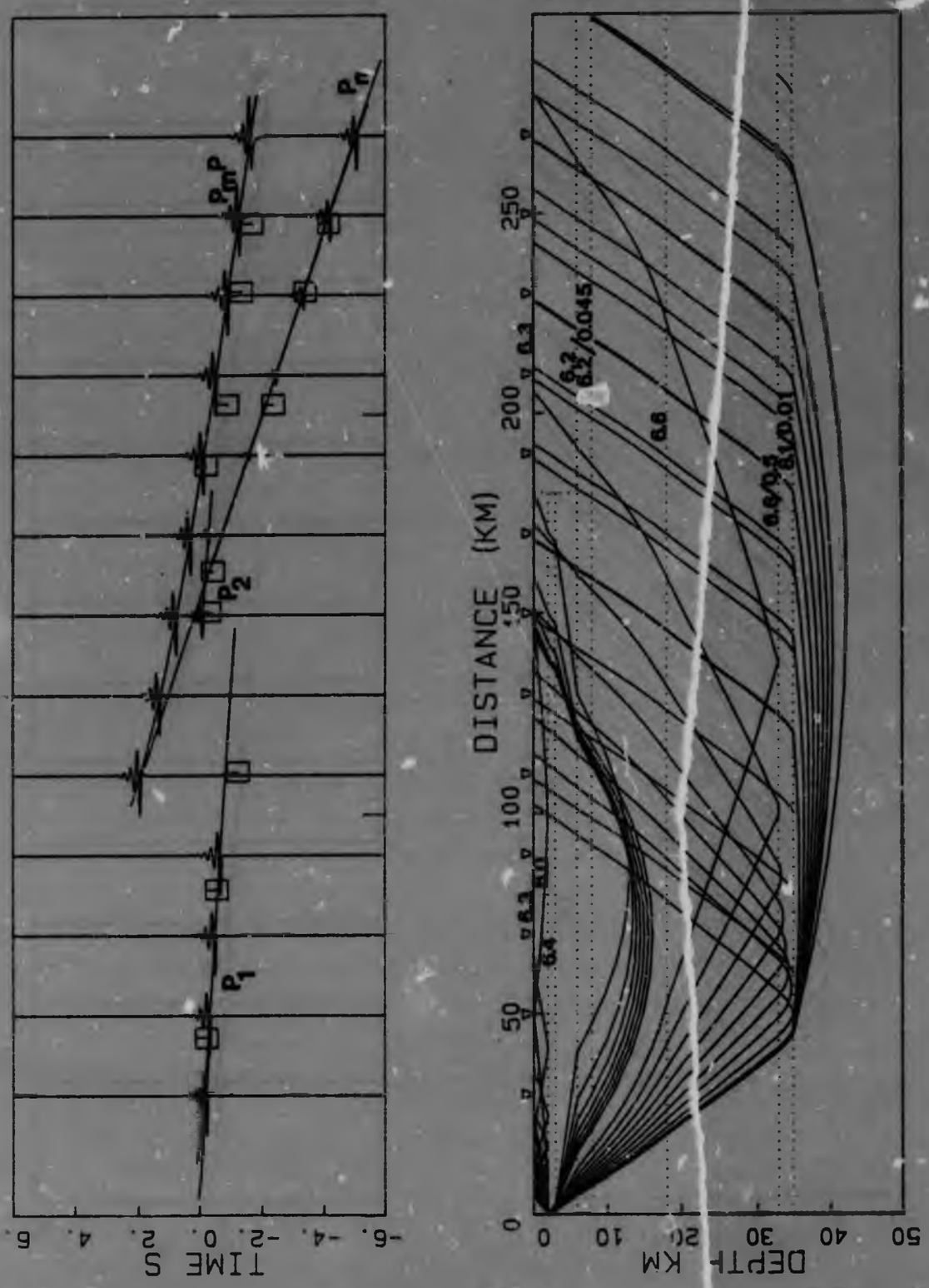


Figure 5.7A. P-wave velocity model, raytrace diagram and synthetic record section for the Klerksdorp - East Rand - Witbank profile. Tremors from the Klerksdorp goldfield.

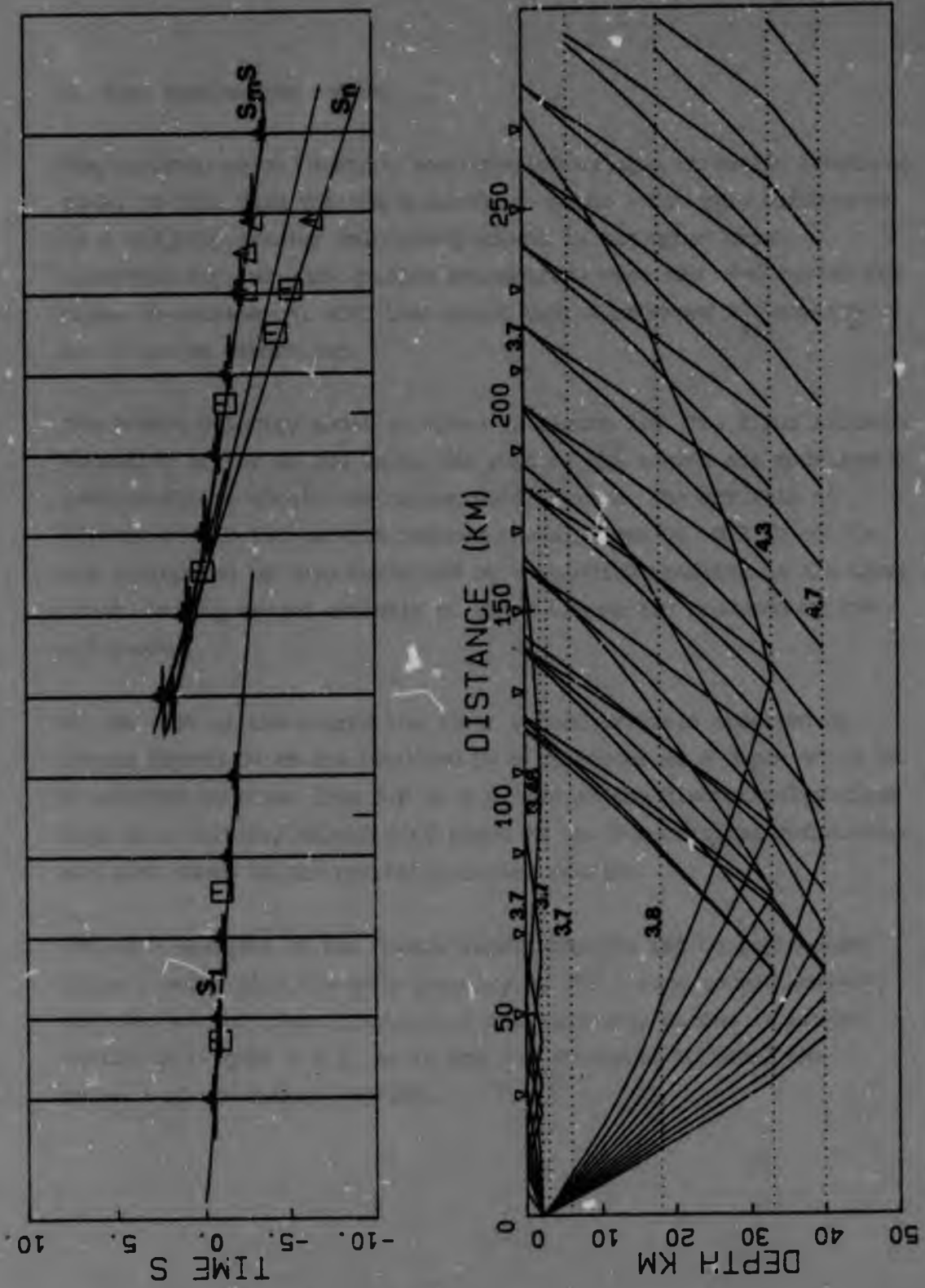


Figure 5.7B. S-wave velocity model, raytrace diagram and synthetic record section for the Klerksdorp - East Rand - Witbank profile. Tremors from the Klerksdorp goldfield.

2. East Rand source region

The observed record section was modelled using a virtually identical model to that used for the Klerksdorp source - the only difference is a slightly greater velocity gradient in the upper crust. Unfortunately, no good quality seismograms were recorded beyond the cross-over distance, with the result that a reversed P_n velocity could not be determined.

The P-wave velocity model is shown in Figure 5.8. The first arrivals extending as far as 100 km to the west of the source are modelled by reverberations within the supracrustal strata. The arrivals at offsets of 110-130 km with reduced travel-times of -0.1 to -0.3 s are reproduced by rays refracted by a velocity gradient in the upper crust. Strong second arrivals on these traces are produced by the $P_m P$ phase.

To the east of the source the clear second arrivals observed on traces beyond 50 km are produced by a reflector at a depth of 14 km. A velocity increase from 6.0 to 6.6 km/s at the discontinuity gives rise to a critical distance of about 70 km. Sub-critical reflections are also shown on the synthetic record section.

The main features of the S-wave record section can be reproduced using a model with the same geometry as the P-wave model. However, correlation and identification of the secondary phases is rather uncertain (Figure 5.2C), so it was not attempted to model the details of the record section.

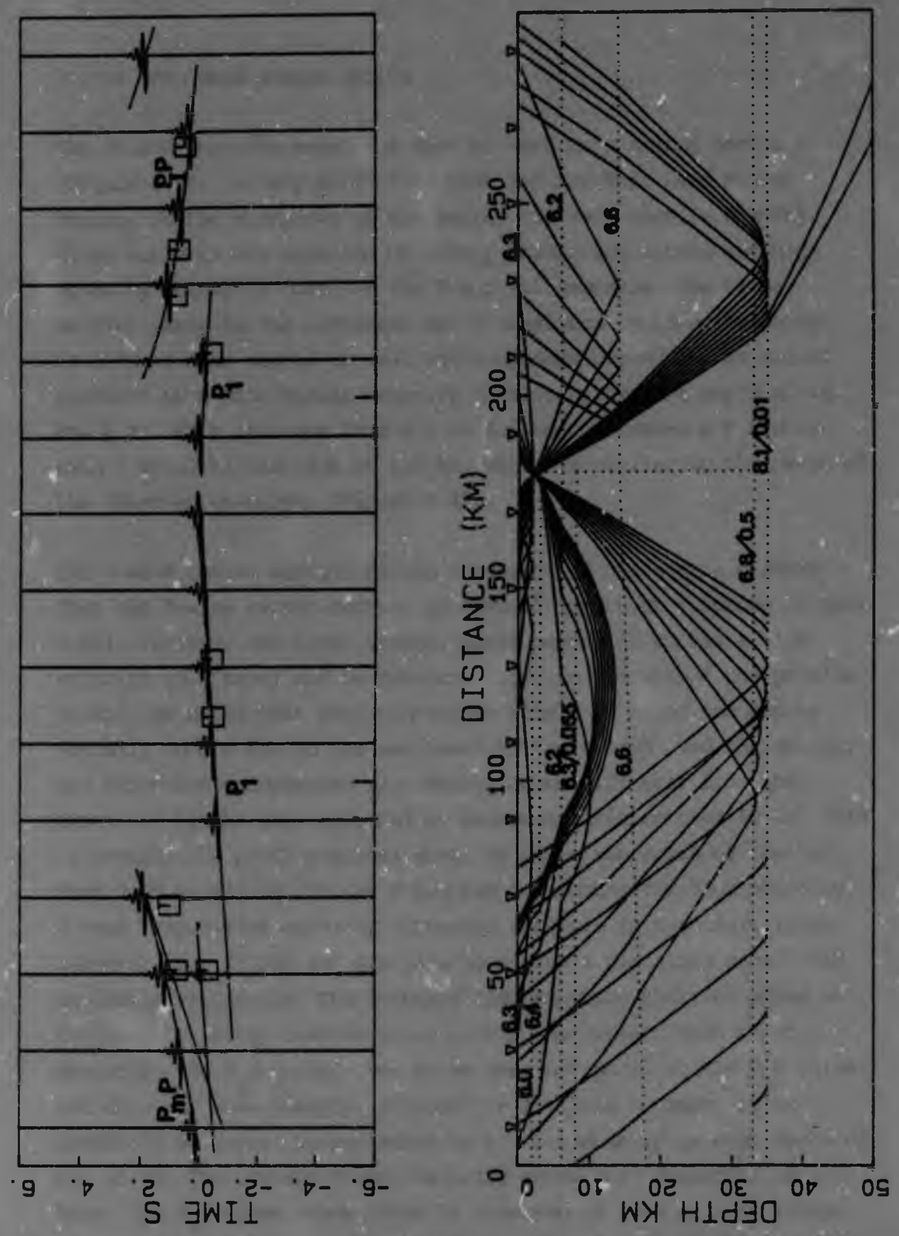


Figure 5.8. P-wave velocity model, raytrace diagram and synthetic record section for the Klerksdorp - East Rand - Witbank profile. Tremors from the East Rand goldfield.

3. Far West Rand source region

The P-wave velocity model for the Far West Rand source region (Figure 5.9A) is very similar to that for the East Rand source region. To the southwest of the source the very fast (6.8 km/s) first arrivals are modelled by energy travelling within the high velocity dolomitic rocks of the Transvaal Sequence. The first arrival phase to the northeast has a considerably lower velocity (6.2 km/s). The second arrival which appears beyond 100 km can be produced by a mid-crustal velocity discontinuity at a depth of 18 km. A velocity increase from 6.2 to 6.6 km/s produces a $P_I P$ phase with a critical distance of 110 km, which is similar to the onset of the observed wavegroup (Figure 5.4B).

The S_I-wave record section to the northeast of the source differs from the P-wave record section in several important respects (Figure 5.9B). Firstly, the first arrival phase beyond 60 km has a high velocity (3.8 km/s) and is detected right to the end of the profile. It must be noted that the seismograms within 50 km of the source actually form a fan to the southeast of the source, and the geology and structure encountered is probably quite different from that traversed by the rays recorded at distances greater than 60 km. This is because the profile passes about 20 km to the south of the Far West Rand goldfield. It was attempted to produce the high velocity S-wave travel-time curve by refracted arrivals in the crystalline basement, but it was not possible to derive a plausible model with realistic velocities. The raytrace diagram shows that the phase is produced by energy reverberating within the supracrustal strata. Secondly, the $S_I S$ travel-time curve does not parallel the $P_I P$ curve, but dips far more steeply. In order to fit this segment, it is necessary to place the reflector at a substantially greater depth of ca. 25 km. The average S-wave velocity above the reflector is 3.8 km/s. The $S_I S$ travel-time curve is observed to have a short length (from 120 to 150 km) and also to be characterised by high amplitude arrivals. Consequently this wavegroup was modelled as originating from a velocity gradient zone. In order to maintain consistency with the P-wave model, a gradient of 0.05 km/s/km is introduced at a depth of 18 km, and continues to a depth of 25 km. The lower crust

3. Far West Rand source region

The P-wave velocity model for the Far West Rand source region (Figure 5.9A) is very similar to that for the East Rand source region. To the southwest of the source the very fast (6.8 km/s) first arrivals are modelled by energy travelling within the high velocity dolomitic rocks of the Transvaal Sequence. The first arrival phase to the northeast has a considerably lower velocity (6.2 km/s). The second arrival which appears beyond 100 km can be produced by a mid-crustal velocity discontinuity at a depth of 18 km. A velocity increase from 6.2 to 6.6 km/s produces a P_IP phase with a critical distance of 110 km, which is similar to the onset of the observed wavegroup (Figure 5.4B).

The S-wave record section to the northeast of the source differs from the P-wave record section in several important respects (Figure 5.9B). Firstly, the first arrival phase beyond 60 km has a high velocity (3.8 km/s) and is detected right to the end of the profile. It must be noted that the seismograms within 50 km of the source actually form a fan to the southeast of the source, and the geology and structure encountered is probably quite different from that traversed by the rays recorded at distances greater than 60 km. This is because the profile passes about 20 km to the south of the Far West Rand goldfield. It was attempted to produce the high velocity S-wave travel-time curve by refracted arrivals in the crystalline basement, but it was not possible to derive a plausible model with realistic velocities. The raytrace diagram shows that the phase is produced by energy reverberating within the supracrustal strata. Secondly, the S_IS travel-time curve does not parallel the P_IP curve, but dips far more steeply. In order to fit this segment, it is necessary to place the reflector at a substantially greater depth of ca. 25 km. The average S-wave velocity above the reflector is 3.8 km/s. The S_IS travel-time curve is observed to have a short length (from 120 to 150 km) and also to be characterised by high amplitude arrivals. Consequently this wavegroup was modelled as originating from a velocity gradient zone. In order to maintain consistency with the P-wave model, a gradient of 0.05 km/s/km is introduced at a depth of 18 km, and continues to a depth of 25 km. The lower crust

then has a slightly lower and uniform velocity of 3.9 km/s. Moho is placed at a depth of 38 km. As this profile does not extend beyond the cross-over distance, the depth to Moho is not well constrained.

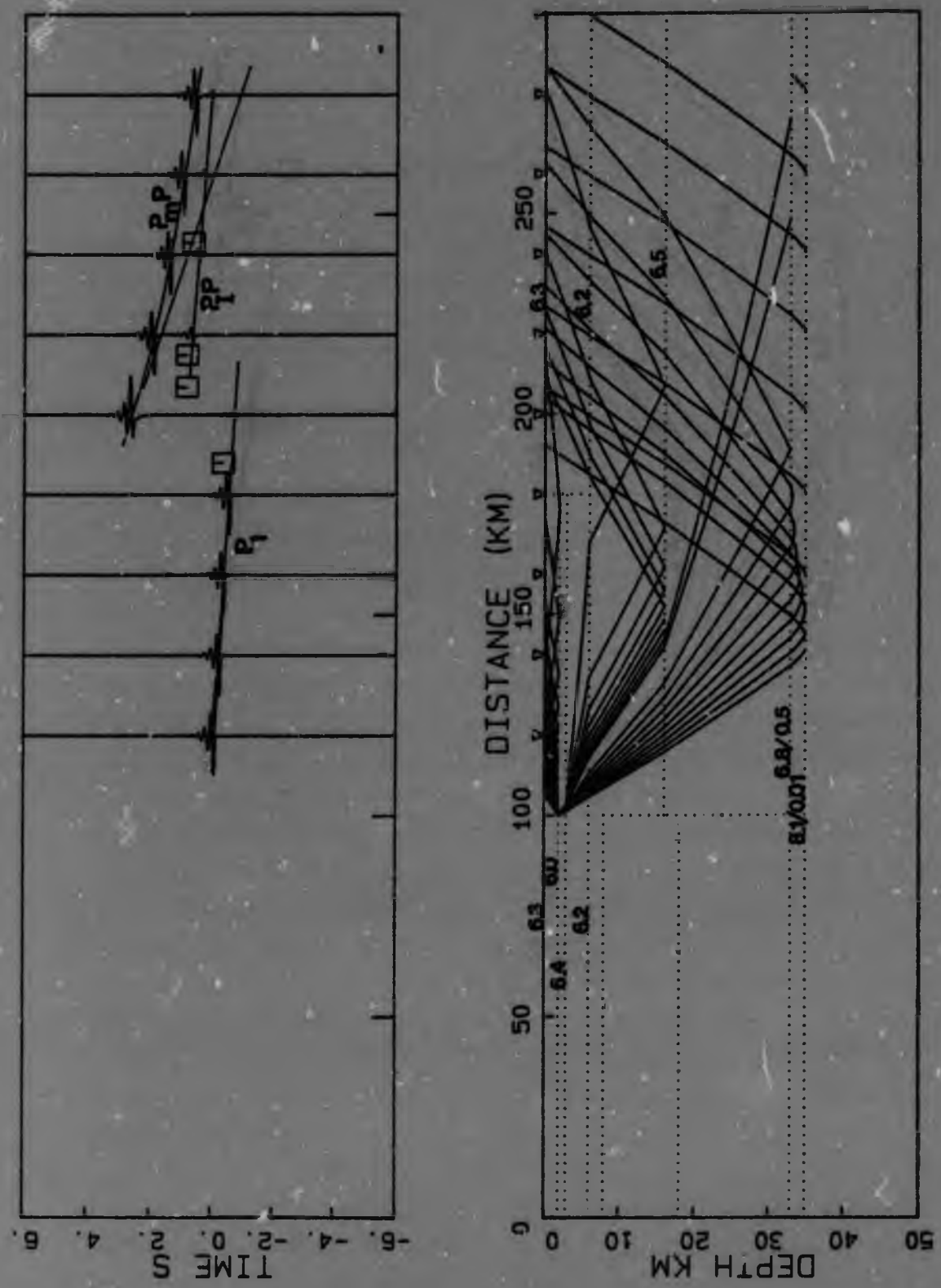


Figure 5.9A. P-wave velocity model, raytrace diagram and synthetic record section for the Klerksdorp - East Rand - Witbank profile. Tremors from the Far West Rand goldfield.

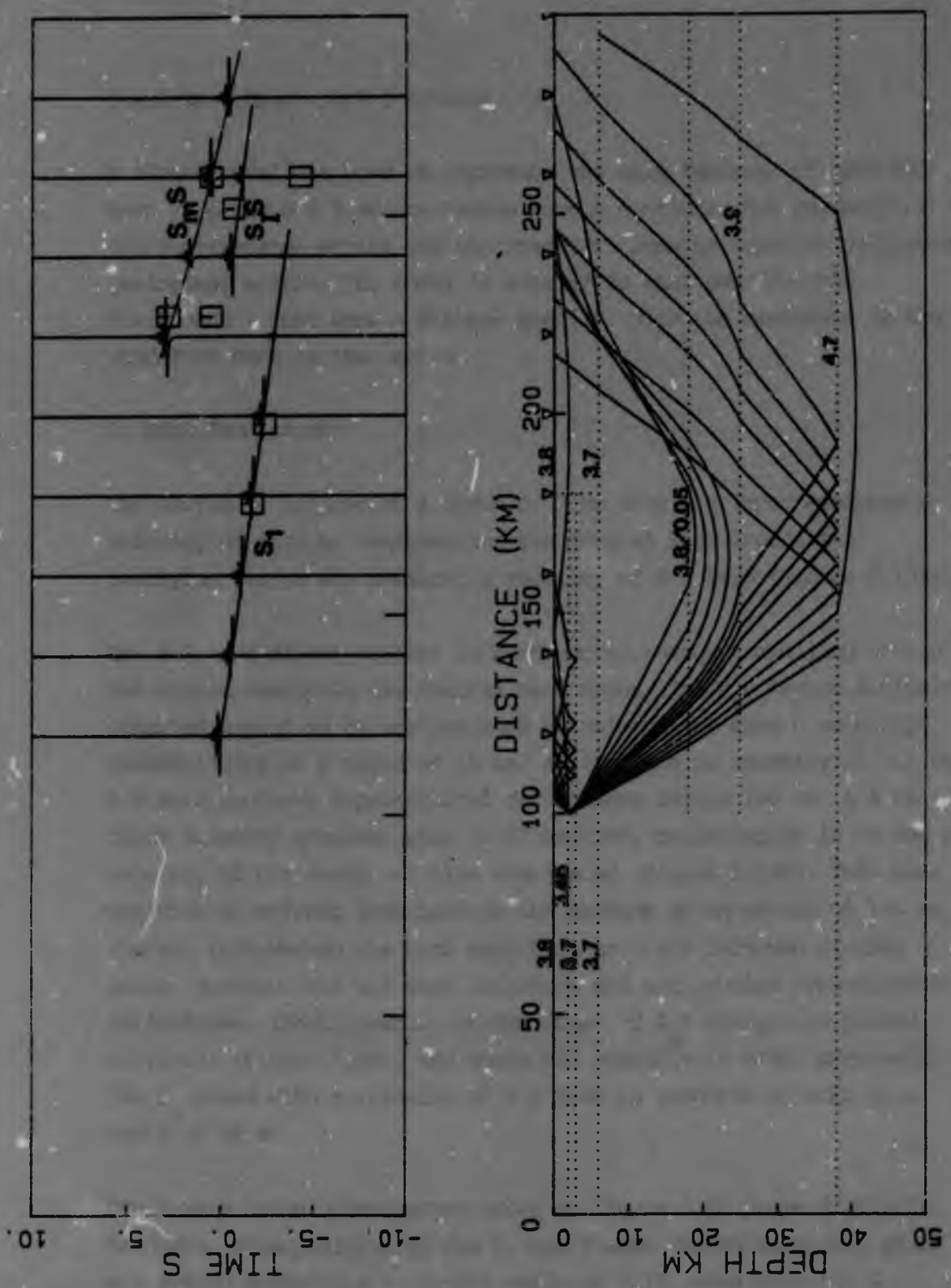


Figure 5.9B. S-wave velocity model, raytrace diagram and synthetic record section for the Klerksdorp - East Rand - Witbank profile. Tremors from the Far West Rand goldfield.

5.4.2 East Rand - O F S profile

A single model was used to reproduce the main features of both the East Rand and O F S source region record sections. The geometry of the supracrustal strata and the Vredefort Dome is based on published geological models. The model is similar to that used for the Klerksdorp - East Rand - Witbank profile, with the exception of the Vredefort Dome in the centre.

1. East Rand source

The source is located at a depth of 2 km within a layer assigned a velocity of 6 km/s, representing the Central Rand Group. The overlying strata are assigned a velocity of 6.4 km/s (Figure 5.10A).

The 6.4 km/s direct arrival is produced by energy travelling within the strata overlying the Central Rand Group. The $P_I P$ second arrivals observed beyond 90 km are produced by reflections from a velocity discontinuity at a depth of 18 km. An increase in velocity of 6.1 to 6.5 km/s produces supercritical reflections beyond 100 km. A 4 km thick velocity gradient zone (0.07 km/s/km, beginning at 18 km and a velocity of 6.3 km/s) was also considered (Figure 5.10B). This zone was able to refract rays back to the surface at an offset of 150 km, thereby reproducing the high amplitude arrivals received at this point. However, the 6.3 km/s interface did not produce supercritical reflections. Identification of the onset of $P_m P$ wavegroups proved difficult (Figure 5.5B), and hence not possible to model precisely. The P_n phase with a velocity of 8.2 km/s is produced by Moho at a depth of 36 km.

The S-wave travel-time curves shown on Figure 5.5C prove difficult to model. Superposition of the P- and S-wave record sections, which are scaled assuming a Poisson's ratio of 0.25, show that the S_n phase is significantly earlier than the P_n phase (by about 1.2 s on the S-wave record section). In addition, the S_n phase is earlier than the reciprocal time on the reversed (O F S source) record section by a 0.7 s. Re-examination of Figure 5.5C shows that the correlation of S_n phases is not very clear, but no other more

convincing alternative is apparent either. I have not found it possible to derive a consistent model from this record section.

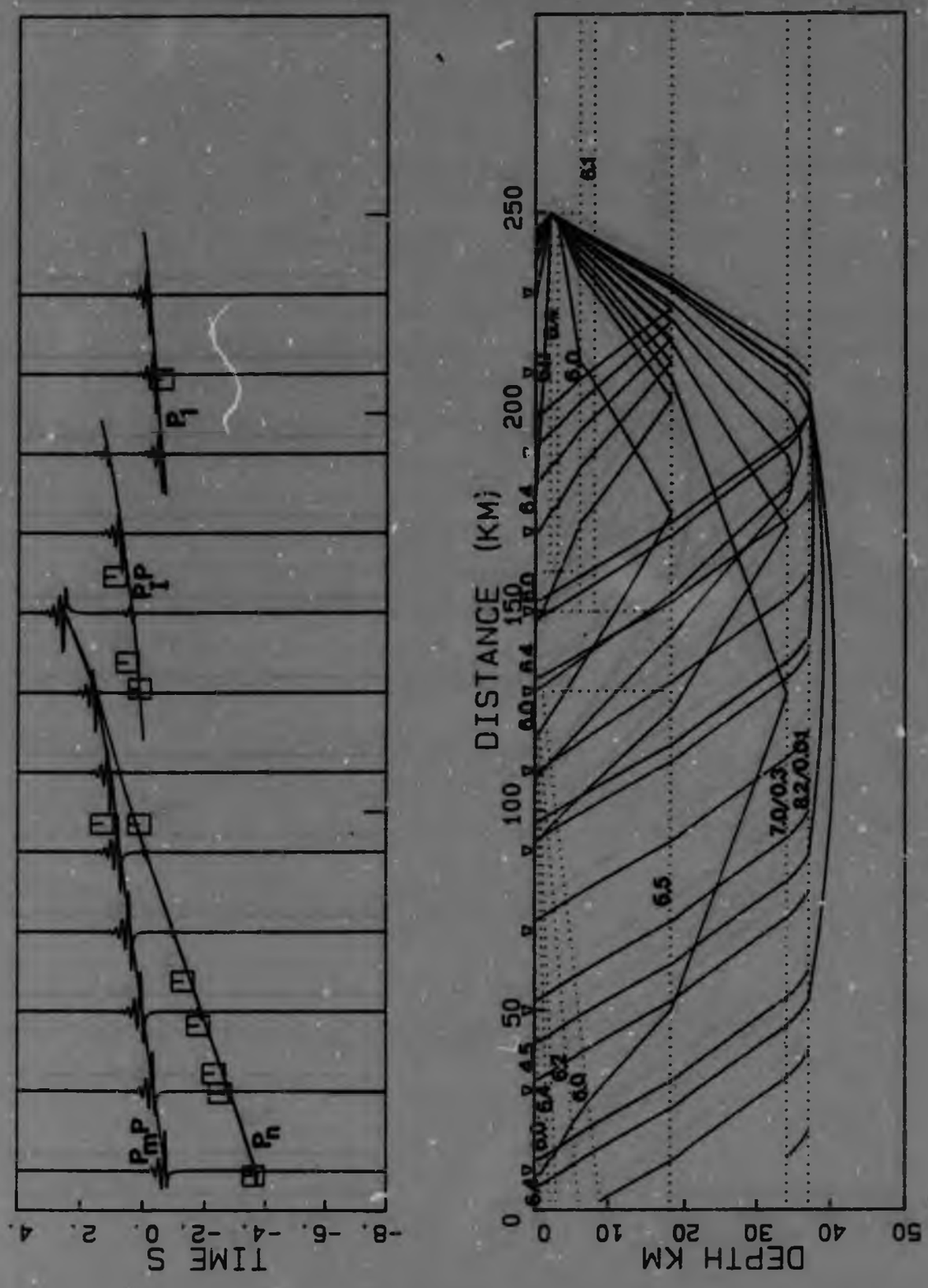


Figure 5.10A. P-wave velocity model, raytrace diagram and synthetic record section for the O. F. S. - East Rand profile. Tremors from the East Rand goldfield.

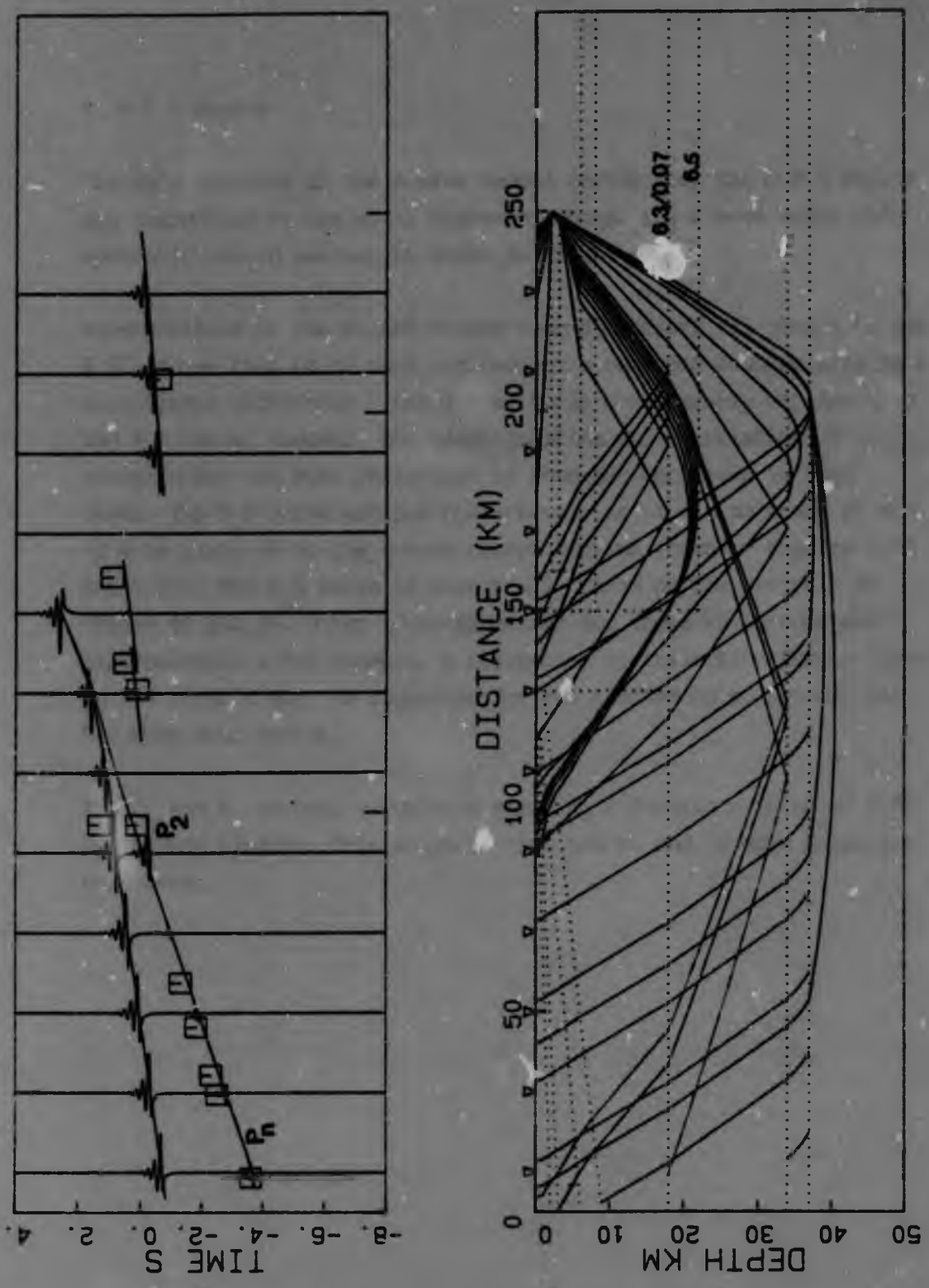


Figure 5.10B. P-wave velocity model, raytrace diagram and synthetic record section for the O. F. S. - East Rand profile. Tremors from the East Rand goldfield. The velocity model is identical to Figure 5.10A, except that the mid-crustal velocity discontinuity is replaced by a velocity gradient.

2. O F S source

The main features of the P-wave record section for the O F S source are reproduced by the model discussed above. The P-wave model and synthetic record section is shown in Figure 5.11.

Superposition of the S- and P-wave record sections (Figures 5.6B and 5.6C) shows them to be very similar, with only one feature showing a significant difference - the $S_m S_m$ curve is considerably earlier than the $P_m P_m$ curve. However, the identification and correlation of arrivals for the Moho reflection is somewhat uncertain in both cases. The $S_m S_m$ curve matches the arrivals at -1.6 s on trace #7 and -2 s on trace #6 on the P-wave record section (compare Figures 5.6B and 5.6C). The $S_m S_m$ curve is essentially based on the arrivals on traces #5 and #6. Other identifications for these wavegroups are also possible - for example, a refraction or reflection from a layer in the lower crust, as suggested for the Klerksdorp source and the Far West Rand source.

The P_n and S_n curves, calculated assuming a Poisson's ratio of 0.25, match very closely. This suggests that the P- and S-wave Mohos are coincident.

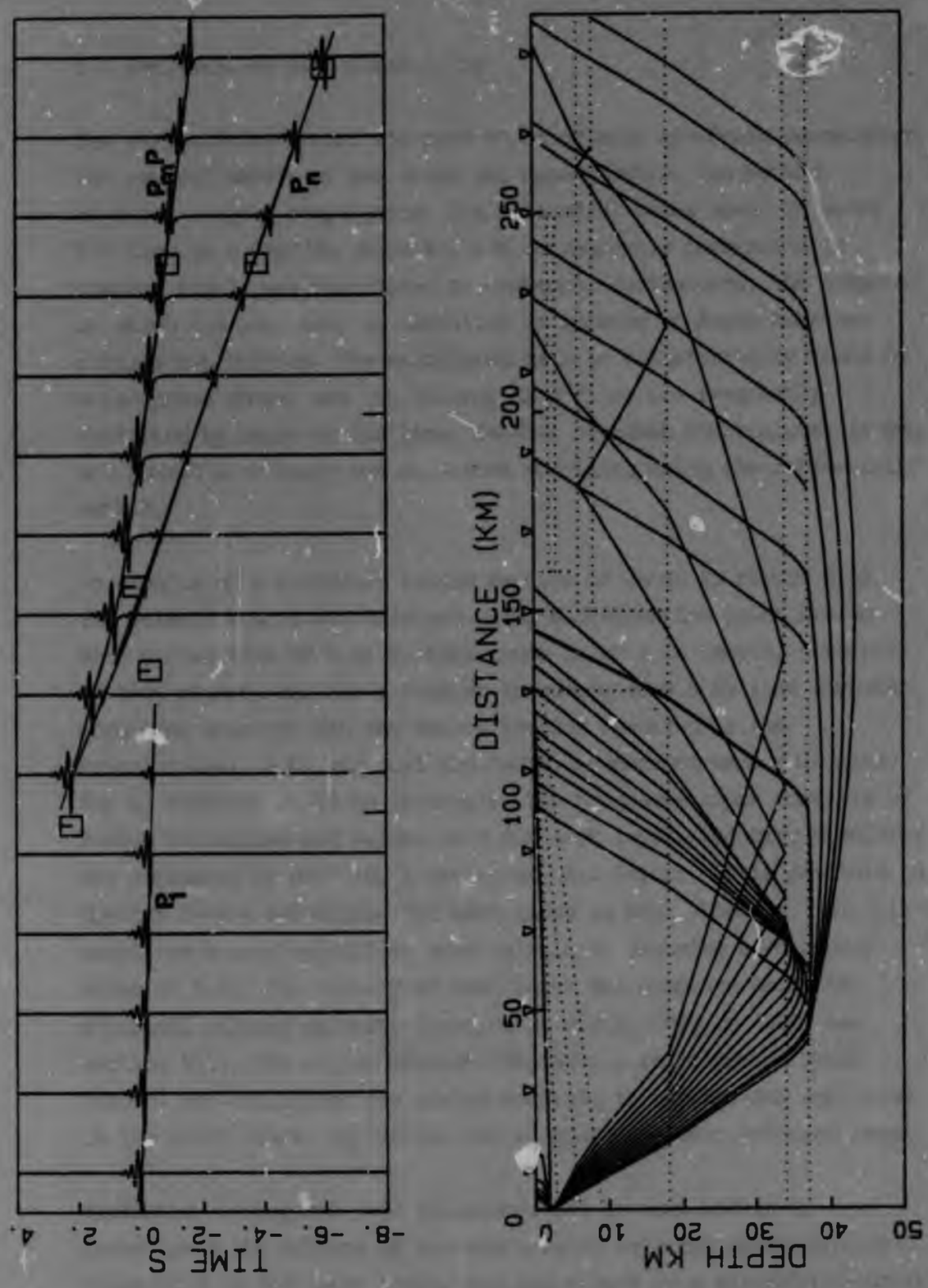


Figure 5.11. P-wave velocity model, raytrace diagram and synthetic record section for the O. F. S. - East Rand profile. Tremors from the O. F. S. goldfield. Velocity model identical to Figure 5.10A.

5.5 Reflectivity method modelling

The reflectivity method was used to calculated synthetic seismograms for several models of the crust and upper mantle. The method requires lengthy computation. A single model takes about 30 hours CPU time on a Vax 780 computer, and consequently permission to compute models was restricted to weekends. Furthermore, the computer on which the programme is installed is located at Anglo-American Corporation offices. The calculated data is transferred by means of a telephone modem, and the lengthy data files are frequently corrupted by noise on the line. Because of these constraints, it was not possible to carry out extensive modelling using the reflectivity method.

An example of a synthetic record section is shown in Figure 5.12. The seismic source was modelled using a dislocation point source with a rise time of 0.05 s. Each trace is 60 s in length, consists of 2048 points, and has a Nyquist frequency of 8.5 Hz (the computer programme does not use the entire Fourier spectrum in its calculations). Both vertical and radial components were calculated for 13 stations at 25 km intervals. The programme input consists of P-wave velocities and values of Q for each layer. Velocity gradients are simulated by defining a series of thin layers. It is possible to specify S-wave velocities for each layer as well. However, for this model the S-wave velocities were calculated assuming a Poisson's ratio of 0.25. The density of each layer was computed using the empirical density-velocity function of Birch (1964, p 4380, see section 5.1). The output wavelet simulates a short period WWSSN record. The amplitudes are scaled accoring to the maximum amplitude on the first trace. Amplitudes are clipped at a user selected level.

Synthetic seismograms were calculated for several models to investigate the effects of the mid-crustal velocity gradient, the value of Q in the lower crust, and the effect of a sub-Moho velocity gradient. It was found that the amplitude of the head wave increases as the sub-Moho velocity gradient is increased.

Figure 5.12A shows the velocity model and full record section. The

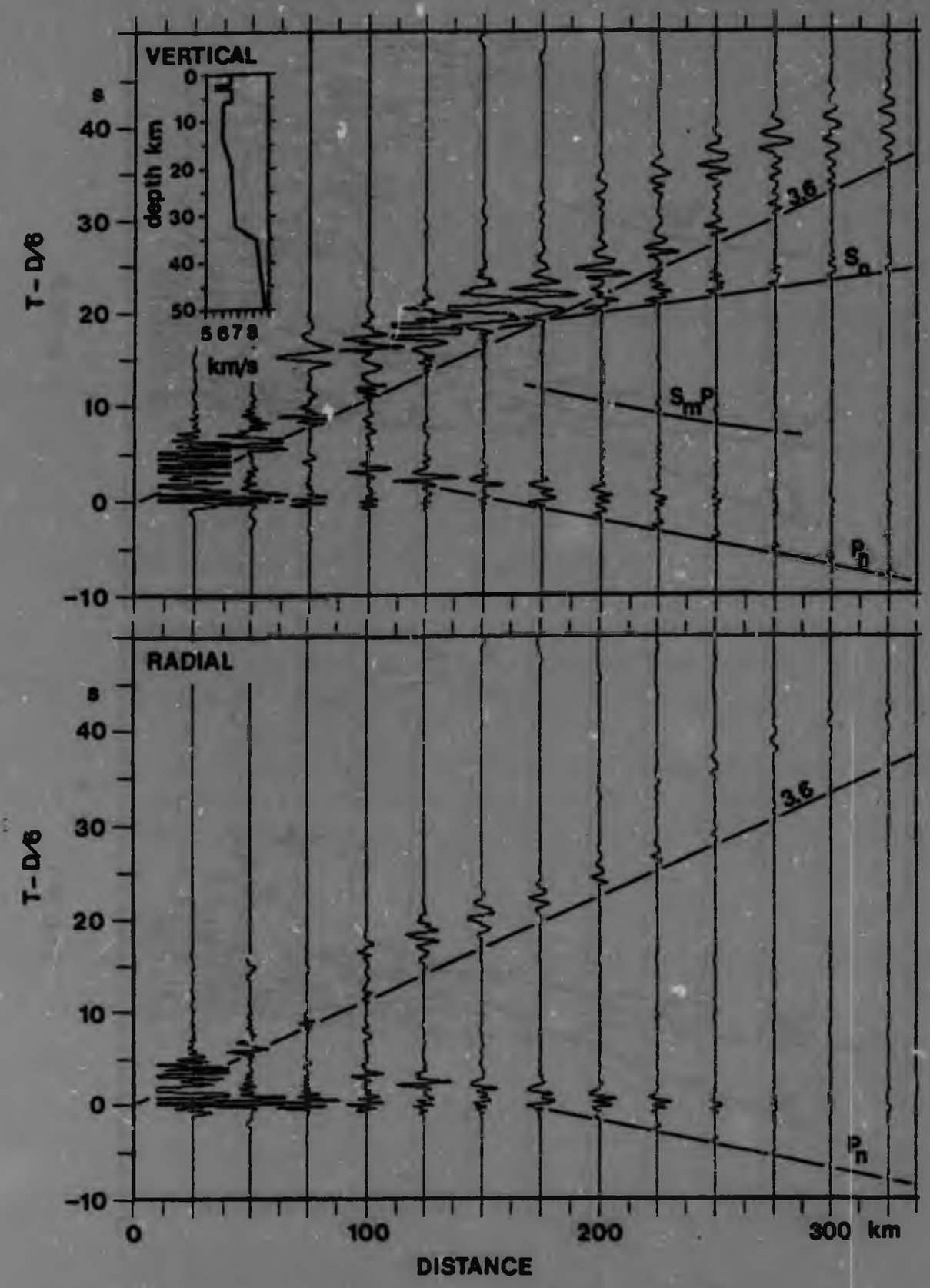


Figure 5.12A. Synthetic record section for a 1-D model of the Kaapvaal Craton computed using the reflectivity method.

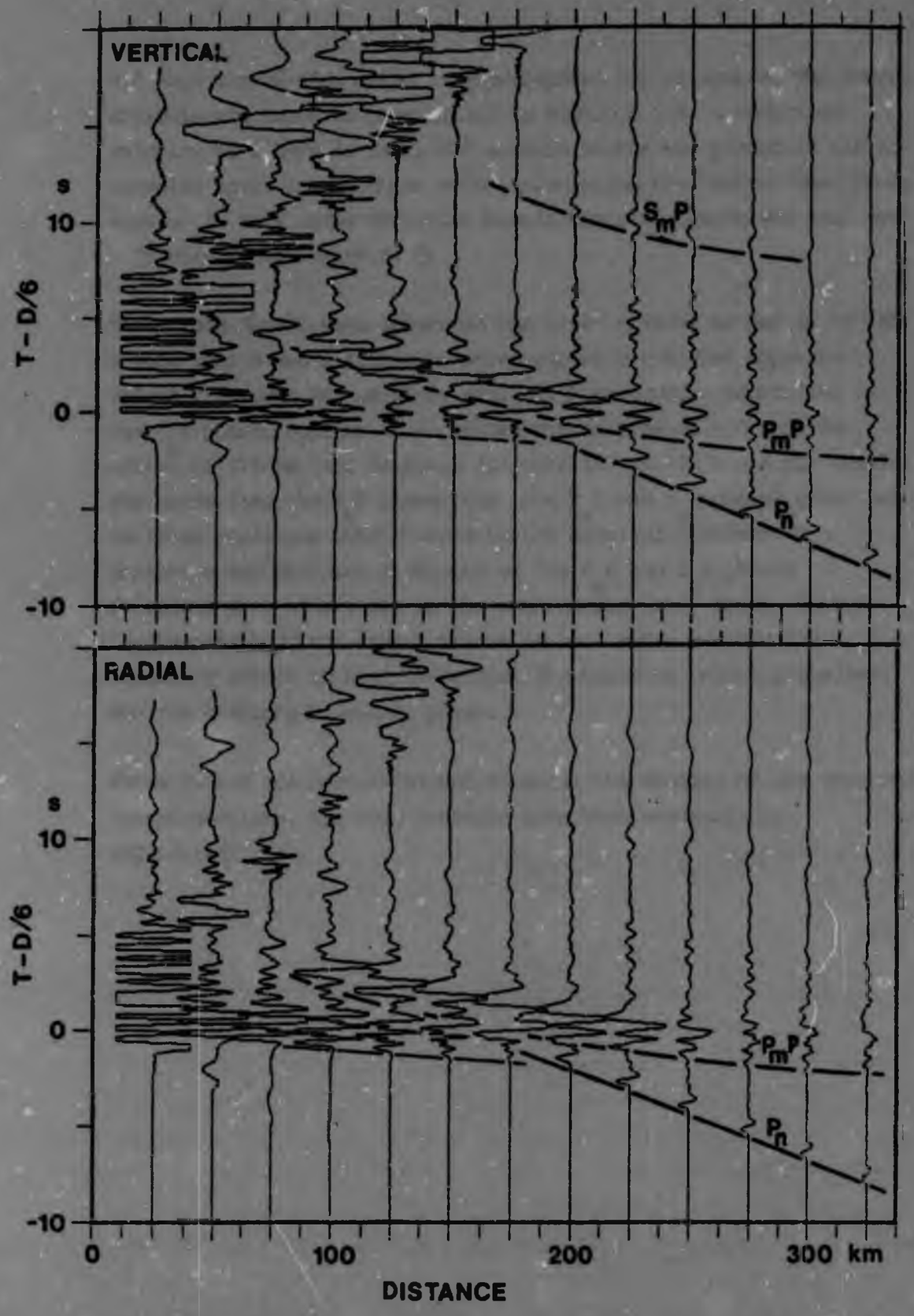


Figure 5.12B. Detail of the P-wave arrivals on the synthetic record section for a 1-D seismic velocity model of the Kaapvaal Craton computed using the reflectivity method.

3.6 km/s travel-time curve is superimposed for reference. The P-wave arrivals are shown in more detail in Figure 5.12B. A reduction velocity of 6 km/s is used. The seismic source was placed in the low velocity layer in the upper crust, simulating the Central Rand Group strata. In this model the crust-mantle transition zone was assigned a relatively low value of Q.

The strong direct wave occurs as the first arrival as far as 100 km. Beyond this a small amplitude wavegroup with a higher apparent velocity emerges as the first arrival. A wavegroup, identified as the $S_m P$ phase, appears at a reduced travel time of +10 s at an offset of 175 km, and persists for over 100 km. It has a far smaller amplitude than the $P_m P$ phase. Both the $P_m P$ and $S_m S$ phases give rise to large amplitude events close to the critical distance. The amplitude and dominant frequency of the $P_m P$ and $S_m S$ phases decreases with offset due to the attenuating lower crust. However the bandwidth of the output traces is too narrow to show the frequency effect to best advantage. The sub-Moho velocity gradient ensures a strong P_n and S_n phase.

While it has not been attempted to model the details of the observed record sections, the main features have been successfully reproduced.

6. TRANS-WITWATERSRAND BASIN DEEP SEISMIC REFLECTION PROFILE

6.1 Objectives

Deep seismic profiling aims at obtaining reflections at near-normal incidence from crystalline rocks in the crust and upper mantle, using the techniques developed by the oil industry for mapping structures in sedimentary rocks. The possibility of obtaining deep reflections was demonstrated in the 1950's and 1960's in the USA (Junger 1951; Widess and Taylor, 1959), Germany (Dohr and Fuchs, 1967) and Canada (Kanesewich, 1965). Deep seismic profiling provides information that is both geophysical and geological in character: not only are models of seismic velocity and attenuation derived; but it is also possible to determine the extent and configuration of reflecting horizons and, sometimes, to trace them to the surface or to a borehole and so identify them.

During the past decade deep reflection profiling has produced new insights into continental structure and evolution due to the establishment of national programmes in north America (COCORP, CALCRUST and LITHOPROBE), Europe (BIRPS, ECORS and DEKORP) and Australia (ACORP). The first deep profile in southern Africa was acquired in 1985 on the Agulhas Bank by Soekor (Durrheim, 1987), and in 1987 a profile across the Limpopo Province was acquired under the auspices of the National Geophysics Programme.

A 112 km, 16 s two-way-time (TWT), seismic reflection profile, stretching from the Ventersdorp Dome, across the Potchefstroom syncline and terminating in the centre of the Vredefort Dome, was acquired during August 1988 for the National Geophysics Programme and the Geological Survey of South Africa. The team which proposed the profile consisted of staff members of the Departments of Geology and Geophysics and the Bernard Price Institute for Geophysical Research (all of the University of the Witwatersrand) under the leadership of Prof L O Nicolaysen. The author was a member of a four person group responsible for supervising the acquisition and data processing by Rockplan (Pty) Ltd.

The objectives of the trans-Witwatersrand Basin deep seismic reflection profile are the following:

a) The profile will illustrate the regional framework in which the basin is set. The crystalline crust and mantle underneath the basin will be compared with the corresponding features outside the basin in order to establish whether a sub-basin geological feature exists which has led to the lengthy period of episodic sedimentation and their preservation in this particular locale.

b) The style of mechanical adjustment which must have taken place on a regional scale during basin subsidence is to be investigated. The profile will reveal whether basining was controlled by a deep-seated array of faults, or whether a quasi-plastic necking in the deep crust took place. The fundamental question to be answered is whether the faulting affecting the supracrustal strata penetrates through the crust, or if a decoupling horizon has developed (Wernicke, 1986).

c) The profile will provide information concerning the structure and tectonic evolution of the supracrustal strata (Dominion, Witwatersrand, Ventersdorp and Transvaal) preserved in the Potchefstroom syncline. The dramatic deformation accompanying the Vredefort event is of particular interest, especially the geometry of the overfolded Vredefort collar rocks.

While the reflection profiling method is able to provide high-resolution images of the geometry of deep crustal reflectors which are critical to inferences concerning the evolution of the continental crust, the method is unable to define what physical properties produce these reflections or to yield accurate depths to interfaces within the crust. Wide-angle refraction profiling is able to provide this complementary information. Coincident seismic reflection/refraction experiments have the unique ability to image lithospheric structure and to provide information necessary to infer the composition and physical state of the continental crust (Mooney and Brocher, 1987). The trans-Witwatersrand Basin reflection profile intersects both the Klerksdorp - Witbank and O F S - East Rand refraction profiles, enabling joint interpretation to be carried out. The synthesis of the reflection and refraction data sets is described in chapter 7.1.

6.2 Acquisition parameters

Field trials were carried out during April 1988 in the Kroonstad district over a profile 6 km in length. The trials were sponsored by Gencor. The acquisition parameters are noted in Table 6.1. The data were processed using parameters routinely applied by Gencor to Witwatersrand Basin data. We were given access to the record section from 2 - 24 s TWT. Between 2 - 6 s there are prominent reflectors, probably due to supracrustal strata. From 6-10 s there are many short reflecting segments. At 11.8-12.3 s there is another band of reflecting segments, which was interpreted to be the reflection Moho. From 12.3 s to 24 s there are scarcely any reflectors, with the exception of a few scattered segments near 19 s.

Table 6.1. Acquisition parameters for the deep seismic reflection field trials conducted in the Kroonstad district.

SOURCE	
Type	5 in-line Failing Y2700 vibrators
Sweep length	30 s
Sweep range	8 - 60 Hz
Repeat sweeps	8
Spacing	100 m
SPREAD	
Geophone groups	120
Spacing	25 m
Geometry	end on
Spread length	3 km
CDP coverage	0 - 30 - 0 fold
RECORDING	
Sampling	4 ms
Listening time	54 s
Record length	24 s

It was found that the very low frequency end of the vibrator sweep caused considerable damage to the waterlogged gravel roads on which the vibrators operated. Band-pass filtered sections showed that the data was not degraded in any way by eliminating the frequencies

below 15 Hz.

The acquisition parameters for the trans-Witwatersrand Basin line were determined after consideration of the field trial, and a cautious attempt to "trade-off" between the length of the line and acquisition parameters which affect data quality and the final section (the number of repeat sweeps, the fold of the stack, the sweep length and listening time). The geophone group interval was limited to 50 m as longer cable lengths could not be supplied by the only contractor operating in southern Africa. The acquisition parameters used for the entire profile are listed in Table 6.2.

Table 6.2. Acquisition parameters for the trans-Witwatersrand Basin deep seismic reflection profile.

SOURCE	
Type	5 in-line Failing Y2700 vibrators, 10m pad separation
Sweep length	28 s
Sweep range	12 - 61.5 Hz
Repeat sweeps	6, 4m move-up between sweeps, pattern centered between stations
Spacing	100 m
SPREAD	
Geophones	SM4/UB, 10Hz
Geophone groups	120
Geophone pattern	24 geophones/array
Station interval	50 m
CDP interval	25 m
Geometry	split straddle 3225-(50)-275-0-275-(50)-3225
Spread length	6.45 km
CDP coverage	0 - 30 - 0 fold nominal
RECORDING	
Sampling	4 ms
Listening time	44 s
Record length	16 s
Low-cut filter	out
High-cut filter	62.5 Hz, 72db/Oct
Notch	out
Tape format	SEG-D, 9 track

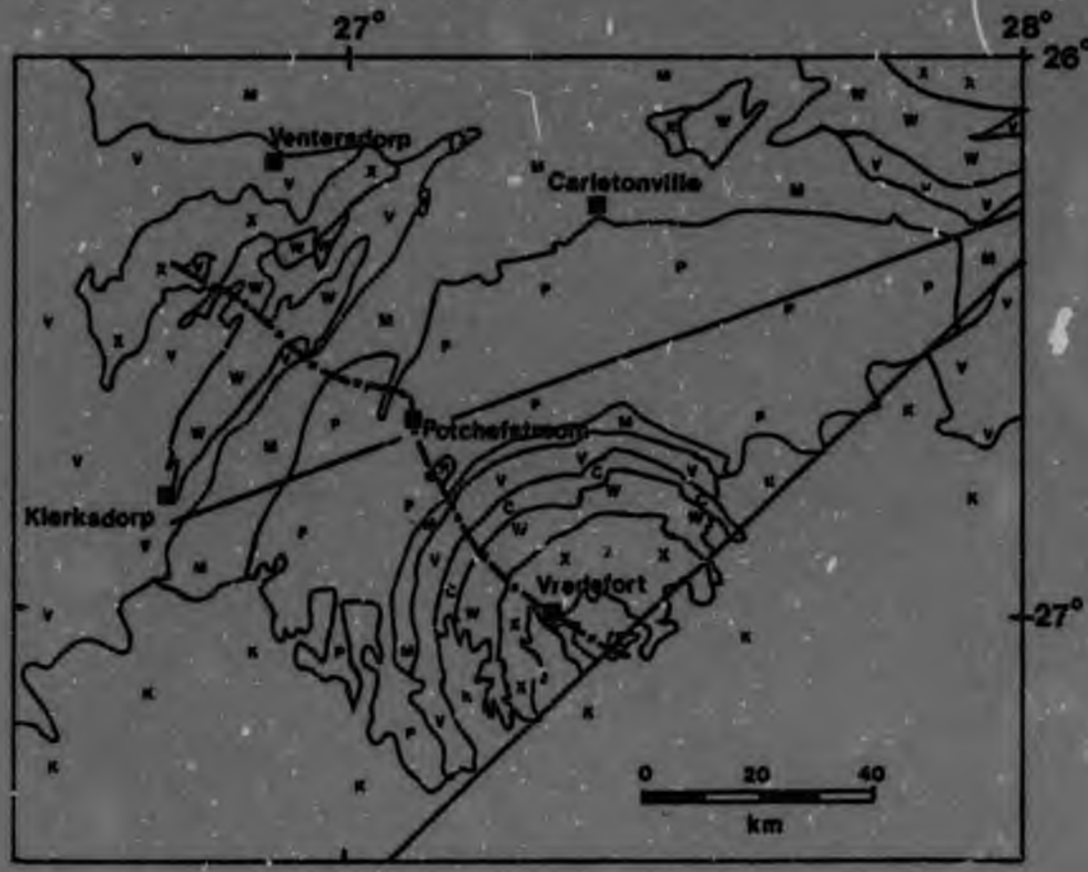


Figure 6.1. Location of the deep reflection seismic profile. The reflection profile is shown by a chained line, and the refraction profiles by solid lines. Geology: X - Basement Complex, W - Dominion and West Rand Groups, C - Central Rand Group, V - Ventersdorp Supergroup, M - Black Reef Formation and Malmani Subgroup, P - Pretoria Group, K - Karoo Sequence, R - Roodekraal Complex.

Data acquisition proceeded without incident. It took 18 field days to complete the 112 km profile (Figure 6.1). Acquisition commenced at the northwestern end of the line, near the town of Ventersdorp. Some degradation of data quality was experienced when passing over the outcropping dolomitic rocks of the Transvaal Sequence, which are known to have an extremely irregular bedrock surface, and are sometimes cavernous. This results in strong scattering of the energy in the near surface, which may completely swamp the deeper reflections (March, 1988). Undershooting was used to pass through the town of Potchefstroom and Vredefort, resulting in a reduction of CDP coverage. When passing through the mountainous collar of the Vredefort structure, crooked roads also resulted in a reduction of coverage.

It had been originally planned to sum the repeat sweeps in the field and correlate in the processing centre. However, a hardware malfunction made field summation impossible, and both steps had to to be carried out at the processing centre. Consequently, the entire set of over 200 field tapes is available for reprocessing.

A brute stack of the first 30 km of the profile was examined while the survey was in progress. The data appeared to be of good quality, and many strong, continuous reflectors were apparent. However, it was decided not to gain and reduce the fold of the stack in an attempt to increase the line length, but to adhere to the original acquisition parameters. This decision was subsequently vindicated, as the final section shows that the northwestern segment (which was acquired first) contains the greatest number of deep crustal reflectors. A relaxation in the acquisition parameters would have made it far more difficult to assess the degree to which changes in the basement geology are responsible for the change in the seismic character observed on the record section.

6.3 Data processing parameters

Reflection seismic data have been routinely gathered in the Witwatersrand basin by mining companies for gold and uranium exploration since 1982. The geological environment is very different to that encountered in hydrocarbon prospects, and several factors

have been identified which require a modification of the processing sequence (March, 1988).

a) The indurated Proterozoic strata have very high seismic velocities (generally greater than 6 km/s) and densities, and very low reflection coefficients (of the order of 5%) are encountered. However, attenuation is also very low, and so reflections are reliably obtained.

b) Due to the very high formation velocities, the step-out on the CDP gather is very small when compared to that encountered in oil-field prospecting, restricting the sensitivity of conventional velocity analysis. The determination of the interval velocity is consequently very error prone, and probably only reliable in the first 1 second. For the trans-Witwatersrand Basin profile we were limited by the available cable length to a spread of 6 km. A split straddle configuration was selected as we anticipated that steep and variable dips would be encountered as the profile traversed the Potchefstroom synclinorium.

c) Very little multiple activity appears to be present in the data in spite of clear primary reflections. This is probably due to the low reflection coefficients, and the fact that there is generally no significant change in reflection coefficient or general increase in seismic velocity with depth. This is in contrast to the usual oil-field geology where the shallow reflection coefficients are generally much greater than those of deep horizons and velocity increases with depth, with the result that multiple energy arriving simultaneously with the deeper reflections has travelled a smaller distance and although reflected twice, has encountered far larger reflection coefficients than the deep primary reflection.

d) The migration of data with high seismic velocity and no regular increase in velocity with depth is one of the most difficult parts of the processing. In practice it is usual to regard the velocity of the whole section as virtually homogeneous. The structure of the Witwatersrand Basin is known to be complex, and out-of-plane energy may be recorded on the section. Although gross structural information can be obtained from a migrated section, it is necessary to treat the data with caution until the interpretation can be confirmed by loop closure or a full three-dimensional survey.

e) Reflected refractions arise when the head wave generated at an interface by energy arriving at the critical angle encounters a

discontinuity such as a dyke or fault. The head wave is reflected back along the interface and continues to radiate energy back to the surface. This gives rise to an arrival on the CMP gather which is difficult to distinguish from a primary reflection. Near-vertical structures such as faults and dykes are known to be common in the mining areas, and reflected refraction arrivals are thus likely to be present in the data. At present no automated process exists to remove these arrivals from a record section.

The data processing sequence was planned taking the above considerations into account, and is described in Table 6.3. The unmigrated stacked section was released on Open File at the S A Geological Survey in January 1989. Finite-difference migration was carried out at the University of the Witwatersrand. Only the upper 8 s of the section was migrated, as the difficulty of using wave equation methods to migrate deep continental data is well known (Warner, 1987). It was found that a migration velocity of 6000 m/s was the most satisfactory, and caused many curved events to collapse to point reflectors.

Table 6.3. Data processing sequence applied to the trans-Witwatersrand Basin deep seismic reflection profile.

1. Demultiplex
2. Edit
3. Statics - field statics applied to floating datum
4. F-K filter - full on at 3000 m/s
5. Scale - whole trace equalisation followed by spherical divergence correction
6. Sort
7. Deconvolution - minimum phase predictive deconvolution
8. Scale - automatic gain control using 100 ms windows
9. NMO - revised velocities derived
10. Statics - data corrected from floating datum to regional datum of 1300 m
11. Autostatics - surface consistent residual statics
12. NMO - revised velocities applied
13. Mute
14. Statics - data corrected to regional datum
15. Autostatics
16. Autostatics
17. Stack
18. Scale - whole trace equalisation
19. Filter - time variant bandpass filter

    6-12-62-74 Hz 0 - 8000 ms

    6-12-46-58 Hz 5000 - 16000 ms
20. Coherency

6.4 Interpretation of the record section

The detailed interpretation of the structure and tectonic evolution of the supracrustal formations is beyond the scope of this thesis, and consequently the upper part of the section is only briefly described. My prime interest is in the reflection seismic signature of the crystalline basement. The geologically mapped contacts between formations were projected down dip to identify the reflections marking these interfaces, and to determine the "seismic

fabric" of each unit. Where possible, the interpretation has been constrained by borehole information. An interpretation of the record section is shown in Figure 6.2.

6.4.1 Supracrustal Strata

The strata mapped at the surface can be projected down dip with little disturbance to at least 2 s TWT (see Figures 6.3A, 6.3B and 6.3C). The Dominion and West Rand Group strata are characterised by numerous strong, continuous reflections, while the Central Rand Group is seismically transparent. The contact between the Central Rand Group and Ventersdorp Supergroup is marked by a distinct reflection. The discordance in dip between the strata of the Witwatersrand triad (Dominion, Witwatersrand and Ventersdorp rocks) and the Transvaal Sequence is clear, the unconformity being marked by another reflection. The Transvaal strata also produce continuous reflectors.

The northwestern segment of the profile shows Dominion and West Rand Group strata preserved in several half-grabens formed within the granitic basement. The strata dip to the southeast at ca. 30°. The faults forming the southeastern margins are interpreted to be reverse faults reactivated during the Ventersdorp rift episode. The fault traces appear to flatten with depth, and do not penetrate deeply into the basement. Transvaal strata are preserved in a minor syncline northwest of Potchefstroom. The onset of the major Witwatersrand Basin synclinorium is clearly evident below these Transvaal strata. Moving inward from the environs of the northwest dipping low-angle fault at Potchefstroom, structural complexity increases. The Roodekraal intrusion is marked by a seismically transparent zone which does not seem to have a large depth extent.

Although a far more complete geologic succession crops out along the collar of the Vredefort dome, this succession is only sparsely represented by reflectors. In one possible interpretation, overturned Dominion and basal West Rand Group strata are imaged by a set of reflectors which dip to the southeast within the upper 1 s TWT, and then to the northwest between 1-2 s TWT (Figure 6.4)

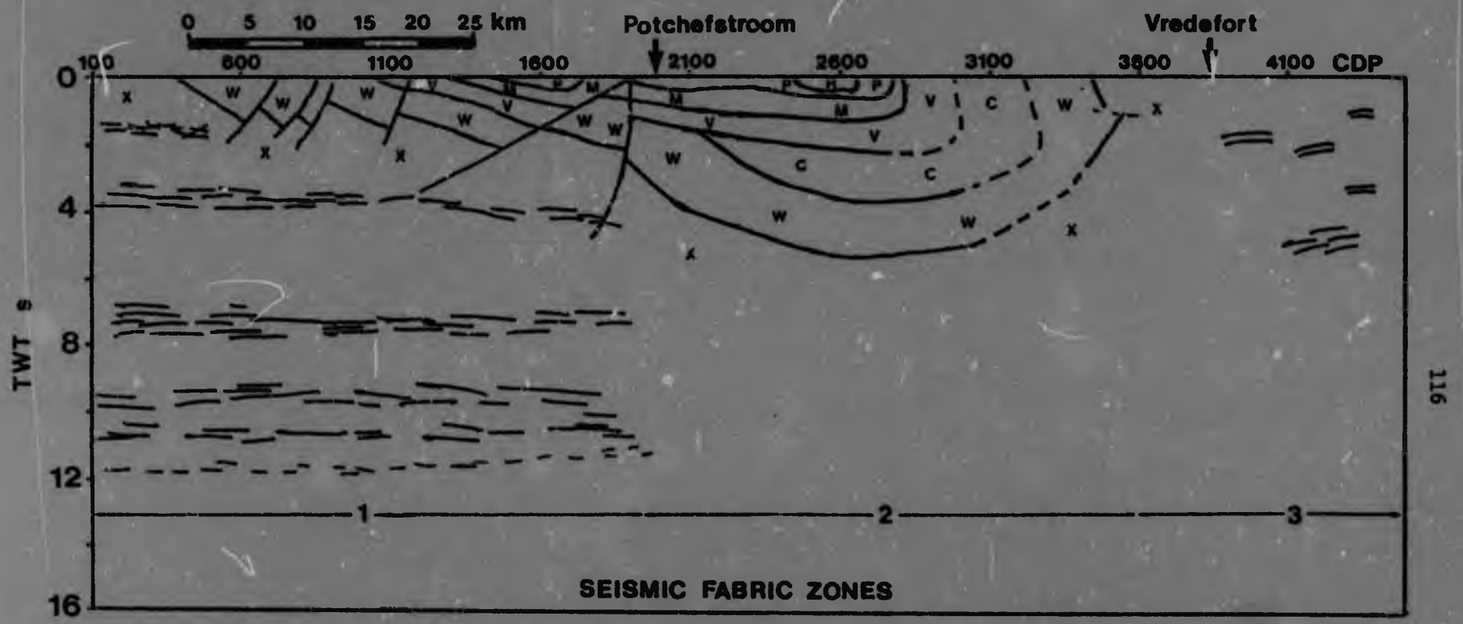


Figure 6.2. Interpretation of the trans-Witwatersrand Basin deep seismic reflection profile.
Geology: X - Basement Complex, W - Dominion and West Rand Groups, C - Central Rand Group,
V - Ventersdorp Supergroup, M - Black Reef Formation and Malmani Subgroup,
P - Pretoria Group, R - Roodeltraal Complex.

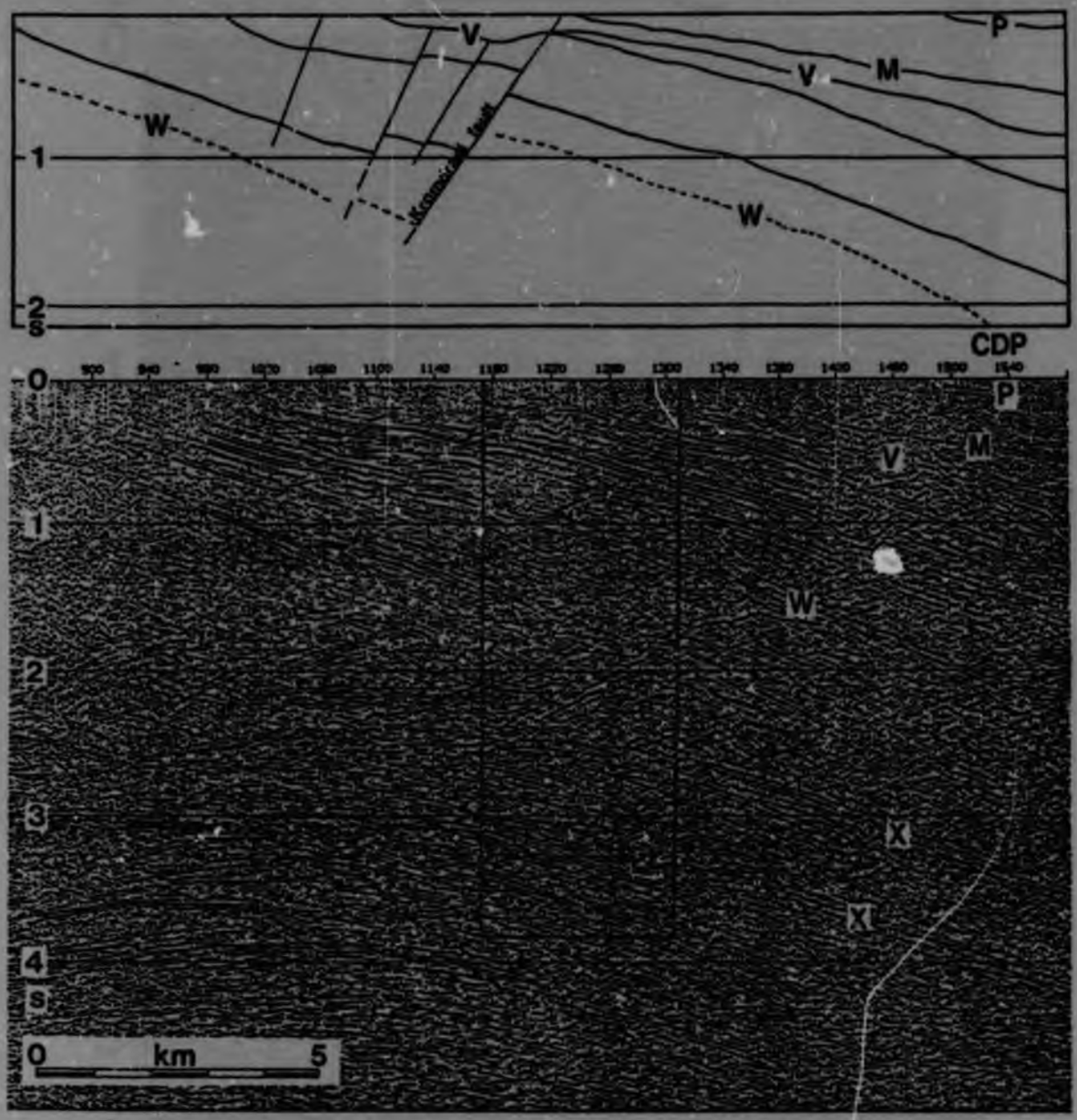


Figure 6.3A. Unmigrated panel (CDP 900-1540) from the trans-Witwatersrand Basin deep seismic reflection profile. An interpretation of the upper 2 s TWT is shown above. X - reflectors in the Basement Complex, W - base of Dominion and West Rand Groups, V - base of Ventersdorp Supergroup, M - base of Black Reef Formation and Malmani Subgroup, P - base of Pretoria Group. The box on the section shows the position of the panel shown in greater detail in Figure 6.3B.

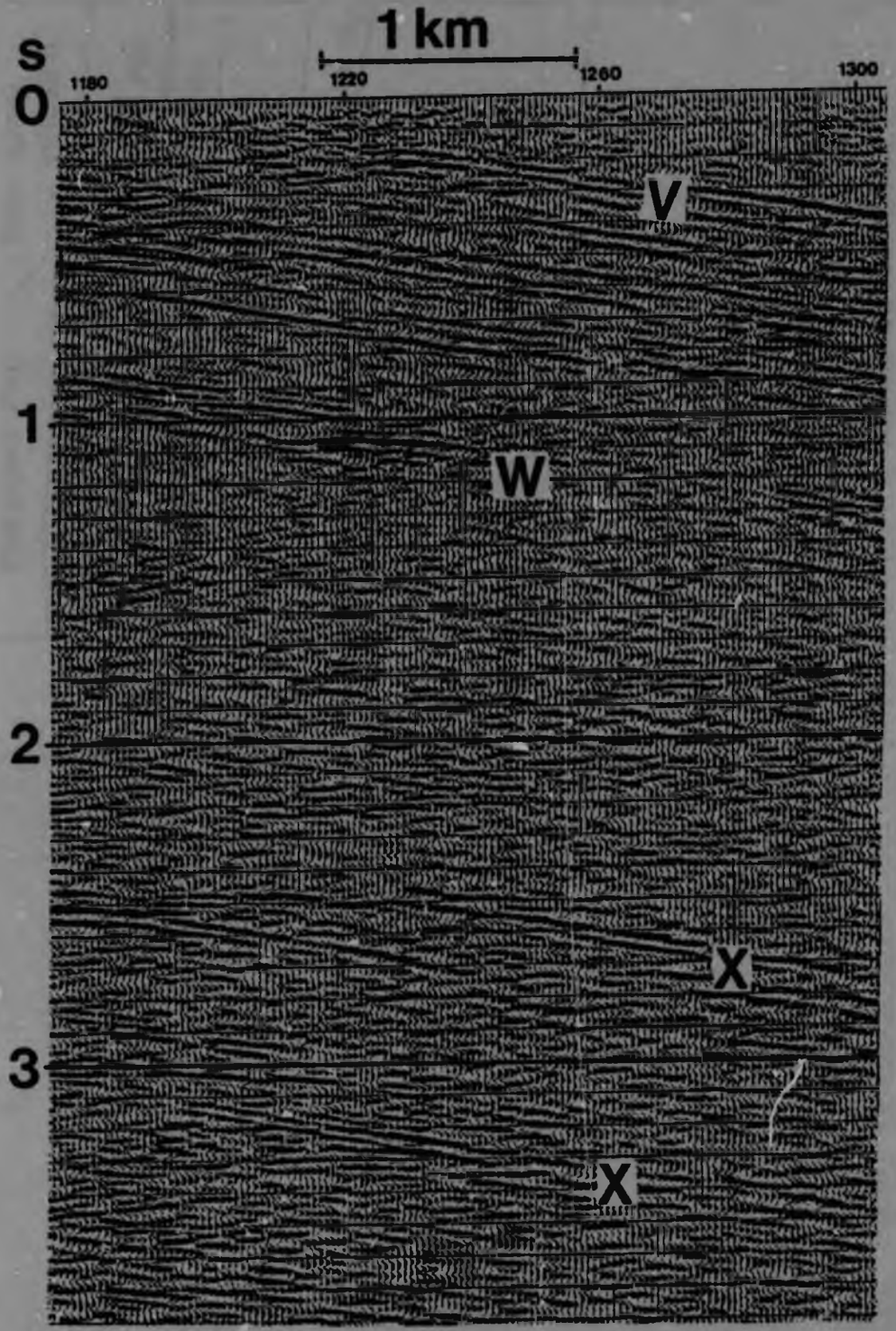


Figure 6.3B. Migrated panel (CDP 1180-1300) from the trans-Witwatersrand Basin deep seismic reflection profile. X - reflectors in the Basement Complex, W - base of Dominion and West Rand Groups, V - base of Ventersdorp Supergroup, M - base of Black Reef Formation and Malmani Subgroup, P - base of Pretoria Group.

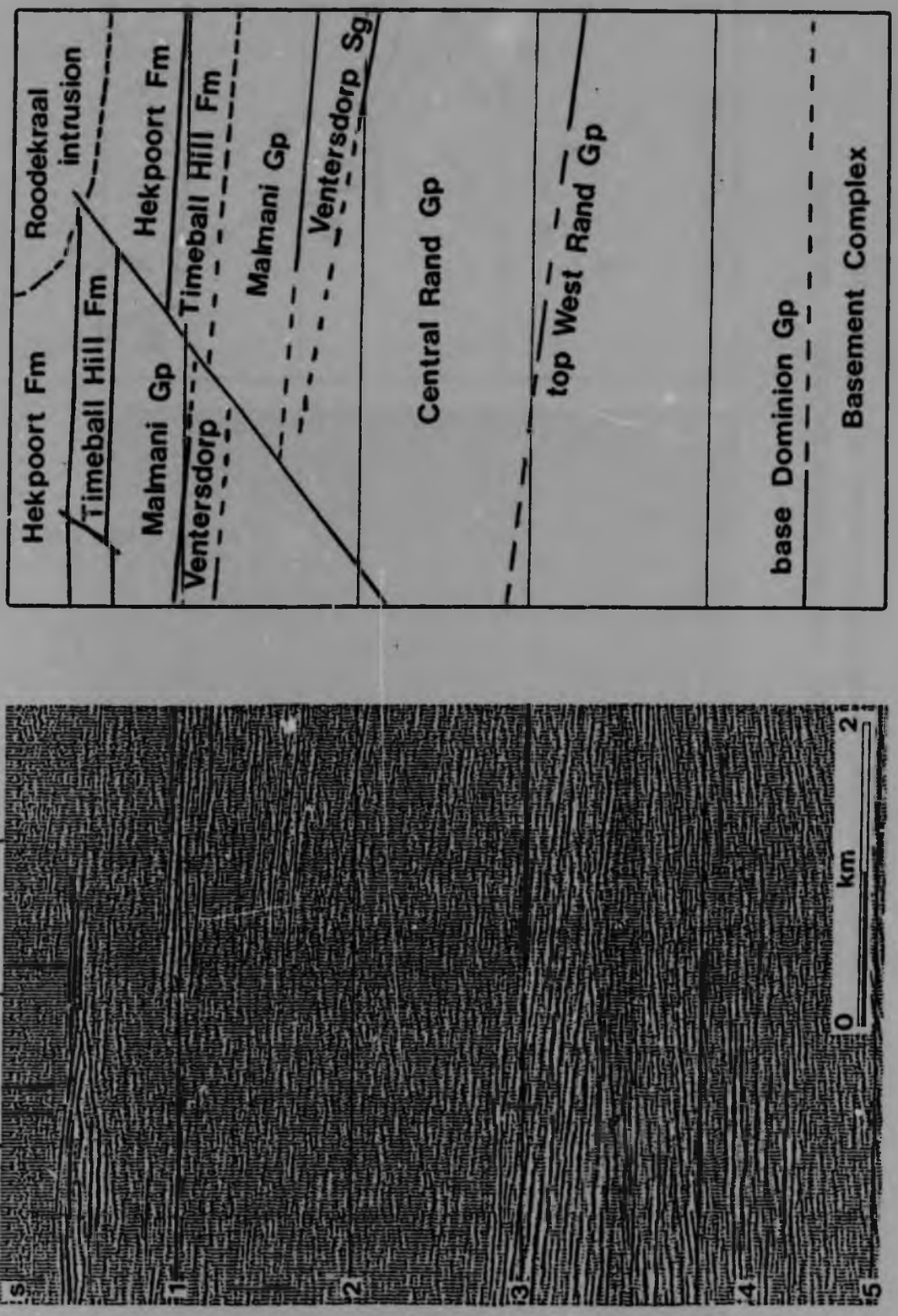


Figure 6.3C. Unmigrated panel (CDP 2540-2700) from the trans-Witwatersrand Basin deep seismic reflection profile and interpretation.

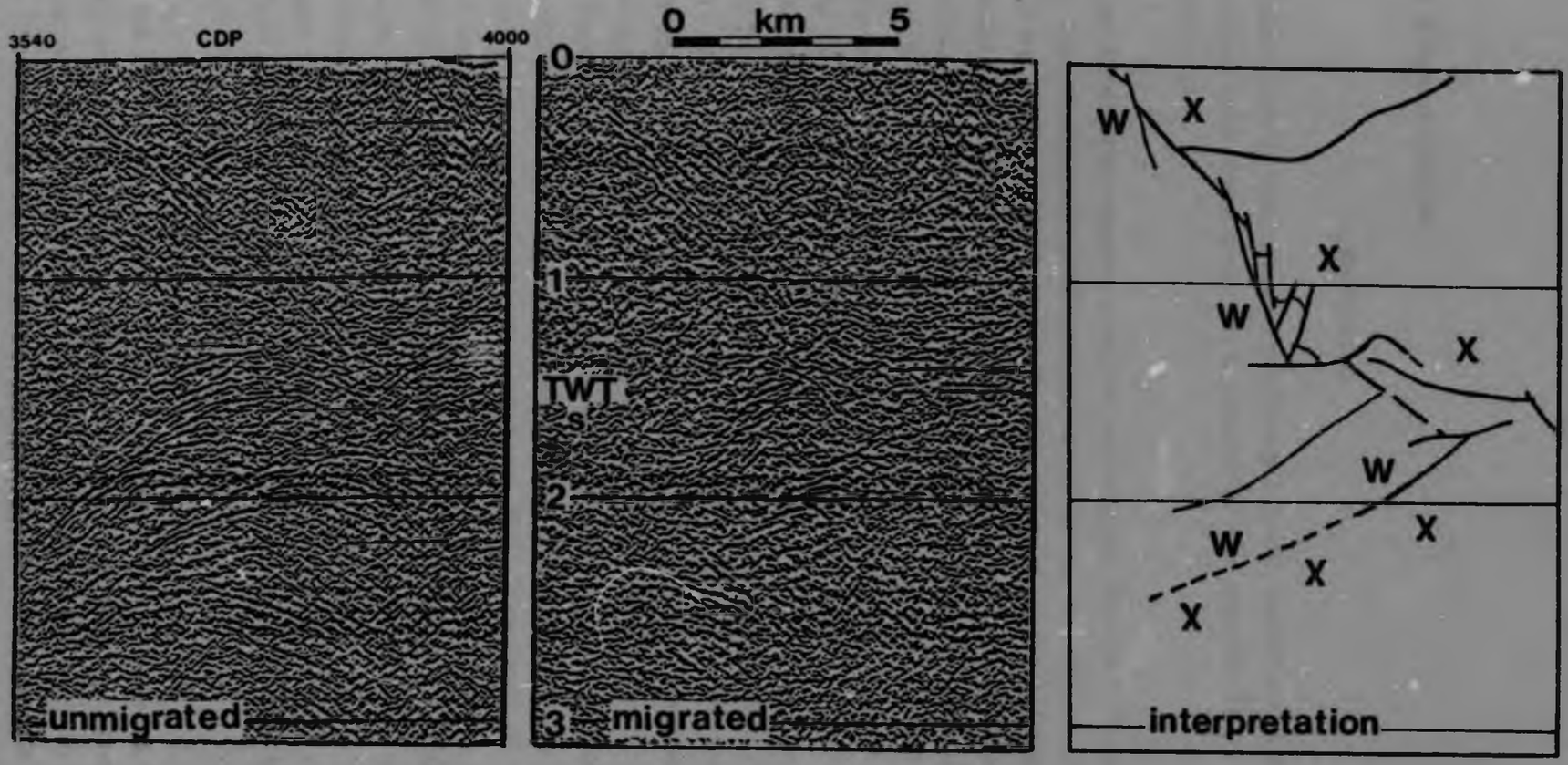


Figure 6.4. Panel (CDP 3540-4000) from the trans-Witwatersrand Basin deep seismic reflection profile showing the collar of the Vredefort Dome.

6.4.2 Basement Complex

Description

The lower part of the trans-Witwatersrand Basin record section can be divided into three zones on the basis of the seismic fabric (Figure 6.1).

(1) The first zone extends from the outcropping Basement Complex rocks (the Ventersdorp Dome) on the northwestern end of the profile as far as Potchefstroom. It is characterised by numerous layered subhorizontal reflectors, both isolated and in complex packages, extending from the surface to 12 sec TWT. The upper 4 s TWT is shown in Figure 6.5A. The reflectors have remarkable continuity and sharpness, many extending for distances greater than 10 km, the length of the continuous events increasing with depth. Virtually all the events show some curvature on the unmigrated section. The events above 1.5 s TWT tend to collapse to a focus after migration (Figure 6.5B). Bands of strong reflection which are continuous for more than 20 km occur from 2.4-2.8 s TWT and 3.4-4.4 s TWT. These reflective bands appear to parallel the base of the supracrustal strata within the Witwatersrand Basin (Figure 6.3A). Between 6 and 12 s there are numerous sub-horizontal reflections, whose horizontal length generally does not exceed a Fresnel zone (for a frequency of 20 Hz and a velocity of 6 km/s, the first Fresnel zone radius at a depth of 20 km is 3 km). Consequently, these reflections do not arise from a planar interface, but probably from undulating interfaces or an ensemble of lenses. The gradual decrease in reflectivity at 12 s is thought to mark the crust-mantle transition. The absence of a "reflection Moho" suggests a smooth transition from crustal to mantle velocities (Braile and Chiang, 1986).

(2) The second zone extends from Potchefstroom to the collar of the Vredefort structure. It is characterised by the complete absence of reflected energy between 6 s TWT and the base of the section at 16 s TWT. The boundary between this zone and the zone of numerous subhorizontal reflectors is vertical and abrupt. The possibility

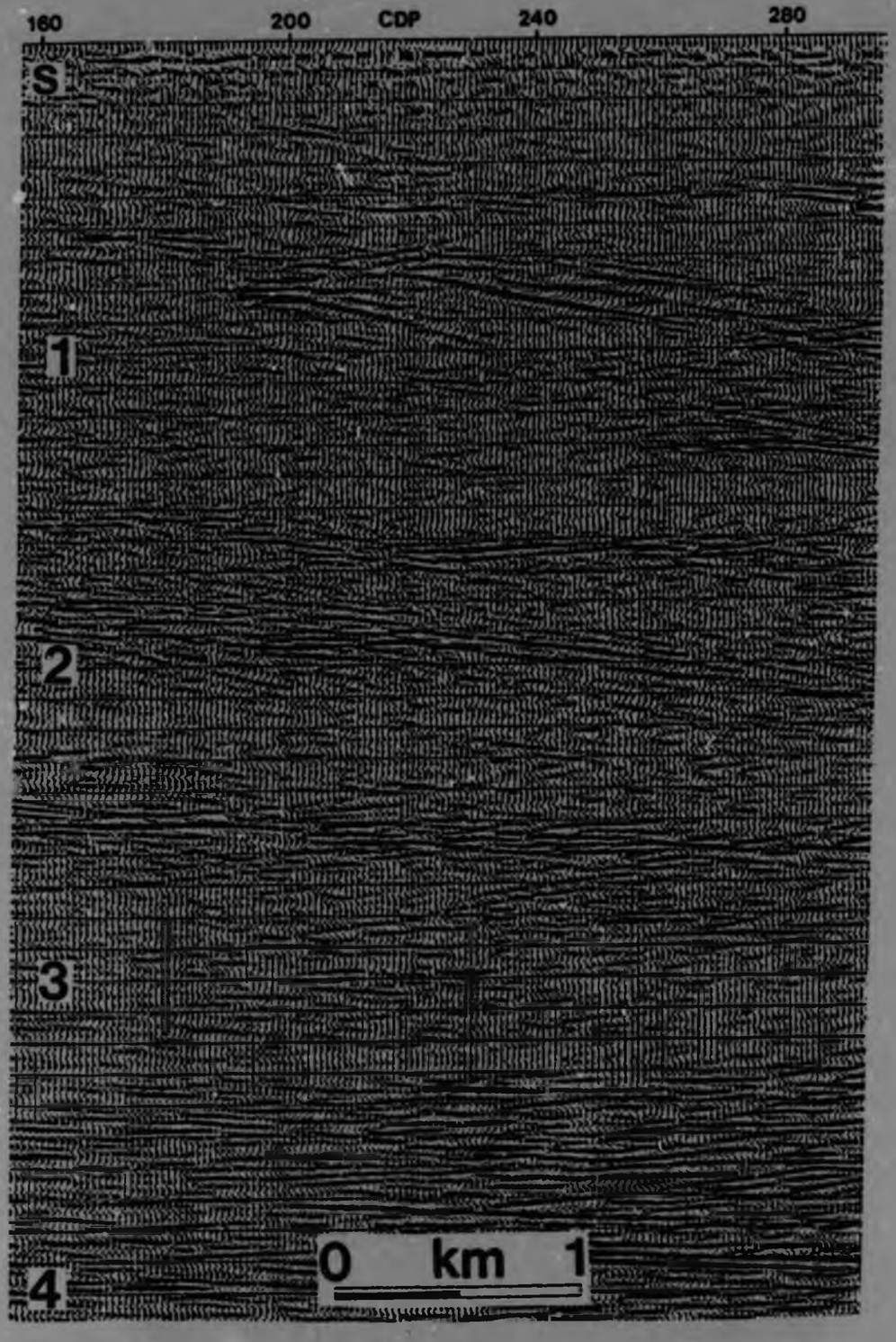


Figure 6.5A. Migrated panel (CDP 160-290) from the trans-Witwatersrand Basin deep seismic reflection profile. This panel shows the reflective character of the Ventersdorp Dome.

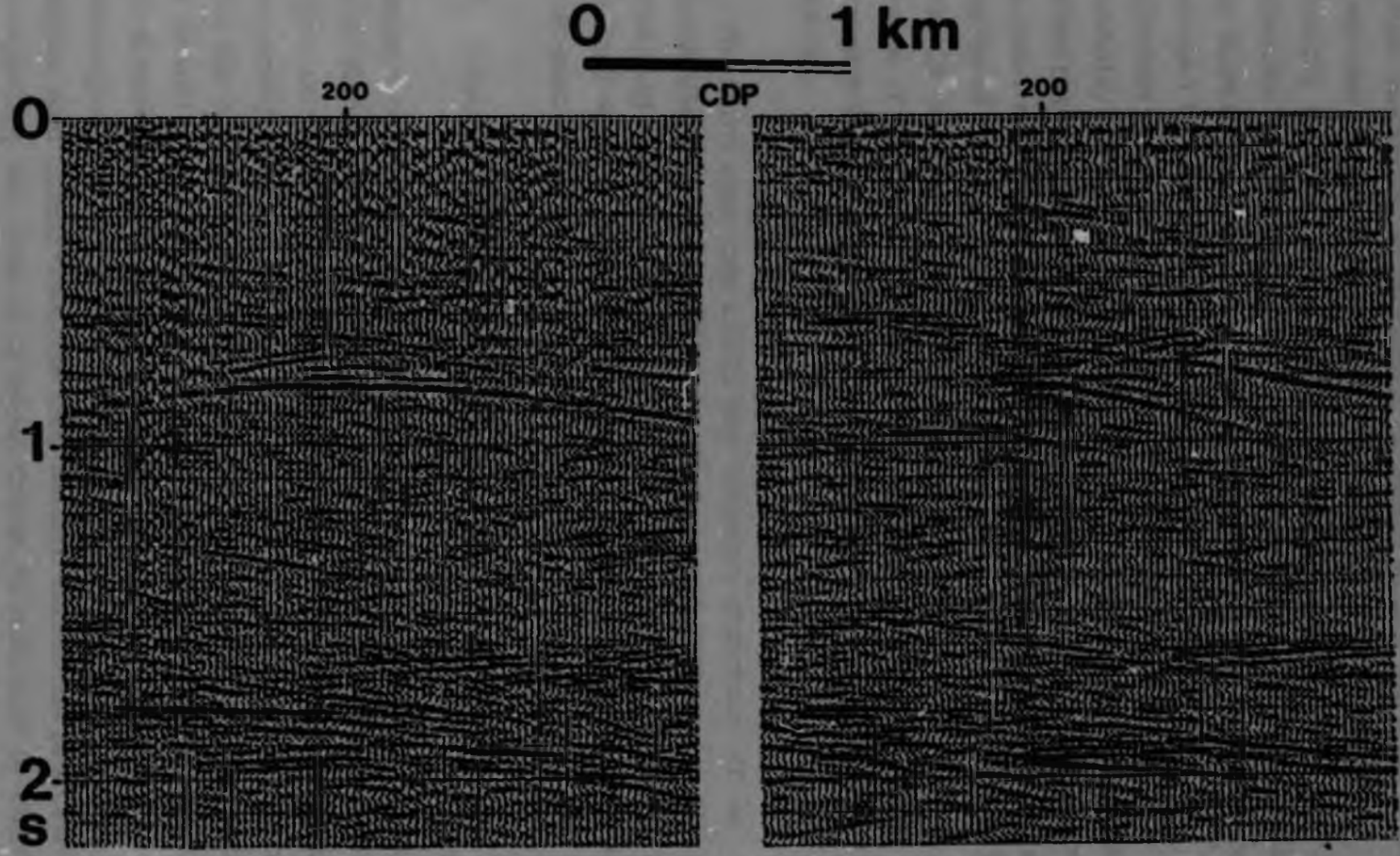


Figure 6.5B. Collapse of a diffraction in the Ventersdorp Dome to a focus (CDP 200, 820 ms TWT) after finite difference migration using a migration velocity of 6000 m/s.

that the absence of deep reflected energy is due to either near-surface scattering or entrapment of energy within the supracrustal strata was carefully considered. The absence of outcropping dolomitic rocks and the sharp definition and continuity of the reflectors in the upper 2 s of the section discount the possibility that significant energy has been lost by scattering or coherence destroyed by poor surface statics. Although a large number of reflectors occur in the upper 3 s of the section, none are abnormally strong. When the generally low values obtained for the reflection coefficients in the Witwatersrand Basin are considered, the total entrapment of energy within the supracrustal strata is considered very unlikely. Consequently I am convinced that the lower crust is genuinely seismically transparent, due either to the absence of layers with a contrast in acoustic impedance, or an extremely complex structure. No vestige of a reflection Moho is detected.

(3) The third zone lies within the Vredefort structure. It is characterised by occasional inclined (curving) reflectors. The reflecting segments are not more than 2 km in length. There is no distinct depth at which the reflection character changes, and so no crust-mantle transition is identified.

Origin of reflections within the continental crust

Numerous conditions capable of producing seismic reflections can exist within the continental crust. It must also be remembered that significant geological boundaries may not have an acoustic contrast and consequently may fail to produce a reflection. Another problem with the reflection seismic technique is that it is most efficient in detecting horizontal or near-horizontal layering. Exposures of the Basement Complex of the Kaapvaal Craton reveal considerable petrological and structural complexity, and underline the need for caution when interpreting the deep seismic reflection profile. In interpreting data from an Archaean Craton it must also be remembered that the features causing reflections represent the current state of the lower crust. The effects of the most recent tectonic event will usually be dominant, although former structures may be reworked

(Blundell and Raynaud, 1986, p 294).

A "typical" deep seismic reflection record section has been derived from numerous profiles of the continental crust acquired over a wide range of tectonic and age provinces in Europe and north America. It consists of an upper crust largely devoid of reflection, except those from either sedimentary basins or occasional medium to low-angle structures generally thought to be faults; and a highly reflective lower crust with the Moho at the base of the reflectivity (McGeary, 1987, p 235; Klemperer et al., 1987, p 219). Examination of outcropping of drilled samples has suggested different explanations for reflectivity in the upper crystalline crust (Klemperer et al., 1987, p 218). Effects implicated to some degree include:

a) primary lithological variation within fault zones;
b) lithological variation due to metasomatic activity along a fault zone;
c) anisotropic fabrics;
d) and trapped fluids.

The physics of the origin of reflections from the lower crust is still not understood (Matthews et al., 1987, p 211). Hypotheses on the origin of the reflective lower crust may be crudely divided into three classes:

a) primary lithological layering, typically igneous layering or mafic sills;
b) reflective ductile strain banding formed from the original lithological contrasts;
c) contrasts in the physical properties of the rock, including the fluid content (Klemperer, 1987, p 219).

Reflective lower crust is not universally found. Old, cold and rigid shields do not show pronounced layering in the lower crust except for some exceptions where intrusion or recent tectonic activity are suspected (Meissner et al., 1987, p 322).

Several particular deep crustal reflector patterns have been noted to recur in reflection profiles, and many suggestions have been offered to explain their origin (Hatcher, 1986; Matthews and Cheadle, 1986; Blundell and Raynaud, 1986).

a) Layered subhorizontal reflectors may be due to layered rocks,

granulite banding, cumulate layering, unconformities, thrusts and thrust stacks, mylonite or cataclastic zones, intrusive sills, zones of ductile flow, lenses of horizontally foliated rocks containing fluids in intergrain cracks and in fractures, lenses of partial melt, constructive interference due to laminations with alternating higher and lower seismic velocities (maximum amplitudes arise from layers a quarter wavelength thick).

b) Inclined reflectors may be due to angular unconformities, dipping layered rocks, imbricate thrusts, root zone and suture structures, duplex and footwall ramps.

c) Curving reflectors due to plutons, open folds and refolded folds.

d) Transparent zones due to acoustically homogeneous rocks, extremely complex structures, or acoustically layered rocks where the layering is thin relative to the seismic wavelength.

Discussion

The observation of strong, continuous reflectors in the upper crystalline crust of the Ventersdorp Dome is extremely unusual, especially when the lengthy tectonic history of the area is considered, as well as its juxtaposition to a block of transparent basement. Although well logs from the crystalline portion of the upper crust display velocity perturbations of the proper wavelength and magnitude to produce large amplitude reflections, it is commonly transparent (Mooney and Brocher, 1987, p 731). Mooney and Brocher (1987) attempt to explain this paradox by suggesting that the velocity perturbations in the upper crust are probably neither well laminated nor of long scale length because this portion of the crust behaves nonductilely; extension and compression are achieved brittlely by cataclasis and folding, producing short features with steep dips not well imaged using conventional seismic profiling methods.

Strongly laminated reflection fabrics in the upper crystalline basement have been recorded in two localities in north America: from 2-4 s over Precambrian granites and gneisses near the Picacho Mountain core complex in south-central Arizona (the reflections were originally interpreted as overthrust sediments, and were drilled to

a depth of 5492 m); and from 4-10 s in the Snake Range metamorphic core complex in eastern Nevada. Both areas lie in the Basin and Range Province, and experienced large amounts of extension in the Tertiary. The laminated reflection fabric is attributed to ductile stretching and contemporaneous magmatic intrusion during this episode (McCarthy, 1986, p 290). In this context, it is interesting to note that both Tankard et al. (1982) and Burke et al. (1985) have alluded to comparisons of the Ventersdorp Supergroup with the modern Basin and Range Province.

The Ventersdorp Dome represents a major zone of basement uplift, but is very poorly exposed. Sporadic fresh outcrops in the centre of the dome reveal an homogeneous, massive, medium- to coarse-grained granodiorite. Very coarse grained pegmatites occur throughout the granite (Robb and Meyer, 1985, p. 6). A normal simple shear model has been used by Clendenin et al. (1988) to explain the structural evolution of the Ventersdorp Supergroup. In terms of this model, the Ventersdorp Dome is interpeted to lie within the zone of maximum crustal extension (Clendenin et al., 1988, p. 9).

The character of the curved events in the upper crust on the western section of the trans-Witwatersrand Basin profile is very similar to events on the Hardeman County COCORP profile identified as diffractions after considering the geometry of the events on the main profile and cross-lines (Schilt et al., 1981). Curved events on the trans-Witwatersrand Basin profile which do not collapse to a focus after migration could well represent reflections from features out of the plane of the profile. In the absence of cross-lines, it is impossible to resolve this question.

The strongly reflective bands at 2.4-2.8 s and 3.4-4.4 s are a prominent feature of the northwestern part of the profile. Modelling shows that similar seismic fabrics are produced by an undulating reflective surface (Blundell and Raynaud, 1986, p 292) and by zones consisting of many reflective lenses packed together (Reston, 1987). There are a wide range of geologic structures which could produce these reflector geometries. These include: igneous intrusions or diapiric upwelling; strongly folded or corrugated surfaces of significant impedance contrast with the radius of curvature < 10 km;

and extensive faulting juxtaposing rocks of differing impedance.

The Ventersdorp Dome lies some 100 km west-southwest of the Johannesburg Dome. Both domes form part of the crescent-shaped basement arch forming the boundary of the main Witwatersrand Basin known as the Rand anticline. The Johannesburg Dome, which has been mapped in detail, is composed of two main varieties of gneiss: (1) mesocratic biotite tonalitic gneisses and (2) leucocratic biotite tonalite and trodhjemite gneisses. In places the gneisses show layering which defines tight fold closures with axial plane foliation. Layered gneisses or migmatites underlie nearly the entire northern half of the Johannesburg Dome, and the gneisses displaying polyphase folding (Tankard et al, 1982, p.34). Anhaeusser (1973) attributes the formation of the layered gneisses to a complex interplay of processes involving stoping and assimilation of supracrustal greenstones by granitic fluids followed by potash metasomatism. The deformation in the gneisses is attributed to partial mobilization which resulted in "flowage folding". Greenstone remnants are preserved within the gneiss. This structurally and petrologically complex crust might be expected to give rise to a transparent seismic signature, and may well represent the rocks forming the basement to the Potchefstroom syncline.

The core of the Vredefort structure has been interpreted as representing a section of the crust turned "on edge". Within the Vredefort middle crust, pods of mafic granulites are found within the leucogranulite (Hart et al., 1981). The reflection seismic signature is in accord with that likely to be produced by steeply dipping rocks containing occasional pods of reflective material.

7. STRUCTURE OF THE KAAPVAAL CRATON

7.1 Synthesis of the seismic refraction, reflection and surface wave models

The deep seismic soundings carried out for this study have confirmed the results of the experiments conducted in the 1950's (Willmore et al., 1952; Gane et al., 1956; Hales and Sacks, 1956) as far as the first order features of the seismic structure are concerned (i.e. crust and upper mantle velocities, crustal thickness). The difficulties in determining the precise source location and origin time, and the range of source locations and source mechanisms used to compile each record section, have not allowed any significant improvement in the determination of these parameters. However, as more source regions have been considered, and the profiles reversed, the results have been extended over a larger area of the Craton. The particular merit of this study lies in the digital recording of the seismograms which has allowed record sections to be compiled, and the character of the various wavegroups to be studied; and the use of far more sophisticated interpretation methods. This has enabled the second order features (e.g. upper-lower crust transition, crust-mantle transition, attenuation) to be investigated. The result is a more detailed and better constrained model of the seismic structure of the Craton.

The crustal shear velocity model for the Kariba-Pretoria path derived by Bloch et al. (1969) from the inversion of surface waves includes two low velocity layers (from 12-16 km and 24-28 km). The S-wave record sections obtained in this study do show considerable complexity, but it has not proved possible to deduce the intra-crustal structure with confidence

Coincident seismic reflection and refraction experiments have a unique ability to image lithospheric structure and to provide the information necessary to infer the composition and physical state of the continental crust (Mooney and Brocher, 1987). The refraction method provides a broadband signal, good seismic velocity and physical property information, and is sensitive to velocity

gradients; while the reflection method provides high resolution and enables a complete 2-D structural interpretation to be made (Braile and Chiang, 1986, p 259).

The trans-Witwatersrand Basin deep reflection profile intersects both the refraction profiles described in this study. In the case of the Klerksdorp - East Rand - Witbank profile, the intersection is about 5 km southeast of Potchefstroom. This point is 40-50 km from the Klerksdorp goldfield and about 120 km from ERPM (see Figure 6.1). Consequently the energy arising from Klerksdorp tremors reflected at this point will be received at offsets of 80-100 km which is just beyond the critical distance, and head waves recorded beyond the cross-over distance would have sampled the crust-mantle boundary below the intersection point. No seismograph was located at a sufficient offset to detect wide-angle reflections or refractions from the ERPM source. The deep seismic reflection profile intersects the East Rand - OFS refraction profile near the farm Inlandsee in the centre of the Vredefort Dome. This is approximately 120 km from both source regions. Wide-angle reflections should be detected at offsets of 240 km, and head waves would have sampled this section of the crust. Consequently the refraction model and the reflection seismic section are directly comparable.

The synthesis of the refraction and reflection models of the Kaapvaal Craton leads to the following conclusions:

a) The uppermost layer of the crust consists of Phanerozoic and Precambrian supracrustal sediments and volcanics ranging in thickness from 0-10 km with seismic velocities in the range 3.5-6.8 km/s, and includes several major velocity discontinuities. The reflection seismic data provides a high resolution image of the disposition of these formations. In the refraction seismic record sections the high velocity dolomites, lavas and indurated shales are manifested by emergent first arrivals with a high velocity. The station spacing is far too great to enable any useful image of the supracrustal strata to be derived from the refraction data.

b) The refraction record sections indicate that a velocity inversion exists within the upper crust. This is attributed to the

lower seismic velocity of the upper crystalline crust compared to the overlying Dominion and West Rand Group rocks.

c) The refraction record section also reveals the existence of a mid-crustal P-wave velocity gradient, particularly beneath the Potchefstroom syncline. The velocity increases from 6.2 km/s at a depth of 8 km to 6.5 km/s at depth of about 12 km. The velocity gradient gives rise to a high-amplitude, low-frequency caustic at offsets of 160-180 km. On other record sections the transition is marked by a sufficiently abrupt velocity discontinuity to give rise to reflections, where it may be termed the Conrad discontinuity. Prominent bands of strong reflectivity are found at a comparable depth (3.4-4.4 s TWT) on the northwestern segment of the reflection profile, with a reflective lower crust extending to 12 s TWT.

d) The refraction data shows that the lower crust has a uniform velocity in the range 6.5-6.8 km/s. The reflection seismic fabric of the lower crust changes from strongly reflective in the northwest to transparent elsewhere. There does not appear to be a precise coincidence between the start of the reflective lower crust, and the intracrustal velocity increase. A similar conclusion has been reached by Wever (1989), after considering some 50 coincident reflection and refraction profiles.

e) The refraction data is interpreted to indicate a velocity gradient zone 1-3 km thick at the base of the crust. This zone gives rise to high-amplitude, low-frequency (< 5 Hz), dispersed $P_m P$ and $S_m S$ arrivals at offsets greater than 150 km. Occasional $S_m P_m$ reflections with a dominant frequency of 2-3 Hz are also observed. No "reflection Moho" is observed. A decrease in reflectivity at ca. 12 s TWT is thought to mark the base of the crust. The Vibroseis™ sweep commenced at 12 Hz, and the wavelengths are too short to be reflected by the gradient.

Models of the Moho boundary consisting of a thick zone of rather smooth transition from crustal to mantle velocities, or more generally without a stack of thin layers with strong velocity contrasts between them giving rise to interference effects, are unlikely to turn back large amounts of energy at normal incidence

and high frequencies. However, at wide-angle and low frequency the reflection coefficient is similar to that for models with first-order discontinuities or velocity laminations at the base of the crust (Braile and Chiang, 1986).

Similar results were obtained on the ECORS "North of France" section over the Precambrian Brabant massif. Reflection profiling showed only a transparent lower crust, and virtually no indication of a crust-mantle boundary; while a refraction/wide-angle reflection survey using an explosive source produced clear low-frequency arrivals (<10 Hz) from the Moho reflector (Hirn et al., 1987, p 292). This was interpreted as indicating a smooth crust-mantle velocity transition.

f) The refraction data indicates that the upper mantle has a seismic velocity of ca. 8.2 km/s. A head wave (P_n) is observed which reaches an amplitude minimum at an offset of ca. 180-200 km, and then increases in amplitude again. This suggests a sub-Moho velocity gradient of at least 0.01 km/s/km.

g) The reflection seismic fabric beneath the Potchefstroom synclinorium and within the Vredefort Dome are essentially similar, with a transparent character from 6-16 sec TWT. The Inlandsee profile shows occasional short reflecting segments. This signature indicates either a lower crust that is acoustically homogeneous or of considerable complexity. The refraction data strongly supports the second possibility. The difference in frequency between the P_n and P_mP phases is interpreted as indicating attenuation in the lower crust, to which both scattering by velocity inhomogeneities and absorption may have contributed.

7.2 Geological and geophysical synthesis

In this chapter the seismic model of the Kaapvaal Craton is integrated with the results of other geophysical and geological investigations.

Outcrops of the Basement Complex in the vicinity of the Witwatersrand Basin have generally not been mapped in detail, but provisional work indicates a diversity of granite types and textures (Robb and Meyer, 1986, p 188; Drennan et al., 1987). For example, the gneisses of the Johannesburg Dome have undergone intensive deformation and extensive metasomatism. In contrast, outcrops of the poorly exposed Ventersdorp Dome reveal a homogeneous, massive granodiorite.

Geophysical methods, which have [illegible] map the depth dimension more effectively, also [illegible] distance of different "crustal blocks". Heat flow measurements indicate a significant difference between the basement underlying the Witwatersrand Basin and the basement forming the Hartebeesfontein and Ventersdorp Domes (Jones, 1988). The magnetic field over the Kaapvaal Craton has also been interpreted to indicate large crustal domains. The east-west trending Machavie lineament, which passes just north of Potchefstroom, is believed to mark the boundary between two domains (B. Corner, Witwatersrand University, pers. comm., 1989). The trans-Witwatersrand Basin deep seismic reflection profile also indicates a dramatic change in reflection seismic signature between the Ventersdorp Dome and the basement underlying the Potchefstroom syncline.

The gravity field along the trans-Witwatersrand Basin deep seismic reflection profile has been modelled using a 2-D Talwani type forward modelling approach (Cooper, 1986). While 2-D modelling is certainly an over-simplification, the exercise shows that a plausible model which satisfies both the reflection seismic section and the gravity field can easily be derived (Figure 7.1). The entire gravity anomaly can be attributed to the dense supracrustal rocks filling the Potchefstroom syncline. The dolomitic rocks of the

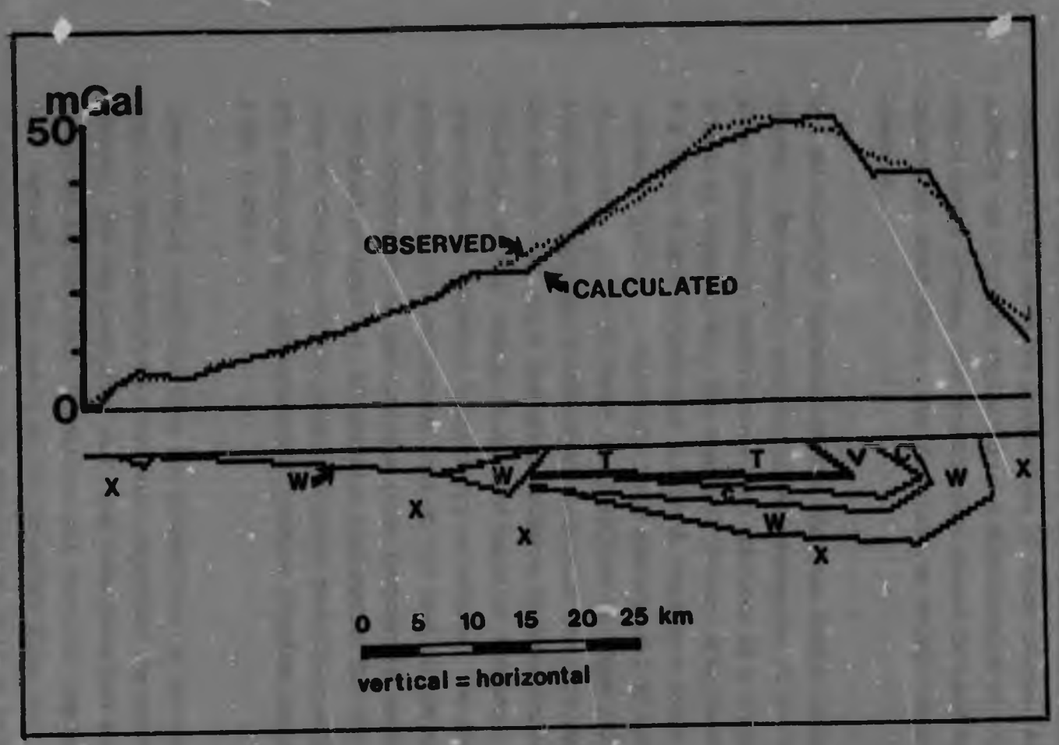


Figure 7.1. 2-D model of the Bouguer gravity anomaly along the trans-Witwatersrand Basin deep seismic reflection profile. The density of the formations with respect to a background of 2.67 g/cm^3 is indicated. Geology: X - Basement Complex (0.0), W - Dominion and West Rand Groups (0.2), C - Central Rand Group (0.0), V - Ventersdorp Supergroup (0.2), T - Transvaal Sequence (0.22).

Transvaal Sequence, lavas of the Ventersdorp Supergroup, and ferruginous shales of the West Rand Group are all considerably denser (about 0.2 g/cm^3) than the quartzites of the Central Rand Group and granitic basement. There is considerable ambiguity concerning the relative proportions of these strata. As the Bouguer anomaly can be fully explained by a distribution of the dense supracrustal strata, the gravity data cannot be used to make inferences about the density distribution within the crystalline basement.

The geo-electric character of the Kaapvaal Craton is particularly unusual. The seismic and electrical parameters of the lower crust under Precambrian regions have been combined in a classification scheme by Jones (1981): the Kaapvaal Craton, with P-wave velocity of 6.8 km/s, S-wave velocity of 3.8 km/s, Poisson's ratio of 0.28 (assuming perfect elasticity), bulk density of 2.95 g/cm^3 and resistivity of 10-150 Ohm.m is classified as "Type III". The Zimbabwe Craton and Southeastern Grenville Province were placed in the same class, while the other Archaean Cratons considered (Ukranian Shield, Baltic Shield and Superior Province) displayed significantly different resistivity structures. The physical properties of the conductive zone at the base of the Kaapvaal Craton are interpreted as indicating a layer composed of serpentinite (hydrated peridotite). Alternative explanation for the conductive zone at the base of the crust are pores containing saline water; or the existence of interconnected graphite (Hyndman and Klemperer, 1989, p 256).

Lower crustal xenoliths from the kimberlites on the Craton are too rare to reach a definite conclusion regarding the petrology. However, the few xenoliths that have been described are all granulite facies rocks. Granulites (of granitic composition) are also exposed in the centre of the Vredefort Dome, and are interpreted to represent rocks originally 10-15 km below the cratonic surface. It is also probable that the Cratonic lower crust differs from the garnet granulite which constitutes the lower crust of the Namaqua-Natal Province. The seismic velocity of the lower

crust beneath the Craton and Namaqualand Metamorphic Complex are 6.4-6.7 and 6.6-6.9 km/s respectively. The seismic velocities of granulites at the base of the crust increases as the amount of garnet increases. For example, the velocity of diorite (adjusted to 1 GPa and 25°C) is 6.6 km/s with little or no garnet, and increases to 7.2 km/s when the amount of garnet is the maximum expected (Drummond, 1988, p 111). It is concluded that the lower crust of the Kaapvaal Craton is more felsic than the lower crust of the lower crust of the Namaqua-Natal Province, with an average dioritic composition. It is unlikely that the lower crust is entirely uniform in composition; rather, that it is comprised of a mixture of rock types. It is probable that lower crust reflectivity is due to mafic intrusions embedded in a more felsic lower crust.

Petrological interpretations of compressional wave models of the crust are tenuous, since a wide range of rocks can usually satisfy a given P wave velocity. More reliable constraints on lithospheric composition are possible with a knowledge of both compressional and shear wave velocity, which enables Poisson's ratio to be calculated. Poisson's ratio is sensitive to variables such as quartz and feldspar content and the presence of fluids (Holbrook et al., 1988, p 12 081). As quartz has an extremely low Poisson's ratio, rocks with a high quartz ratio will also display a low Poisson's ratio and vica versa. Increasing feldspar content gives high Poisson's ratios as a consequence of relatively high compressional wave velocities compared to the respective shear wave velocities. In general, high contents of olivine, garnet, pyroxene and amphibole produce high compressional and shear wave velocities and relatively high Poisson's ratios (Kern, 1982, p 24).

The P- and S-wave velocities at the base of the Kaapvaal Craton are 6.8 and 3.8 km/s respectively, indicating a Poisson's ratio of ca. 2.8. This indicates a low quartz content of the rock. A crust-mantle transition zone including serpentinised peridotite is capable of explaining the seismic velocities and Poisson's ratio (Kern, 1982), as well as the existence of an electrically conductive zone.

A borehole situated near the centre of the Vredefort Dome has

intersected serpentinised hornblende-bearing harzburgite. The rocks in the central region of the Vredefort structure are interpreted to be lower crustal rocks which experienced uplift of more than 36 km during the Vredefort cryptoexplosion event 2.0 Ga ago. The serpentinised ultramafic rocks described above have major and trace element chemistry similar to that of fertile oceanic lithosphere, and are interpreted to represent upper mantle beneath this region of the Kaapvaal Craton (Hart et al., in press).

The seismic velocity obtained for the mantle (8.1 to 8.2 km/s) is in accord with predominantly peridotite composition, as indicated by xenoliths.

7.3 Comparison with other Archaean Cratons

The are several fundamental questions regarding the evolution of the earth which seismic studies of the Archaean crust may eventually help to answer. These include the following:

a) Did tectonic styles evolve with time, leaving systematic differences in the structures and lithologies of Archaean, Proterozoic and Phanerozoic crust ?

b) Are particular kinds of upper crust associated with specific kinds of lower crust, or are upper and lower crust generally unrelated ?

c) Are there Precambrian Mohos where lower crust and adjacent uppermost mantle have been attached and intact since the Precambrian?

d) Why does Proterozoic crust seem to have a greater tendency to be covered by Phanerozoic sedimentary rocks than Archaean crust ? (Gibbs, 1986, p. 95)

In an attempt to answer the questions noted above, and in order to establish whether or not a "typical" Archaean crustal signature exists, seismic studies from other Archaean cratons are reviewed and compared with the results from the Kaapvaal Craton. Observed velocity-depth models for the Archaean shield areas are shown in Figure 7.2.

Description

1. Superior Province, Canadian Shield

The Superior Province is dated at 2.4-3.0 Ga, the oldest rocks being of sedimentary and volcanic origin, and has many granitic intrusions. It is flanked in the south by the Proterozoic Grenville Province, which is characterised by moderate to high grade metamorphism and a complex structural style, thought to indicate significant uplift and erosion (Berry and Fuchs, 1973, p 1394). A seismic refraction study of the Superior Province found the upper crust (from 1 or 2 km to the Conrad discontinuity) to be essentially homogeneous with a velocity of 6.2 km/s, except for a low-velocity

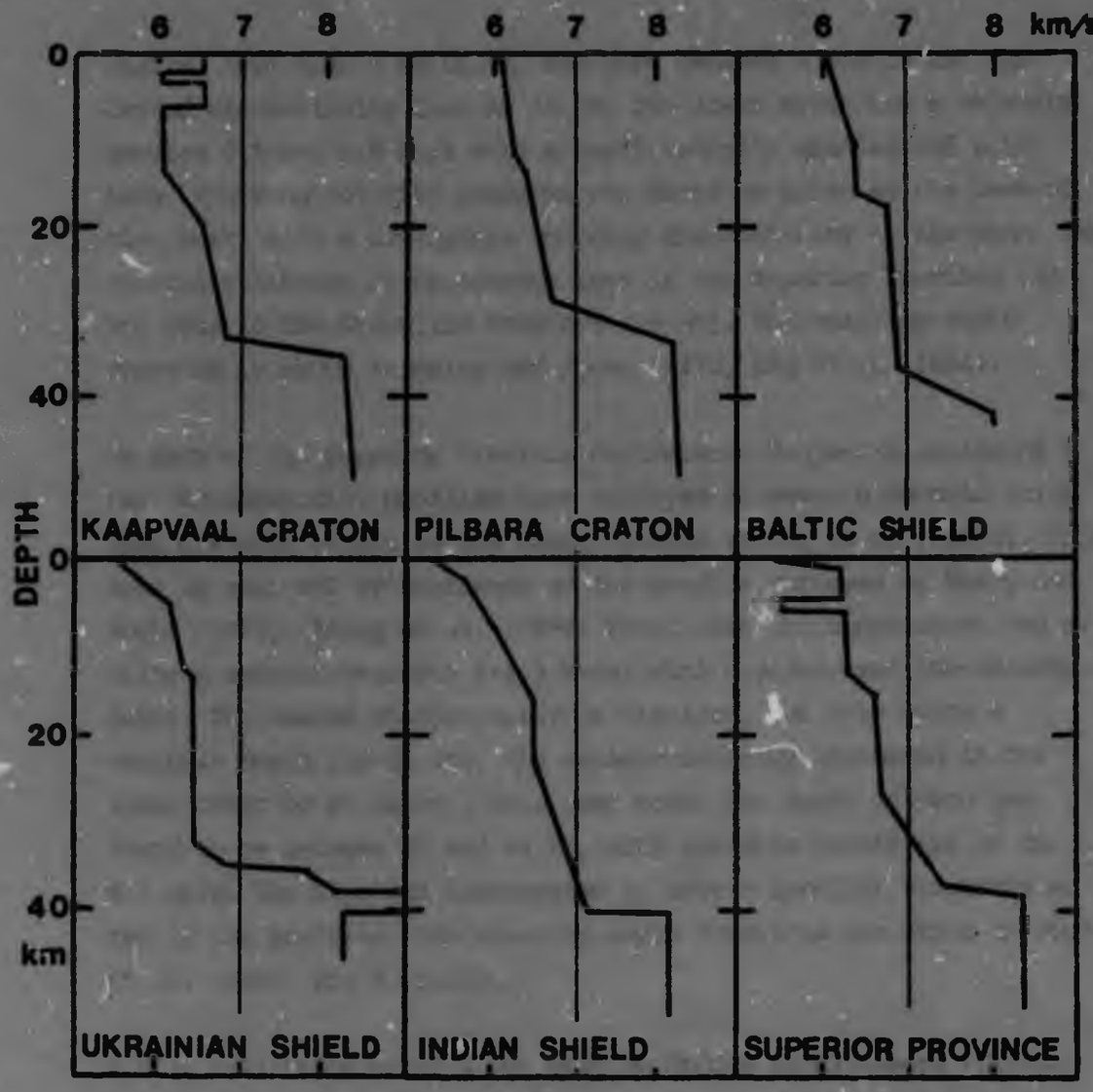


Figure 7.2. Velocity-depth models for Archaean Cratons (from this study and Drummond and Collins, 1986, p 370).

channel less than 5 km thick, and base between 6 and 15 km. The Conrad discontinuity lies at 14 km. The lower crust has a velocity between 6.5 and 6.8 km/s with a small velocity gradient of 0.02 km/s. A strong velocity gradient was found to exist at the base of the crust, with a negligible velocity discontinuity at the Moho. The crustal thickness is on average less in the Superior Province (34 km) than in the Grenville Province (39 km). The velocity-depth function is shown in Berry and Fuchs (1973, fig 37, p. 1424).

As part of the Superior Province Geotraverse Project a series of 4 seismic refraction profiles were surveyed in western Ontario using open pit mine blasts as the energy source (Young et al., 1986). This area is some 500 km southwest of the profile surveyed by Berry and Fuchs (1973). Young et al. (1986) found that the upper crust had a uniform seismic velocity (<6.3 km/s) with a widespread low-velocity layer. The Conrad discontinuity is distinct, but with quite a variable depth (13-21 km). The seismic velocity increased in the lower crust to at least 7 km/s near Moho. The depth of Moho was found to be between 37 and 44 km, with sub-Moho velocities of ca. 8.1 km/s. The Moho was interpreted to have a lamellar structure on two of the profiles. The velocity-depth functions are shown in Young et al. (1986, fig 9, p.153).

A deep reflection profile was shot by COCORP in Minnesota (Gibbs, 1986, p. 97). The seismic signature of the crust beneath the granite-greenstone terrane is characterised by numerous complex, variably-dipping reflections and diffractions. Occasional reflections with migrated two-way times of 13-15 s are thought to originate from the base of the crust.

2. Wyoming Province

The COCORP Wind River deep reflection profile crosses the best exposure of Archaean rocks in the U S A (Smithson et al., 1980). The upper crust is marked by relatively few reflections, with the exception of an 8 km long dipping reflector between 2-3 s TWT. It is interpreted to be due to an iron formation, mafic dyke, or other layered metamorphic sequence. The data between 7 and 10 s shows a

pattern that migration moves into a synform. The seismic signature is interpreted to be due to folded, multi-layered rocks, such as pyroxene granulite and granitic gneiss. This suggests that the lower crust has a complexity similar to that found where deeply eroded granulite facies rocks are exposed at the surface. It is concluded that it is unlikely that the crust has been thickened by underplating since the Archaean (Smithson et al., 1980, p 304).

The COCORP Montana Plains survey images the crystalline continental basement on a regional scale. The Archaean basement is complexly reflective from the base of the Paleozoic and Mesozoic sedimentary cover to the Moho. The upper crust is not, in general, acoustically transparent. The base of the crust is characterized by a relatively abrupt decrease in reflectivity. Lower crustal laminated zones and prominent Moho reflections are generally absent, with the exception of the lowermost crust beneath the Williston Basin, which is strongly reflective (Latham, et al., 1988).

3. Baltic Shield

The northern part of the FENNOLORA refraction profile traverses Precambrian basement complexes ranging in age from 1.8-2.8 Ga (which are adjacent to the Kola nucleus, site of the world's deepest borehole). Interpretation of the data shows alternating velocity maxima and reversals in the upper and middle crust, which are attributed to anisotropic seismic laminations; steepening velocity gradients in the lower crust and seismic velocities in excess of 7 km/s between 34 km and Moho; Moho depths between 44 and 49 km; and sub-Moho velocities significantly greater than 8.0 km/s (8.2 - 8.4 km/s) (Olsen and Lund, 1986). The velocity-depth function is summarized in Olsen and Lund (1986, fig 5, p. 125). It is speculated that the higher velocities and gradients and anisotropic laminations may be a consequence of thickening of an initially thin (10-20 km) primitive crust by early Precambrian lithospheric evolutionary processes e.g. underplating, ensialic orogeny, intracontinental subduction etc (Olsen and Lund, 1986, p. 125).

Two short reflection profiles were recorded as part of the European Geotraverse POLAR-profile. Clear reflectors are recorded in the

upper crust down to ca. 5.5s TWT. Energy is also received in between 11-14 s TWT (Lund and Heikkinen, 1987).

4. Ukranian Shield

The Ukranian Shield forms the core of the ancient east European Platform. Seismic measurements were made by Sollogub et al. (1973), and the travel-times and amplitudes subsequently reinterpreted by Jentsch (1979). The derived models start with a seismic velocity of 5 5 km/s at the surface, increasing to 6.1 km/s at 5 km, and reaching 6.4 km/s at 13 km depth. In order to account for the $P_g/P_m P$ amplitude ratio, the velocity between 13 and 30 km was kept constant at 6.4 km/s or even slightly reduced, and a thin high velocity layer introduced immediately below the Moho. The Moho itself was modelled as a 7 km broad transition zone at which the velocity increase from 6.4 to 8.2 km/s.

5. Indian Shield

The western part of the Indian wide-angle DSS traverse crosses an Archaean granite-greenstone terrane. The record section reveals an east-dippping imbricate reflection pattern persisting to at least mid-crustal depths. Some of these east-dipping reflection zones correspond with late Archaean thrust faults, and many persist through the crust and may even offset Moho (Gibbs, 1986, p 99, figs 3c and 3d).

6. Pilbara Craton and Yilgarn Block, W Australia

The Archaean Pilbara craton of northwestern Australia is a granite-greenstone terrane with ages generally greater than 2.4 Ga. The Hamersley basin developed across the craton in the late Archaean. Since the Proterozoic this region has only been subjected to mild epeirogenic uplift. The typical refraction seismic model of the Pilbara craton has the following features: a high-velocity near-surface layer in some areas due to dense, metamorphosed banded ironstones and basic volcanics in the Hamersley basin; the velocity increases from 6 km/s near the surface to 6.7 km/s at 28 km, with a low-velocity layer sometimes developed in the upper crust; a steep

increase in seismic velocity to in the lowermost crust to reach 8.2 km/s at a depth of 34 km (Drummond and Collins, 1986, fig 2a). A preliminary refraction seismic depth-velocity function for the Yilgarn block is very similar to that described for the Pilbara craton (Drummond and Collins, 1986, fig 7, p. 370).

Several short deep seismic reflection profiles were surveyed in the Yilgarn block as part of the western Australia Geotraverse. Probable reflections were of very low-amplitude, and of little continuity. The lack of any distinctive reflection character and definitive vertical velocity information made it impossible to correlate reflection events from one area to another along the Geotraverse (Mathur et al., 1977; Moss and Dooley, 1988, p 233).

7. Zimbabwe Craton

A crude model of the Zimbabwe Craton shows it to have a crustal velocity of 6.5 km/s, Moho at a depth of 40 km, and a sub-Moho velocity of 8.4 km/s (Stuart and Zengeni, 1987).

Discussion

In broad terms the velocity-depth model for the Kaapvaal Craton is similar to that observed on other Archaean cratons. Several generalizations can be made regarding the seismic structure of Archaean cratons.

a) The upper crystalline crust has seismic velocities in the range 6.2-6.4 km/s. Low velocity zones are not commonly developed.

b) The transition from upper to lower crust occurs at a depth which ranges from 12-18 km. It is generally marked by a gradient rather than a first order discontinuity.

c) The lower crust has seismic velocities in the range 6.5-6.8 km/s. Velocities > 7 km/s are not frequently observed.

d) The crust-mantle transition is generally a gradient zone 2-5 km thick over which velocities increase from ca. 6.8 km/s to ca. 8.1 km/s.

e) The depth of the Moho is between 35 and 40 km, with a slight positive velocity gradient beneath.

f) The reflection seismic fabric of the Archaean crust is generally transparent, with occasional diffractions and short (less than the Fresnel zone) dipping reflectors.

g) Seismic Q is generally high.

The most significant deviations of the Kaapvaal Craton from this generalised model are considered to be the following:

a) The strongly reflective character of the crystalline basement between the Vanteredorp Dome and Potchefstroom.

b) The relatively low values of seismic Q found to exist within the crystalline basement, particularly at the base of the crust.

7.4 Comparison with adjacent geological provinces

The seismic velocity structure of the Kaapvaal Craton is compared with that of adjacent younger geological provinces. The velocity-depth models are shown in Figure 7.4.

The Kaapvaal Craton is rimmed to the south and southwest by the Proterozoic Namaqua-Natal Province. A refraction seismic investigation of the Namaqualand Metamorphic Complex shows that the lower crust is comprised of a substantial proportion of intermediate velocity (6.6-6.9 km/s) rocks. Moho was found to be at a depth of 42 km (Green and Durrheim, in press). The Namaqua-Natal Province is in turn rimmed by the Pan-African (670-530 Ma) Damara Province. A refraction survey was conducted in the Damara Orogen of Namibia in 1975. Three profiles were observed in order to study the crustal structure and the nature of the crust-mantle boundary. In the central zone of the Damara Orogen two velocity inversions were found in the upper crust; and the crust-mantle boundary was found to be a transition zone of variable width rising slightly from a depth of 47 km towards the Atlantic coast. The profile in the southern zone of the Orogen showed relatively high velocities (up to 6.6 km/s) in the upper and middle crust and also in the lower crust (7.2 km/s). Finally, the profile on the Kalahari Craton (to the south of the Orogen, and consisting of the fused Kaapvaal Craton and Namaqua-Natal Province) showed no velocity inversions in the upper crust; and the Moho appears as a more distinct discontinuity split into an upper level at 47 km and a lower level at 60 km approximately (Baier et al., 1983).

The basement rocks of the southern Cape also are included in the Damara Province. The region is also the locus of the most recent tectonic events affecting southern Africa: the Cape Orogeny (280-230 Ma), and the fragmentation of Gondwana (135-115 Ma). Several refraction surveys were conducted on the Agulhas Bank in the 1960's as part of the International Indian Ocean Expedition. Using gravity and seismic refraction data, Graham and Hales (1965) interpreted a section through the Agulhas Bank along a line bearing south-southeast, and crossing the coastline 20 km east of Cape Seal. Their

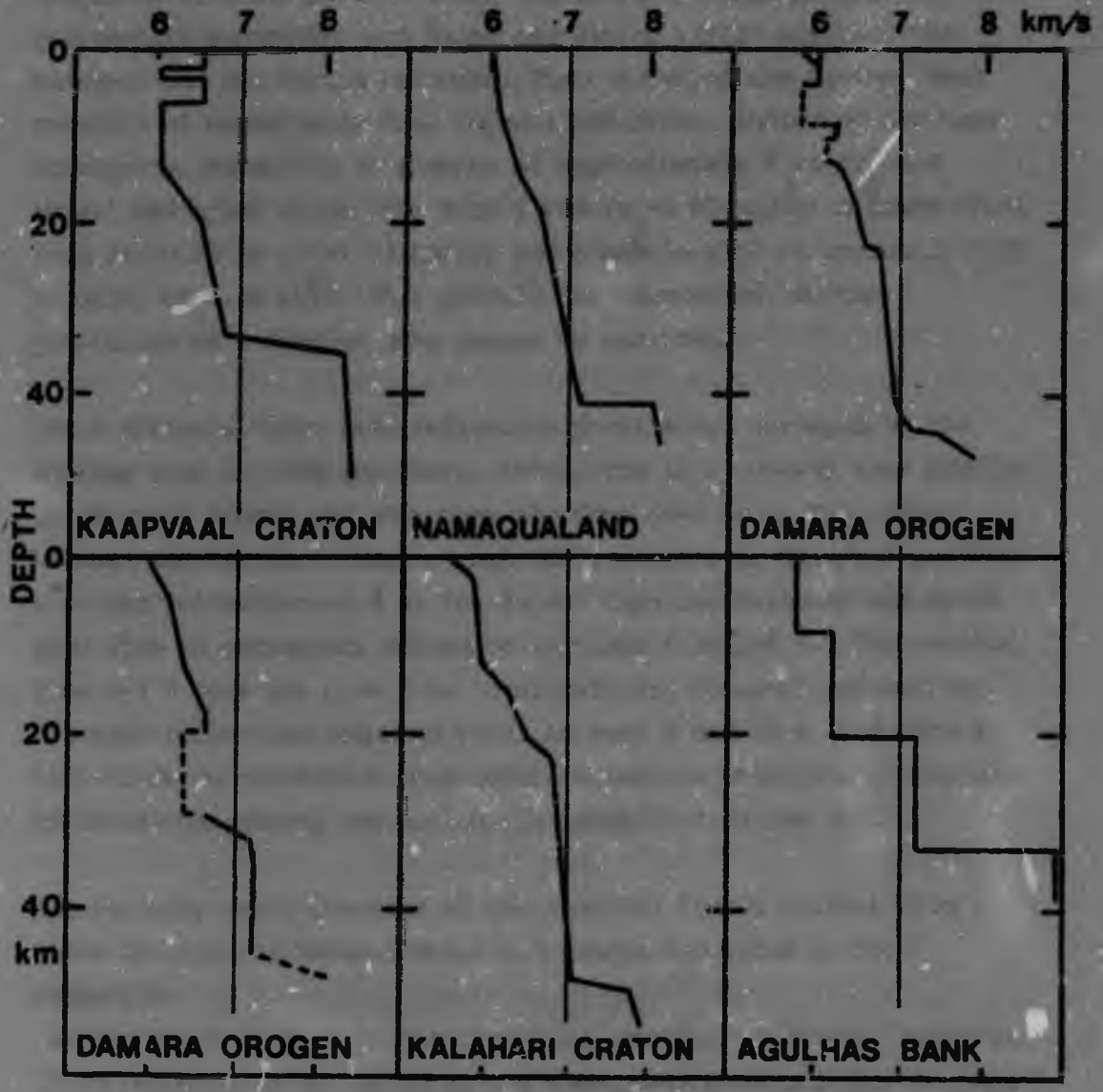


Figure 7.3. Velocity-depth models for southern Africa (from this study; Green and Durrheim (in press); Baier et al.. 1983; Hales and Nation, 1972).

model indicates a layer of sediments (v_p < 5 km/s) with an average thickness of 5.3 km; and a crust (v_p =6.4 km/s) extending to a depth of 30-33 km. A refraction profile approximately coincident with longitude 21°E was shot in 1968. Spence (1970) interpreted the sedimentary structure, and Hales and Nation (1972) analysed the basement and and mantle arrivals. Their model of the Agulhas Bank consists of essentially four layers: sediments, including the Cape Supergroup, extending to a depth of approximately 8 km (v_p =5.8 km/s); and upper crust from 8 to 21 km (v_p =6.21 km/s); a lower crust from 21 to 33 km (v_p =7.24 km/s); and a mantle with an unusually high velocity of 8.95 km/s. This profile was unreversed, so the possiblity of a dipping Moho cannot be excluded.

South Africa's first deep reflection profile was surveyed on the Agulhas Bank in 1985 (Durrheim, 1986). The 12 s two-way time profile is 46 km in length and straddles the Cape Seal Arch. The contact between the marine sediments and the pre-Mesozoic basement produces a strong reflection at 2 s. The folded Cape and Kaaimans sediments give rise to occasional strong reflections from 2-6 s. The section from 6-9 s does not give rise to significant coherent reflections. Strongly reflecting segments occur between 9 and 10 s, and with a time-to-depth conversion made using refraction velocities, this zone of occasional strong reflections is identified as the Moho.

The velocity-depth function of the Kaapvaal Craton differs from those obtained in Namaqua-Natal and Damara Provinces in two respects:

a) The depth to Moho in the Craton is somewhat shallower, being ca. 35 km compared to ca. 42 km in the Namaqualand Metamorphic Complex and ca. 47 km in the Damara Orogen.

b) The seismic velocities in the lower crust of the Craton are smaller (6.4-6.7 km/s) than observed in Namaqualand (6.6-6.9 km/s), the Damara Orogen (6.6-7.0 km/s), and the Agulhas Bank (ca. 7.2 km/s). This implies that the lower crust of the Craton is more felsic than that of the younger Provinces.

7.5 Implications for crustal evolution.

Many processes act on the continental crust following its primary derivation. The most significant processes are probably:

(a) stretching and shortening, accompanied by thinning and thickening respectively;

(b) redistribution of crustal rocks laterally by erosion, transport and sedimentation, or by thrusting or thin-skinned sliding;

(c) differentiation, in which a potassic upper crust and a more refractory lower crust are formed from a more uniform crust;

(d) accretion at the edges, either at magmatic arcs or by the addition of exotic terranes (decretion is the reverse process);

(e) overplating by ophiolite emplacement or extrusion of magmas across the surface or intrusion into the near-surface rocks;

(f) underplating by upper mantle partial melts at the base of the crust (sub-crustal erosion is the reverse process).

Processes (a) to (c) involve the rearrangement of material within the crust, while (d) to (f) involve the addition to or removal of material from the crust (Drummond and Collins, 1986, p 367).

The view that underplating (basaltic melt beneath granitic crust) may have been an important process in the growth of continental crust during the Archaean is expressed by several workers (e.g. Fyfe, 1974; Kröner, 1984). Underplated crust will be revealed by the elevation of seismic velocities. Depending on the composition of the underplated material and the local thermal structure, seismic velocities in the added layer will be in a range of values intermediate between velocities appropriate for crust and mantle materials (7.0 - 7.8 km/s), or values interpreted to be more typical of mantle materials (7.8 - 8.1 km/s) (Furlong and Fountain, 1986). All Archaean cratons for which detailed velocity-depth models are available (Baltic, Ukranian and Indian Shields, the Superior Province of Canada, Yilgarn and Pilbara blocks of Australia) lack the high lower-crustal velocities expected in underplated areas.

It is thought that the continental crust preserved in the Kaapvaal Craton had formed prior to 2.5 Ga (Harris et al., 1987, p. 87). The

model Nd ages were obtained from a surface location and xenoliths from two kimberlite pipes. Harris et al. (1987, p 92) conclude that the trace element data from granitoids and the high erosion rates implied by isotopic studies of sediments suggest that the growth of the Kaapvaal Craton during the Archaean was by underplating rather than lateral accretion. The absence of high seismic velocities within the lower crust of the Kaapvaal craton is believed to demonstrate the lack of significant underplating. The Kaapvaal Craton seems unaffected by the post-Archaean tectonism which occurred to the southeast of the Craton in the Proterozoic Namaqua-Natal Province, where intermediate velocities in the lower crust suggest underplating (Green and Durrheim, in press). Other evidence supporting this contention is provided by kimberlite studies. The equilibration temperatures for inclusions within diamonds from the Premier Mine kimberlite cluster near Pretoria are interpreted to mean that the Craton had already grown to its full areal extent and cooled to approximately the present thermal gradient at the time of diamond formation (Nixon, 1987, p 410). These kimberlites are dated at 1.25 Ga (Dawson, 1980, p 16). An argument used to support underplating as a major mechanism of Archaean crustal growth is the reported absence of significant areas of ophiolitic rocks, analogues of the modern ocean crust, on Archaean cratons (Fyfe, 1974). The recent reinterpretation of the Barberton Sequence of the eastern Kaapvaal Craton as an ophiolite succession is of significance in this context (De Wit et al., 1988).

The seismic structure of southern Africa is very similar to Australia, where seismic refraction studies (neglecting Archaean provinces) show that the average seismic velocity of the crust increases with its thickness, the increase being achieved wholly in the lower crust. This is attributed to a greater degree of underplating in the older provinces. Hoever, the Archaean Pilbara Craton does not fit this trend, and does not appear to have any significant amount of underplated material at the base of the crust (Drummond and Collins, 1986).

The geophysical and geological evidence for a layer of hydrated mantle rock at the base of the crust, with chemistry similar to that of oceanic lithosphere, is consistent with the model of mid-Archaean

tectonism proposed by Tredoux et al. (1989, p 811). In their model the simatic lithosphere of southern Africa formed intraoceanic thrust stacks which continuously underplated granite-greenstone terrains to form an mafic-ultramafic "keel" to the continental (sialic) lithosphere. The "keel" grew by tectonic inslicing, to attain a depth of at least 150 km by 3.0 Ga ago, and has remained intact since that time.

Comparison of four seismic refraction data sets from southern Africa indicates that the component of intermediate velocity rocks (6.6-7.3 km/s) within the lower crust increases as the age of the most recent crust building event affecting the region decreases. These differences might be attributed to variations in the principal mechanisms of crustal growth between Archaean and Proterozoic times.

8. CONCLUSIONS

The achievements of this study are summarized in the statements below.

1. A major new seismic data set covering the central portion of the Archaean Kaapvaal Craton has been acquired. Mine tremors have been recorded on three-component seismographs at 50 stations on the Craton. Most of the observations were made on two profiles which stretched from Klerksdorp to Witbank and from Boksburg to Welkom. The source-receiver distances ranged from 10 to 300 km. Observations took 30 months to complete, and in this time about 650 tremors were recorded, many of the events at several stations.

2. Tremors, instead of explosives, were used as the energy source for the deep seismic sounding investigation. This was made possible by the frequent and localized occurrence of mining-induced tremors in the deep-level gold mines of the Witwatersrand Basin. Tremors have the following advantages:

a) They are rich in shear energy, enabling joint interpretation of the P- and S-body waves.
b) Tremors have a wide bandwidth. The larger events ($M_L > 3$) have significant energy at frequencies as low as 3 Hz, enabling reflections from gradient zones to be detected.
c) They are cheap sources of energy, as no holes have to be drilled or explosives expended.

The major disadvantages of using tremors are the following:

a) The source location and origin time are not precisely known.
b) The tremors used to compile a record section have a variety of magnitudes, focal mechanisms, and source locations. Consequently, there is considerable variation in the character of the seismograms, which makes phases correlation more difficult.

3. Several methods not previously used for seismic refraction studies at Witwatersrand University were implemented. The most significant are:

a) The use of a microcomputer (XT and AT compatibles) for analog to

digital conversion, signal processing, and raytrace modelling.

b) The use of an advanced graphics package designed for the display of reflection seismic record sections to display the data.

c) The reflectivity method has been used to compute complete synthetic seismograms.

4. This study has yielded a significantly more detailed and better constrained seismic model of the Kaapvaal Craton than hitherto available. The previous investigations were conducted three decades ago. These workers were unable to unequivocally distinguish between a single-layer crust, a model incorporating an intermediate velocity lower crust, or a model with a velocity gradient throughout the crust. The seismic model of the crust derived from the wide-angle observations of tremors has the following features:

a) Supracrustal strata 0-10 km thick, with velocities of 3.5-6.8 km/s.

b) The upper part of the crystalline basement has a uniform velocity of 6.0-6.2 km/s. This forms a low velocity layer ca. 10 km thick, as the overlying Dominion and West Rand Groups have significantly higher seismic velocities.

c) The boundary between upper and lower crust is sometimes marked by a velocity gradient, which gives rise to a high amplitude caustic at offsets of 150 - 180 km. In other areas the transition is sufficiently abrupt for reflections to be generated.

d) The lower crust has a rather uniform seismic velocity in the range 6.4-6.7 km/s.

e) The crust-mantle transition takes place over a distance of 1-3 km.

f) The Moho is at a depth of ca. 35 km. A slight velocity gradient (at least 0.01 km/s/km) exists beneath the Moho.

g) The lower crust has a low value of Q revealed by the low dominant frequency of the $P_m P$ phase. The attenuation is due to both anelastic absorption and scattering. The correlation length of the scatterers of seismic energy is estimated to be ca. 60 m.

5. The improvement in the model is attributed to the following factors:

a) Use of digital data allowing manipulation of the seismograms and the construction of record sections. This facilitated phase correlation and identification, especially of the later arrivals.
b) During the studies carried out in the 1950's, only the Central Rand was a significant source of tremors. Many new gold mines have been established in the intervening years. During this study tremors from the Far West Rand, Klerksdorp and the O F S gold fields were recorded. This enabled the profiles to be reversed, and a greater area of the Craton to be investigated.
c) Modern seismic ray-tracing and synthetic seismogram methods were used to interpet the data.

6. The 16 s TWT trans-Witwatersrand Basin seismic reflection profile was acquired for the National Geophysics Programme during 1988. The reflection profile intersects both refraction profiles, allowing a joint interpretation to be made. The refraction and reflection data sets are complentary: the refraction method provides a broadband signal and good velocity and physical property information; while the reflection method provides high resolution and enables complete 2-D structural interpretation.

7. The deep reflection seismic section has the following features:
a) The disposition of the supracrustal strata has been reliably established. The faults displacing the supracrustal strata cannot be traced deep into the basement.
b) There appears to be a significant difference between the basement underlying the Potchefstroom synclinorium and that beneath the Ventersdorp Dome. The crystalline basement is divided into three domains on the basis of the seismic fabric: from the Ventersdorp Dome to Potchefstroom the crust is strongly reflective; beneath the Potchefstroom synclinorium it is essentially transparent; and the interior of the Vredefort structure has occasional short reflecting segments.
c) The strong reflectivity could be due to a wide variety of features including primary lithological layering, reflective ductile banding, igneous intrusions and sills. Strong reflectivity in the upper crystalline crust is an unusual feature. One of the best analogies is a metamorphic core complex

in the Basin and Range Province of north America. The reflectivity is probably an overprint of the most recent tectonic episode (possibly the intrusion of sills and ductile strain banding formed as a result of extension in Ventersdorp times), and does not provide and insight into the mechanism of basining.

d) The seismically transparent zone beneath the Potchefstroom synclinorium could be due either to a homogeneous or extremely heterogeneous crust. The wide-angle tremor data favours the latter option, because of the strong absorption and scattering experienced by the $P_m P$ phase.

e) No "reflection Moho" is detected. The reflectivity of the crust diminishes at ca. 12 s TWT. The failure to detect the Moho is attributed to the relatively gradual crust-mantle transition, which did not reflect the frequencies (> 10 Hz) used in the reflection seismic survey. The $P_m P$ and $S_m P$ reflections observed in the wide-angle experiment had frequencies < 3 Hz.

8. The petrology of the lower crust of the Craton and the underlying mantle is deduced from a consideration of seismic velocities, Poisson's ratio, seismic attenuation, xenolith compositions, electrical conductivity and petrophysical data.

a) The upper crystalline crust is composed of rocks of granitic to granodioritic average composition.

b) The upper to lower crust transition takes place over several kilometers, with the average composition becoming more mafic.

c) The lower crust is composed of felsic granulite (no garnets) with a dioritic average composition. Reflective layering is probably due to intrusive mafic sills.

d) The crust-mantle transition is marked by a zone several kilometers thick containing increasing amounts of serpentised peridotite. This accounts for the relatively high Poisson's ratio, high seismic attenuation and high electrical conductivity observed at the base of the crust.

c) The mantle consists predominantly of peridotite.

7. The velocity/depth model for the Kaapvaal Craton is essentially similar to models derived for other Archaean cratons: upper crust velocities 6.0-6.4 km/s; lower crust velocities 6.6-6.9 km/s, Moho

at 35-40 km marked by a velocity gradient from 1-5 km thick. Unusual features of the Kaapvaal Craton are the seismically attenuative and electrically conductive lower crust. Only the Zimbabwe Craton has a similar electrical structure.

8. When compared with seismic models of the younger Proterozoic terranes adjacent to the Kaapvaal Craton, the Craton is found to have a significantly thinner crust, and smaller velocities in the lower crust indicating a more felsic composition.

9. It is inferred that the lithospheric "keel" of the proto-Kaapvaal Craton grew to a depth of 150 km during the Archaean by tectonic inslicing and underplating of simatic lithosphere. The Kaapvaal Craton has not grown by underplating since its consolidation at ca. 2.6 Ga. The Craton is probably composed of several "crustal blocks", although data are too sparse to delineate them at this stage.

10. An increase in the component of intermediate rocks (6.6-7.3 km/s) and crustal thickness with time is indicated by seismic refraction studies of the Archaean Kaapvaal Craton, Proterozoic Namaqua-Natal Province, and the Pan-African (670-530 Ma) Damara Province. This suggests a change in the dominant mode of crustal growth during earth history, with underplating becoming more important since the Archaean.

REFERENCES

Anhaeusser, C. R., The geology and geochemistry of the Archaean granites and gneisses of the Johannesburg-Pretoria dome, Geol. Soc. S. Afr. Spec. Publ. 3, 361-385, 1973.

Arnott, F. W., Seismicity in the Welkom area, O. F. S. (with special reference to the origin of the 1976-12-8 Event), M. Sc. dissertation. Univ. Witwatersrand, Johannesburg, 1981.

Baier, B., H. Berckhemer, D. Gajewski, R. W. Green, Ch. Grimsel, C. Prodehl and R. Vees, Deep seismic sounding in the area of the Damara Orogen, Namibia, South West Africa, in Intracontinental Fold Belts, edited by H. Martin and F. W. Eder, 885-900, Springer-Verlag, Berlin, 1983.

Berry M. J. and K. Fuchs, Crustal structure of the Superior and Grenville Provinces of the northeastern Canadian Shield, Bull. Seism. Soc. Am., 63, 1393-1432, 1973.

Birch, F., Interpretation of the seismic structure of the crust in the light of experimental studies of wave velocities in rocks, in Contributions in geophysics in honor of Beno Gutenberg, edited by H. Benioff, M. Ewing, B. F. Howell Jnr. and F. Press, 158-170, Pergamon, London, 1958.

Birch, F., Density and composition of the mantle and core, J. Geophys. Res., 69, 4377-4387, 1964.

Bloch, S., A. L. Hales and M. Landisman, Velocities in the crust and upper mantle of southern Africa from multi-mode surface wave dispersion, Bull. Seism. Soc. Am., 59, 1599-1629, 1969.

Blundell, D. J. and B. Raynaud, Modeling lower crust reflections observed on BIRPS profiles, in Reflection Seismology: a global perspective, M. Barazangi and L. Brown (eds.), Geodynamics Series, 13, 287-296, American Geophysical Union, Washington, 1986.

Boland, A. V., R. M. Ellis, D. J. Northey, G. F. West, A. G. Green, D. A. Forsyth, R. F. Mereu, R. P. Meyer, P. Morel-a-l'Huissier, G. G. R. Buchbinder, I. Asudeh and R. A. W. Haddon, Seismic delineation of upthrust Archaean crust in Kapuskasing, Northern Ontario, Nature, 335, 711-713, 1988.

Borchers, R., Exploration of the Witwatersrand system and its extensions, in The geology of some ore deposits in southern Africa, vol 1, S. H. Haughton (ed.), 1-23, Geol. Soc. S. Afr.,

Johannesburg, 1964.

Bott, M. H. P., The Interior of the Earth, Edward Arnold, London, 1971.

Braile, L. W. and C. S. Chiang, The continental Mohorovicic discontinuity: results from near-vertical and wide-angle seismic reflection studies, in Reflection Seismology: a global perspective, M. Barazangi and L. Brown (eds.), Geodynamics Series, 13, 257-272, American Geophysical Union, Washington, 1986.

Braile, L. W. and R. B. Smith, Guide to the interpretation of crustal refraction profiles, Geophys. J. R. astr. Soc., 40, 145-176, 1975.

Brune, J. N., Tectonic stress and the spectra of seismic shear waves from earthquakes, J. Geophys. Res., 75, 4997-5009, 1970.

Brune, J. N., Correction: Seismic stress and the spectra of seismic shear waves from earthquakes, J. Geophys. Res., 76, 5002, 1971.

Burke, K., W. S. F. Kidd and T. Kusky, Archean foreland basin tectonics in the Witwatersrand, South Africa, Tectonics, 5, 429-456, 1986.

Burke, K., W. S. F. Kidd and T. Kusky, Is the Ventersdorp rift system of southern Africa related to a continental collision between the Kaapvaal and Zimbabwe Cratons at 2.64 Ga ago?, Tectonophysics, 115, 1-24, 1985.

Campbell, G. and D. G. Peace, Seismic reflection experiments for gold exploration, Wits. Basin, Republic of South Africa, paper presented at the 46th Meeting of the European Association of Exploration Geophysicists, London, 19-22 June, 1984.

Carswell, D. A., W. L. Griffin and P. Kresten, Peridotite nodules from the Ngopetsoeu and Lipelaneng kimberlites, Lesotho: a crustal or mantle origin, in Kimberlites II: the mantle and crust-mantle relationships, edited by J Kornprobst, 229-243, Elsevier, Amsterdam, 1984.

Cerveny, V., I. A. Molotkov, and I. Psencik, Ray Method in Seismology, Univerzita Karlova, Praha, 1977.

Christensen, N. I., Seismic velocities, in Handbook of Physical Properties of Rocks, Vol. 2, edited by R. S. Carmichael, CRC Press, Boca Raton, 1982.

Clendenin, C. W., E. G. Charlesworth, S. Maske and A. A. de Gasparis, Normal simple shear model for the evolution of the

early Proterozoic Venterasdorp Supergroup, South Africa, Inform. Circ. Econ. Geol. Res. Unit. Univ. Witwatersrand, Johannesburg, 201, 20 pp, 1988.

Cook, N. G. W., The seismic location of rockbursts, Proc. 5th Rock Mech. Symp., Pergamon, Oxford, 493-516, 1963.

Cooper, G. R. J., GRAV2D: An interactive 2-D gravity modelling programme for the IBM PC, Dept. of Geophysics, Univ. Witwatersrand, 5 pp, 1986.

Corner, B., R. J. Durrheim and L. O. Nicolaysen, The structural framework of the Witwatersrand basin as revealed by gravity and aeromagnetic data, Geocongress '86 Extended Abstracts, 27-30, Johannesburg, 7-11 July, 1986a.

Corner, B., R. J. Durrheim, B. C. Rodney, W. A. Wilsher and W. B. Steenkamp, Aeromagnetic coverage of the Witwatersrand basin and techniques used in its interpretation, Geocongress '86 Extended Abstracts, 211-214, Johannesburg, 7-11 July, 1986b.

Dawson, J. B., Kimberlites and their xenoliths, Springer-Verlag, Berlin, 1980.

Dawson, J. B. and J. V. Smith, Reduced sapphirine granulite xenoliths from the Lace kimberlite, South Africa; implications for the deep structure of the Kaapvaal Craton, Contrib Mineral Petrol, 95, 376-383, 1987.

De Wit, M. J., R. A. Hart and R. J. Hart, The Jamestown Ophiolite Complx, Barberton mountain belt: a section through 3.5 Ga oceanic crust, Journal African Earth Science, 6, 681-730, 1987.

Dietz, R. S., Vredefort ring structure: Meteorite impact scar?, J. Geol., 69, 499-516, 1961.

Dohr, G. and K. Fuchs, Statistical evaluation of deep crustal reflections in Germany, Geophysics, 40, 25-39, 1967.

Dooley, J. C. and F. J. Moss, Deep crustal reflections in Australia 1957-1973 - II. Crustal models, Geophysical Journal, 93, 239-249, 1988.

Drennan, G. R., M. Meyer and L. J. Robb, General charateristics of the Archaean basement west of the Welkom goldfield: applicability to the interpretation of the Colesberg magnetic anomaly trend (working paper), Contrib. to Int. Workshop on Cryptoexplosions and Catastrophes in the Geological Record, Parys, 1987.

Drummond, B. J. and C. D. N. Collins, Seismic evidence for underplating of the lower continental crust of Australia, Earth

Planet. Sci. Lett., 79, 361-372, 1986.

Drummond, B. J., A review of crust/upper mantle structure in the Precambrian areas of Australia and implications for Precambrian crustal evolution, Precambrian Research, 40/41, 101-116, 1988.

Durrheim, R. J., Recent reflection seismic developments in the Witwatersrand basin, in Reflection Seismology: a global perspective, M. Barazangi and L. Brown (eds.), Geodynamics Series, 13, 77-83, American Geophysical Union, Washington, 1986.

Durrheim, R. J., Seismic reflection and refraction studies of the deep structure of the Agulhas Bank, Geophys. J. R. astr. Soc., 89, 395-398, 1987.

Durrheim, R. J., B. Corner and W. A. Wilsher, The gravity field of the Witwatersrand basin and techniques used in its interpretation, Geocongress '86 Extended Abstracts, 215-218, Johannesburg, 7-11 July, 1986.

Evernden, J. F., C. B. Archambeau, E. Cranswick, An evaluation of seismic decoupling and underground nuclear test monitoring using high-frequency seismic data, Rev. of Geophys., 24, 143-215, 1986.

Ewing, W. M., W. S. Jardetzky and F. Press, Elastic waves in Layered Media, McGraw-Hill, New York, 380 pp., 1957.

Fernandez L. M., et al., Seismological Bulletins, monthly Reports of the South African Geological Survey, 1986, 1987, 1988.

Fuchs, K. and G. Miller, Computation of synthetic seismograms with the reflectivity method and comparison with observations. Geophys. J. R. astron. Soc., 23, 417-433, 1971.

Fuchs, K., Synthetic seismograms of PS-reflections from transition zones computed with the reflectivity method, J. Geophys., 41, 445-462, 1975.

Furlong, K. P. and D. M. Fountain, Continental crustal underplating: thermal considerations and seismic-petrologic consequences, J. Geophys. Res., 91, 8285-8294, 1986.

Fyfe, W. S., Archaean tectonics, Nature, 249, 338, 1974.

Gane, P. G., A statistical study of the Witwatersrand earth tremors, J. S. A. S. C. M. M., 155-173, 1939.

Gane, P. G., A. R. Atkins, J. P. F. Sellschop and P. Seligman, Crustal structure in the Transvaal, Bull. Seism. Soc. Am., 46, 293-316, 1956.

Gane, P. G., A. L. Hales and H. A. Oliver, A seismic investigation of the Witwatersrand earth tremors, Bull. Seism. Soc. Am., 36,

49-80, 1946.

Gane, P. G., P. Seligman and J. H. Stephen, Focal depths of Witwatersrand earth tremors, Bull. Seism. Soc. Am., 43, 239-250, 1952.

Gay, N. C., D. Spencer, J. J. van Wyk and P. K. van den Heever, The control of geological and mining parameters on seismicity in the Klerksdorp gold mining district, Proc. 1st Int. Conq. on Rockbursts and Seismicity in Mines, Johannesburg, 1982, N. C. Gay and E. H. Wainwright (eds.), 107-120, SAIMM, Johannesburg, 1984.

Gibbs, A. K., Seismic reflection profiles of Precambrian crust: a qualitative assessment, in Reflection Seismology: the continental crust, M. Barazangi and L. Brown (eds.), Geodynamics Series, 14, 95-106, American Geophysical Union, Washington, 1986.

Giese, P., General remarks on travel time data and principles of correlation, in Explosion Seismology in Central Europe, edited by P. Giese, C. Prodehl and A. Stein, 130-145, Springer-Verlag, Berlin, 1976a.

Giese, P., Depth calculation, in Explosion Seismology in Central Europe, edited by P. Giese, C. Prodehl and A. Stein, 146-161, Springer-Verlag, Berlin, 1976b.

Graham, K. W. T. and A. L. Hales, Surface-ship gravity measurements in the Agulhas Bank area, south of South Africa, J. Geophys. Res., 70, 4005-4011, 1965.

Green, R., A portable multi-channel seismic recorder and a data processing system, Bull. Seism. Soc. Am., 63, 423-431, 1973.

Green, R. W. and P. Chetty, Seismic studies in the basement of the Vredefort structure (working paper), Contrib. to Int. Workshop on Cryptoexplosions and Catastrophes in the Geological Record, Parys, 1987.

Green, R. W. E. and R. J. Durrheim, A seismic refraction investigation of the Namaqualand Metamorphic Complex, South Africa, J. Geophys. Res., in press.

Gupta, R. N, Reflection of elastic waves from a linear transition layer, Bull. Seism. Soc. Am., 56, 511-526, 1966a.

Gupta, R. N, Reflection of elastic waves from transition layers with arbitrary variation of velocity and density, Bull. Seism. Soc. Am., 56, 633-642, 1966b.

Gutenberg, B. and C. F. Richter, Magnitude and energy of earthquakes, Ann. Geofis. (Rome), 9, 1-15, 1956.

Guzman, J. A., A package of computer programs for the evaluation of local earthquakes and publication of the seismological bulletin, Rep. Geol. Surv. S. Afr., Gn 2446, 1978.

Hales, A. L. and D. I. Gough, Isostatic anomaly map of the Republic of South Africa, Map to accompany The Gravity Survey of South Africa. P. J. Smit, A. L. Hales and D. I. Gough, Handb. 3, Geol. Surv. S. Afr, 1962.

Hales, A. L. and J. B. Nation, A crustal structure profile of the Agulhas Bank, Bull. Seism. Soc. Am., 62, 1029-1051, 1972.

Hales, A. L. and I. S. Sacks, Evidence for an intermediate layer from crustal structure studies in the Eastern Transvaal, Geophysical Journal, 2, 15-33, 1959.

Hargraves, R. B., Palaeomagnetic evidence relevant to the origin of the Vredefort ring, J. Geol., 78, 253-263, 1970.

Harris, N. B. W., C. J. Hawkesworth, P. van Calsteren and F. McDermott, Evolution of continental crust in southern Africa, Earth Planet. Sci. Lett., 83, 85-93, 1987.

Hart, R. J. and M. A. G. Andreoli, A geological traverse of the Vredefort structure: the natural equivalent of a 15 km borehole into the Archaean Kaapvaal Craton, South Africa, Geocongress '86 Extended Abstracts, 823-826, Johannesburg, 7-11 July, 1986.

Hart, R. J., M. A. G. Andreoli, C. B. Smith, M. L. Otter and R. Durrheim, Ultramafic rocks in the centre of the Vredefort structure: possible exposure of the upper mantle ? Chemical Geology, in press.

Hart, R. J., L. O. Nicolaysen and N. H. Gale, Radioelement concentrations in the deep profile through Precambrian basement of the Vredefort structure, J. Geophys. Res., 86, 10639-10652, 1981.

Hartnady, C., P. Joubert, and C. Stowe, Proterozoic Crustal Evolution in Southwestern Africa, Episodes, 8, 236-244, 1985.

Hatcher, R. D., Interpretation of seismic reflection data in complexly deformed terranes: a geologist's perspective, in Reflection Seismology: the continental crust, M. Barazangi and L. Brown (eds.), Geodynamics Series, 14, 9-12, American Geophysical Union, Washington, 1986.

Helmstaedt, H. and J. J. Gurney, Kimberlites of southern Africa - are they related to subduction processes ?, in Kimberlites I:Kimberlites and related rocks, J. Kornprobst (ed.), 425-436,

Elsevier, Amsterdam, 1984.

Hill, D. P., Critically refracted waves in a spherically symmetric radially heterogeneous earth model, Geophys. J. R. astr. Soc., 34, 149-177, 1973.

Hirn, A., B. Damotte, G. Torreilles and ECORS Scientific Party, Crustal reflection seismics: the contributions of oblique, low frequency and shear wave illuminations, Geophys. J. R. astr. Soc., 89, 287-296, 1987.

Holbrook, W. S., D Gajewski, A. Krammer and C. Prodehl, An interpretation of wide-angle compressional and shear wave data in southwest Germany: Poisson's ratio and petrological implications, J. Geophys. Res., 93, 12 081-12 106, 1988.

Hron, M. and C. H. Chapman, Seismograms from Epstein transition zones, Geophys. J. R. astr. Soc., 37, 305-322, 1974.

Hyndman, R. D. and S. L. Klemperer, Lower-crustal porosity from electrical measurements and inferences about composition from seismic velocities, Geophys. Res. Lett., 16, 255-258, 1989.

Jentsch, M., Reinterpretation of a deep-seismic-sounding profile on the Ukranian Shield, J. Geophys., 45, 355-372, 1979.

Jones, A. G., On a type classification of lower crustal layers under Precambrian regions, J. Geophys., 49, 226-233, 1981.

Jones, M. Q. W., Heat flow in the Witwatersrand Basin and environs and its significance for the South African shield geotherm and lithosphere thickness, J. Geophys. Res., 93, 3243-3260, 1988.

Junger, A., Deep reflections in Big Horn County, Montana, Geophysics, 16, 499-504, 1951.

Kanasewich, E. R. and G. L. Cumming, Near-vertical-incidence seismic reflections from the "Conrad" discontinuity, J. Geophys. Res., 70, 3441-3446, 1965.

Kasahara, K., Earthquake mechanics, Cambridge Earth Science Series, 1981.

Kern, H., P- and S-wave velocities in crustal and mantle rocks under the simultaneous action of high confining pressure and high temperature and the effect of the rock microstructure, in High-Pressure Researches in Geoscience, W. Schreyer (ed.), 15-45, E. Schweizerbart'sche Verlagsbuchhandlung, Stuttgart, 1982.

Kind, R., Observations of sPn from Swabian Alb earthquakes at the GRF array, J. Geophys., 45, 337-340.

Kind, R., The reflectivity method for different source and receiver

structures and comparison with GRF data, J. Geophys., 58, 146-152, 1985.

Klemperer, S. L. and the BIRPS group, Reflectivity of the crystalline crust: hypotheses and tests, Geophys. J. R. astr. Soc., 89, 217-222, 1987.

Kozlovsky, Y. A., The world's deepest well, Scientific American, 251, 106-112, 1984.

Kröner, A., Evolution, growth and stabilization of the Precambrian lithosphere, Physics and Chemistry of the Earth, 15, 69-106, 1984.

Latham, T. S., J. Best, T. Chaimov, J. Oliver, L. Brown and S. Kaufman, COCORP profiles from the Montana plains: the Archean cratonic crust and a lower crustal anomaly beneath the Williston basin, Geology, 16, 1073-1076, 1988.

Lawrence, D. A., Seismicity in the Orange Free State gold mining district, Proc. 1st Int. Cong. on Rockbursts and Seismicity in Mines, Johannesburg, 1982, N. C. Gay and E. H. Wainwright (eds.), 121-130, SAIMM, Johannesburg, 1984.

Lilly, P. A., Shock metamorphism in the Vredefort collar: evidence for internal shock sources, J. Geophys. Res., 86, 10689-10700, 1981.

Lomnitz, C., A fast epicentre location program, Bull. Seism. Soc. Am., 67, 425-431, 1977.

Lund, C-E. and P. Heikkinen, Reflection measurements along the EGT POLAR-profile, northern Baltic shield, Geophys. J. R. astr. Soc., 89, 361-364, 1987.

Malan, W. W., Opening address, Rockbursts and Seismicity in Mines Symposium, in Proc. 1st Int. Cong. on Rockbursts and Seismicity in Mines, Johannesburg, 1982, N. C. Gay and E. H. Wainwright (eds.), 3-4, SAIMM, Johannesburg, 1984.

March, D. W., Seismic acquisition and processing in old geological formations, S A Geophys. Ass. Yearbook, 39-41, 1988.

Matthews, D. H. and M. J. Cheadle, Deep reflections from the Caledonides and Variscides west of Britain and comparison with the Himalayas, in Reflection Seismology: a global perspective, M. Barazangi and L. Brown (eds.), Geodynamics Series, 13, 5-20, American Geophysical Union, Washington, 1986.

Matthews, D. H. and the BIRPS group, Some unsolved BIRPS problems, Geophys. J. R. astr. Soc., 89, 209-216, 1987.

Mathur, S. P., F. J. Moss and J. C. Branson, Seismic and gravity investigations along the geotraverse, Western Australia, 1969, Bur. Miner. Resour. Aust. Bull., 191, 1977.

McCarthy, J., Reflection profiles from the Snake Range metamorphic core complex: a window into the mid-crust, in Reflection Seismology: the continental crust, M. Barazangi and L. Brown (eds.), Geodynamics Series, 14, 281-292, American Geophysical Union, Washington, 1986.

McDonald, A. J., Seismicity of the Witwatersrand Basin, M. Sc dissertation (unpubl.), Witwatersrand University, 160 pp., 1982.

McGarr, A., Seismic moments and volume changes, J. Geophys. Res., 81, 1487-1494, 1976.

McGeary, S., Nontypical BIRPS on the margin of the northern North Sea: The SHET Survey, Geophys. J. R. astr. Soc., 89, 231-238, 1987.

Meissner, R., The continental crust. A geophysical approach, Academic Press, London, 1986.

Meissner, R. Th. Wever and R. Bittner, Results of DEKORP 2-S and other reflection profiles through the Variscides, Geophys. J. R. astr. Soc., 89, 319-324, 1987.

Mitchell, B. J., N. K. Yacoub and A. M. Correig, A summary of seismic surface wave attenuation and its regional variation across continents and oceans, in The Earth's Crust, J. G. Heacock (ed.), Am. Geophys. Union Monogr., 20, 405-426, 1977.

Mooney, W. D. and T. M. Brocher, Coincident seismic reflection/refraction studies of the continental lithosphere: a global review, Rev. of Geophys., 25, 723-742, 1987.

Mooney, W. D. and C. Prodehl (Eds.), Proceedings of the 1980 Workshop of the International Association of Seismology and Physics of the Earth's Interior on the Seismic Modeling of Laterally Varying Structures: Contributions based on data from the 1978 Saudi Arabian Refraction Profile, U. S. Geol. Surv. Circ. 937, 158 pp., 1984.

Mooney, W. D. and A. W. Walter, Interpretation of coincident seismic reflection and refraction data in laterally inhomogeneous structure: A discussion of the results, in Interpretations of the SJ-6 seismic reflection/refraction profile, south-central California, USA, edited by A. W. Walter and W. D. Mooney, U. S. Geological Survey Open-file Report 87-73, Menlo Park, 1987.

Moss, F. J. and J. C. Dooley, Deep crustal reflection recordings in Australia 1957-1973 - I. Data acquisition and presentation, Geophysical Journal, 93, 229-237, 1988.

Miller, G, The reflectivity method:a tutorial, J. Geophys., 58, 153-174, 1985

Muller, M. R., Moho depth and crust-mantle velocity contrast determinations for South Africa from teleseismic P-wave spectral ratios, Extended Abstract, S. A. Geophysical Assn. Tech. Mtg., 29-30 June 1989, 145-148, 1989.

Nicolaysen, L. O and J. Ferguson, Diapirs driven by high pore fluid pressure, J. Struct. Geol., 3, 89-95, 1981.

Nicolaysen, L. O. and W. U. Reimold, Shock deformation, shatter cones, and pseudotachylite at Vredefort: a review of major unsolved problems and current efforts to resolve them, Lunar and Planetary Science, XVI, 618-619, 1985.

Nixon, P. H., Kimberlite xenoliths and their cratonic setting, in P. H. Nixon (ed.), Mantle Xenoliths, John Wiley & Sons, Chichester, 1987.

Olsen, K. H. and C-E Lund, Precambrian crustal structure of the northern Baltic Shield from the Fennolora profile: evidence for upper crustal anisotropic laminations, in Reflection Seismology: the continental crust, M. Barazangi and L. Brown (eds.), Geodynamics Series, 14, 121-126, American Geophysical Union, Washington, 1986.

Pavlenkova, N. I., Properties of middle and lower crust in platform areas, Annales Geophysicae, 5B, 651-656, 1987.

Peberdy, E, Geological effects on seismic elastic wave attenuation with specific application to the magnitude assessment, M.Sc dissertation (unpubl.), University of the Witwatersrand, 76 pp., 1986.

Peberdy, E. and R. W. E. Green, Coda Q and site effect of mine tremors for close distances within the Kaapvaal Craton, in review.

Percival, J. A. and Berry, M. J., The lower crust of the continents, in Composition, Structure and Dynamics of the Lithosphere-Asthenosphere System, K. Fuchs, and C. Froidevaux (eds.), Geodynamics Series, 16, 33-60, American Geophysical Union, Washington, 1987.

Potgieter, G. J. and C. Roering, The influence of geology on the

mechanisms of mining-associated seismicity in the Klerksdorp Goldfield, Proc. 1st Int. Cong. on Rockbursts and Seismicity in Mines, Johannesburg, 1982, N. C. Gay and E. H. Wainwright (eds.), 45-50, SAIMM, Johannesburg, 1984.

Pretorius, D. A., The nature of the Witwatersrand gold-uranium deposits, in Handbook of strata-bound and stratiform ore deposits, vol 7, K. H. Wolf (ed.), 29-88, Elsevier, Amsterdam, 1976.

Prodehl, C., The structure of the crust-mantle boundary beneath North America and Europe as derived from explosion seismology, in The Earth's Crust, J. G. Heacock (ed.), Am. Geophys. Union Monogr., 20, 349-369, 1977.

Raynaud, B., The quantitative interpretation of deep seismic reflection data, First Break, 6, 223-231, 1988.

Reston, T. J., Spatial interference, reflection character and the structure of the lower crust under extension. Results from 2-D seismic modelling, Annales Geophysicae, 5B, 339-348, 1987.

Richards, P. G. and W. Menke, The apparent attenuation of a scattering medium, Bull. Seism. Soc. Am., 73, 1005-1021, 1983.

Richter, C. F., Elementary Seismology, W. H. Freeman, San Francisco, 1958.

Robb, L. J. and Meyer, M, Hydrothermally altered granites and their significance in the hinterland of the Witwatersrand basin, Geocongress '86 Extended Abstracts, 27-30, Johannesburg, 7-11 July, 1986.

Robb, L. J. and M. Meyer, The nature of the Witwatersrand hinterland: conjectures on the source-area problem, Inform. Circ. Econ. Geol. Res. Unit, Univ. Witwatersrand, Johannesburg, 178, 25 pp., 1985.

Robinson, E. A., Multichannel Time Series Analysis with Digital Computer Programs, Holden Day, San Francisco, 298 pp., 1967.

Roux, A. T., The application of geophysics to gold exploration in South Africa, in Mining and Groundwater Geophysics/1967, L. W. Morley (ed.), Econ. Geol. Rep. 26, Geol. Surv. Canada, 425-438, 1970.

Rybach, L., A petrological model of the lower continental crust, derived from seismic velocities and from radioactive heat production, Annales. Geophysicae, 5B, 403-408, 1987.

Schilt, F. S., S. Kaufman and G. H. Long, A three-dimensional study

of seismic diffraction patterns from deep basement sources, Geophysics, 46, 1673-1683, 1981.

Schoenberger, M. and F. K. Levin, Apparent attenuation due to intrabed multiples, Geophysics, 39, 278-291, 1974.

Shapira, A., Rg waves from rockbursts in South Africa, Tectonophysics, 156, 267-273, 1988.

Slichter, L. B., The theory of the interpretation of seismic travel-time curves in horizontal structures, Physics, 3, 273-295, 1932.

Slotnick, M. M., Lessons in seismic computing, Society of Exploration Geophysicists, Tulsa, 268 pp., 1959.

Smithson, S. B., J. A. Brewer, S. Kaufman, J. E. Oliver and R. L. Zawislak, Complex Archean lower crustal structure revealed by COCORP crustal reflection profiling in the Wind River Range, Wyoming, Earth Planet. Sci. Lett., 46, 295-305, 1980.

Sollogub. V. B., D. Prosen, C. Dachev, I. Petkov, T. Velchev, E. Andonova, S. Mihailov, E. Mituch, K. Posgay, H. Militzer, C. Knothe, I. Uchman, P. Constantinescu, I. Cornea, S. I. Subbotin, A. V. Chekunov, I. A. Garkalenko, V. E. Khain, V. I. Slavin, B. Beranek, J. Weiss, A. Hridlicka, A. Dudek, M. Zounkova, M. Suk, M. Feifar, B. Milovanovic, M. Roksandic, Crustal structure of central and southeastern Europe by data of explosion seismology, Tectonophysics, 20, 1-33, 1973.

Spence, D. L., A seismic refraction study of sedimentary structure south of Cape Infanta, M. Sc. dissertation (unpubl.), Univ. Witwatersrand, 1970.

Spence, G. D., K. P. Whittall and R. M. Clowes, Practical synthetic seismograms for laterally varying media calculated by asymptotic ray theory, Bull. Seism. Soc. Am., 74, 1209-1223, 1984.

Spottiswoode, S. M., Source mechanisms of mine tremors at Blyvooruitzicht gold mine, Proc. 1st Int. Conf. on Rockbursts and Seismicity in Mines, Johannesburg, 1982, N. C. Gay and E. H. Wainwright (eds.), 29-38, SAIMM, Johannesburg, 1984.

Spottiswoode, S. M., Total seismicity and mine layouts: application of ERR and ESS, Colloquium: Mining in the vicinity of geological and hazardous structures, 4 June 1986, Johannesburg, SAIMM, 1986.

Spottiswoode, S. M. and A. McGarr, Source parameters of tremors in a deep-level gold mine, Bull. Seism. Soc. Am., 65, 93-112, 1975.

Stepto, D., A geological and geophysical study of the central portion of the Vredefort dome structure, Ph. D thesis (unpubl.),

Witwatersrand University, Johannesburg, 1979.

Stuart, G. W. and Zengeni, T. G., Seismic crustal structure of the Limpopo mobile belt, Zimbabwe, Tectonophysics, 144, 323-335, 1987.

Tankard, A. J., M. P. A. Jackson, K. A. Eriksson, D. K. Hobday, D. R. Hunter and W. E. L. Minter, Crustal Evolution of Southern Africa, 3.8 Billion years of earth history, 523 pp., Springer-Verlag, New York, 1982.

Tittmann, B. R., Internal friction measurements and their implications in seismic Q structure models of the crust, in The Earth's Crust, J. G. Heacock (ed.), Am. Geophys. Union Monogr., 20, 197-213, 1977.

Toksöz, M. N. and D. H. Johnston (eds.), Seismic wave attenuation, Soc. Expl. Geophys., Tulsa, 1981.

Tredoux, M. M. J. de Wit, R. J. Hart, R. A. Armstrong, N. M. Lindsay and J. P. F. Sellschop, Platinum group elements in a 3.5 Ga nickel-iron occurrence: possible evidence of a deep mantle origin, J. Geophys. Res., 94, 795-813, 1989.

Trifunic, M. D., Stress estimates for the San Fernando, California, earthquake of February 9, 1971; main event and thirteen aftershocks, Bull. Seism. Soc. Am., 62, 721-750.

Tweedie, K. A. M., The discovery and exploration of Beisa and Beatrix gold and uranium mines in the southern extension of the Welkom goldfield, in C. R Anhaeusser and S. Maske (eds.), Mineral Deposits of South Africa, 541-547, Geol. Soc. S. Afr., Johannesburg, 1986.

Van Calsteren, P. W. C., N. B. W. Harris, C. J. Hawkesworth, M. A. Menzies and N.W Rogers, Xenoliths from southern Africa: a parspective on the lower crust, in J. B. Dawson, D. A. Carswell, J. Hall and K. H. Wedepohl (eds.), The Nature of the Lower Continental Crust, Geological Society Special Publication No 24, 351-362, 1986.

Van den Heever, P., The influence of the geological structure on seismicity and rockbursts in the Klerksdorp goldfield, M. Sc dissertation (unpubl.), Rand Afrikaans University, 156 pp., 1982.

Van Zijl, J. S. V., A deep Schlumberger sounding to investigate the electrical structure of the crust and upper mantle in South Africa, Geophysics, 34, 450-462, 1969.

Van Zijl, J. S. V., Ultra deep Schlumberger sounding and crustal

conductivity structure in South Africa, Geophys. Prosp., 18, 615-634, 1970.

Van Zijl, J. S. V., The relationship between the deep electrical structure and tectonic provinces in southern Africa. Part 1. Results obtained by Schlumberger soundings, Trans. geol. Soc. S. Afr., 81, 129-142, 1978.

Warner, M, Migration - why does'nt it work for deep continental data? Geophys. J. R. astr. Soc., 89, 21-26, 1987.

Wernicke, B, Whole-lithosphere normal simple shear: an interpretation of deep-reflection profiles in Great Britain, in Reflection Seismology: the continental crust, M. Barazangi and L. Brown (eds.), Geodynamics Series, 14, 331-339, American Geophysical Union, Washington, 1986.

Wever, Th., The Conrad discontinuity and the top of the reflective lower crust - do they coincide, Tectonophysics, 157, 39-58, 1989.

Widess, M. B. and G. L. Taylor, Seismic reflections from layering within the Precambrian basement complex, Oklahoma, Geophysics, 24, 417-425, 1959.

Willmore, P. L., A. L. Hales and P. G. Gane, A seismic investigation of crustal structure in the western Transvaal, Bull. Seism. Soc. Am., 42, 53-80, 1952.

Wu, R. S. and K. Aki, Elastic wave scattering by a random medium and the small-scale inhomogeneities in the lithosphere, J. Geophys. Res., 90, 10261-10273, 1985.

Young, R. A., J. Wright and G. F. West, Seismic crustal structure northwest of Thunder Bay, Ontario, in Reflection Seismology: the continental crust, M. Barazangi and L. Brown (eds.), Geodynamics Series, 14, 143-156, American Geophysical Union, Washington, 1986.

conductivity structure in South Africa, Geophys. Prosp., 18, 615-634, 1970.

Van Zijl, J. S. V., The relationship between the deep electrical structure and tectonic provinces in southern Africa. Part 1. Results obtained by Schlumberger soundings, Trans. geol. Soc. S. Afr., 81, 129-142, 1978.

Warner, M, Migration - why does'nt it work for deep continental data? Geophys. J. R. astr. Soc., 89, 21-26, 1987.

Wernicke, B, Whole-lithosphere normal simple shear: an interpretation of deep-reflection profiles in Great Britain, in Reflection Seismology: the continental crust, M. Barazangi and L. Brown (eds.), Geodynamics Series, 14, 331-339, American Geophysical Union, Washington, 1986.

Wever, Th., The Conrad discontinuity and the top of the reflective lower crust - do they coincide, Tectonophysics, 157, 39-58, 1989.

Widess, M. B. and G. L. Taylor, Seismic reflections from layering within the Precambrian basement complex, Oklahoma, Geophysics, 24, 417-425, 1959.

Willmore, P. L., A. L. Hales and P. G. Gane, A seismic investigation of crustal structure in the western Transvaal, Bull. Seism. Soc. Am., 42, 53-80, 1952.

Wu, R. S. and K. Aki, Elastic wave scattering by a random medium and the small-scale inhomogeneities in the lithosphere, J. Geophys. Res., 90, 10261-10273, 1985.

Young, R. A., J. Wright and G. F. West, Seismic crustal structure northwest of Thunder Bay, Ontario, in Reflection Seismology: the continental crust, M. Barazangi and L. Brown (eds.), Geodynamics Series, 14, 143-156, American Geophysical Union, Washington, 1986.

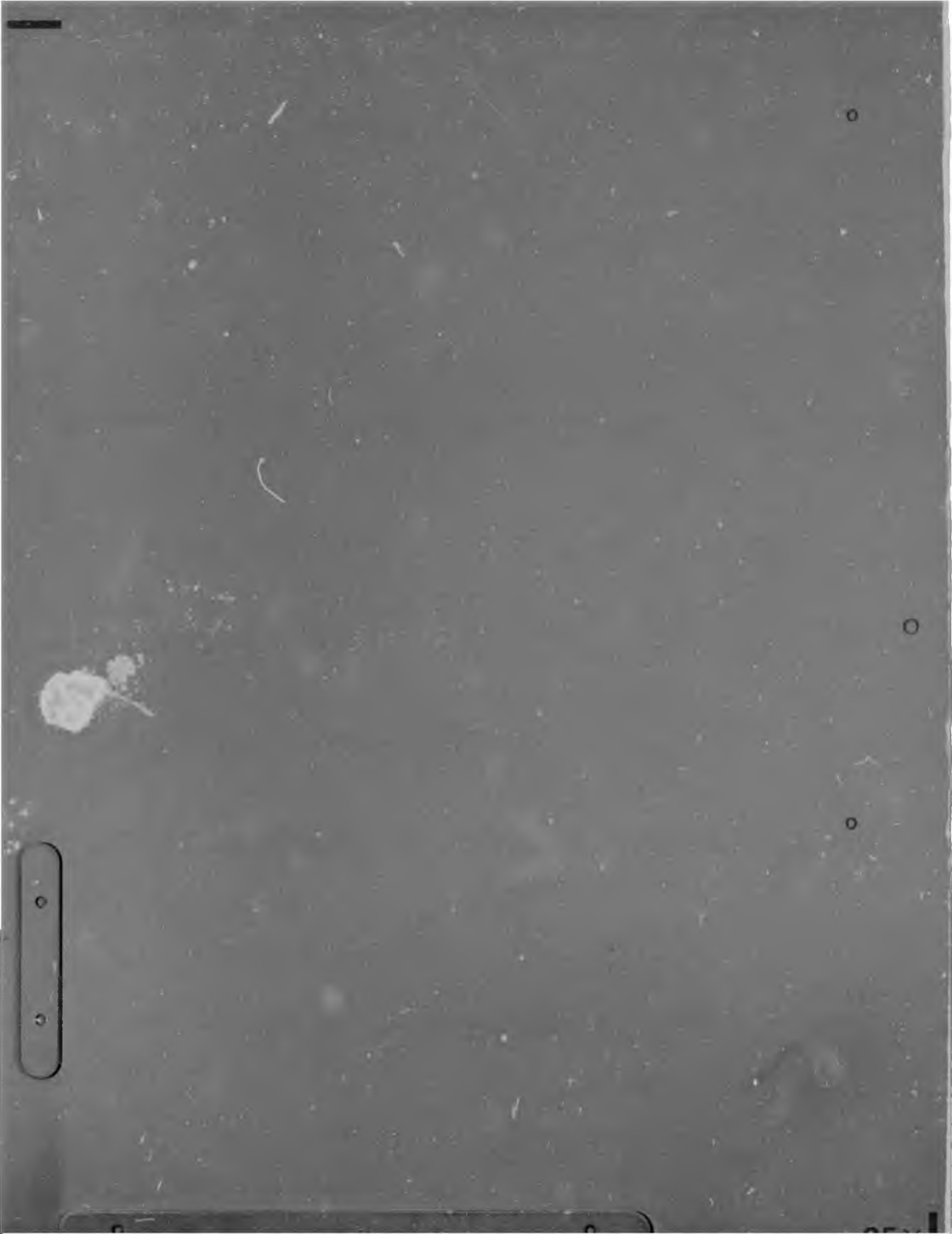
APPENDIX A: SEISMOGRAPH LOCATIONS

Klerksdorp - East Rand - Witbank profile

Station	Farm	Lat	Long
KB-20		27.015	26.526
KB-10	Goedgenoeg 433 IP	26.983	26.601
KB 00			
KB 10	Witkop 438 IP	26.947	26.709
KB 20	Hartebeestfontein 422 IP	26.898	26.801
KB 30	Wildebeestpan 442 IP	26.862	26.873
KB 40	Haaskraal 430 IQ	26.776	27.072
KB 50	Elandsheuvel 436 IQ	26.733	27.151
KB 60	Rietfontein 434 IQ	26.682	27.234
KB 70	Witpoort 419 IQ	26.657	27.344
KB 80	Goedgedacht 408 IQ	26.613	27.426
KB 90	Rhenosterfontein 560 IQ	26.560	27.511
KB100A	Raatskraal 524 IQ	26.548	27.591
KB100B	Doornfontein 522 IQ	26.533	27.609
KB110	Kalbasfontein 365 IQ	26.485	27.690
KB120	Rietfontein 336 IQ	26.451	27.790
KB130	Fonteine 313 IQ	26.405	27.882
KB140	Muldersrus 330 IQ	26.368	27.966
KB150	Patlynn Agric. Holdings	26.325	28.040
KB160	Newmarket	26.288	28.123
KB170	E.R.P.M.	26.259	28.221
KB180	Airfield	26.174	28.313
KB190	Modder East	26.183	28.433
KB200	Modderfontein 236 IR	26.124	28.505
KB210	Olifantsfontein 196 IR	26.089	28.583
KB220	Witklipbank 202 IR	26.046	28.687
KB230	Brakfontein 559 JR	25.999	28.771
KB240	Witpoort 563 JR	25.942	28.857
KB250	Hartbeesfontein 537 JR	25.906	28.948
KB260	Doornbult	25.885	29.019

East Rand - O F S profile

Station	Farm	Lat	Long
BW 20	Waterval 150 IR	26.406	28.085
BW 30	Nooitgedacht 177 IR	26.466	28.010
BW 40	De Deur 539 IQ	26.537	27.953
BW 50	Houtkop	26.607	27.893
BW 60	Vanderbijlpark	26.683	27.824
BW 70	Driefontein 581 IQ	26.744	27.770
BW 80	Weilbach 115	26.816	27.682
BW 90	Vergenoeg 162	26.880	27.630
BW100	Ontevreden 278	26.959	27.5[illegible]
BW110	Oudewerf 275	27.044	27.51[illegible]
BW120	Mara 1084	27.099	27.480
BW130	Rondebeuwel 266	27.184	27.353
BW140	De Wets Rust 230	27.243	27.273
BW150	Doornpan 1220	27.319	27.237
BW160	Denbigh 1229	27.364	27.167
BW170	Driekop 630	27.462	27.119
BW180	Enkeldoorn 67	27.512	27.032
BW190	Trutersrust 1758	27.602	26.997
BW200	Bronkhorstlaagte 1828	27.671	26.914
BW210	Scotland Noord 178	27.726	26.796
BW220	Lusthof 158	27.802	26.821
BW230	Bedela 54	27.963	26.710



Author Durrheim R J
Name of thesis A Seismic investigation of the Kaapvaal Craton 1989

PUBLISHER:
University of the Witwatersrand, Johannesburg
©2013

LEGAL NOTICES:

Copyright Notice: All materials on the University of the Witwatersrand, Johannesburg Library website are protected by South African copyright law and may not be distributed, transmitted, displayed, or otherwise published in any format, without the prior written permission of the copyright owner.

Disclaimer and Terms of Use: Provided that you maintain all copyright and other notices contained therein, you may download material (one machine readable copy and one print copy per page) for your personal and/or educational non-commercial use only.

The University of the Witwatersrand, Johannesburg, is not responsible for any errors or omissions and excludes any and all liability for any errors in or omissions from the information on the Library website.